Diffusion Mechanisms, Measurements, and Models with Applications in Bioremediation of Trichloroethylene and Breakdown Products

A Thesis

Presented in Partial Fulfillment of the Requirements for the

Degree of Master of Science

with a

Major in Chemical Engineering

in the

College of Graduate Studies

University of Idaho

by

Jonathan R. Counts

Major Professor: James Moberly, Ph.D.

Committee Members: Kristopher Waynant, Ph.D.; Mark Roll, Ph.D.

Department Administrator: Eric Aston, Ph.D.

May 2020

Authorization to Submit Thesis

This thesis of Jonathan R. Counts, submitted for the degree of Master of Science with a Major in Chemical Engineering and titled "Diffusion Mechanisms, Measurements, and Models with Applications in Bioremediation of Trichloroethylene and Breakdown Products," has been reviewed in final form. Permission, as indicated by the signatures and dates below, is now granted to submit final copies to the College of Graduate Studies for approval.

Major Professor: _____ Date: _____
James Moberly, Ph.D.

Committee Members: _____ Date: _____
Kristopher Waynant, Ph.D.

_____ Date: _____
Mark Roll, Ph.D.

Department

Administrator: _____ Date: _____
Eric Aston, Ph.D.

Abstract

Trichloroethylene (TCE) is a persistent groundwater pollutant remaining from decades of use as a dry cleaning solvent and general degreaser. Having low solubility and a higher density than water, it often exists as a Dense Non-Aqueous Phase Liquid (DNAPL) at the bottom confining layer of aquifers, posing a unique remediation challenge. Bioremediation using anaerobic bacteria has proven successful, but high concentrations of TCE and proton buildup from degradation can incapacitate microbes, leaving the system "stuck". In addition, incomplete degradation of TCE results in by-products cis-1,2-dichloroethene (cDCE) and highly toxic vinyl chloride (VC). Encapsulation of microbes in a hydrogel bead to facilitate diffusion of pollutant and adsorption of acid may allow total remediation of problem systems. In this work, a series of membranes of various compositions are tested and diffusion coefficients determined for all species of interest using the diaphragm cell method. In Chapter 3, this information is used in a model to optimize hydrogel bead size and composition for bioremediation applications.

Laboratory measurements of diffusion coefficients are time-consuming and may not be feasible for a diverse range of membrane types. It would be highly advantageous to build a correlation relating membrane properties to diffusivity. This would eliminate the need for repeated measurements using hazardous chemicals. Such a model would also allow rapid estimates of diffusion coefficients, expanding the likelihood of adoption of diffusion/reaction systems. Chapter 2 relates solute size, charge, and interactions within hydrogel membranes to steady state effective diffusivity for several molecules including hydrochloric acid. Increased understanding of the mechanisms of proton diffusion may have applications beyond bioremediation, including fuel cells and biomedical implants. Chapter 4 details future work which may improve efficacy of encapsulated cell systems.

Acknowledgements

My sincere gratitude goes out to all the faculty, staff, and professors in the College of Engineering and especially the Chemical and Materials Engineering Department at the University of Idaho. Their positive attitude, devotion to students, and passion for research made it a joy to come to work every day. I would like to thank all the undergraduate researchers who assisted this research and greatly added to its scope, especially Thomas Christensen II, Laura Nutter, Addie White, Isabell Strawn, Chad Larson, and John Sanchez. I give special thanks to Dr. Waynant, whose constant support, ideas, and energetic presence at meetings greatly helped. Most of all I would like to thank and acknowledge my major professor Dr. James Moberly not only for his support and guidance but especially for taking me on as his graduate student when I was at the proverbial 'crossroads'. Thank you so much Dr. Moberly for opening a series of doors when I was considering shutting the first one.

This material is based upon work supported by the National Science Foundation under Grant No. (1805358). Any opinions, findings, and conclusions or recommendations expressed in this material are those of the author(s) and do not necessarily reflect the views of the National Science Foundation.

Dedication

I would like to dedicate this thesis to my mother Nora Counts and twin brother David Counts. The two of you are great motivators, even when you're not around. I would also like to include the Chemical and Materials Engineering Administrative Assistant, Gail Bergman in this dedication – you are an absolute gem of a human being.

Table of Contents

List of Tables

List of Figures

List of Equations

Chapter 1: Introduction to Diffusion and TCE

1.1 The TCE problem

Chlorinated aliphatic hydrocarbons (CAHs) such as trichloroethylene (TCE) are long-lasting, carcinogenic groundwater pollutants. TCE was used for nearly a century in America as a dry-cleaning solvent and degreasing agent[1], seeing extensive use as a degreaser in military bases and nuclear power plant operations[2]. Approximately 60% of National Priority List sites are contaminated with TCE, and nearly every state in the union has significant contamination[3]. TCE is produced industrially by chlorination of ethylene dichloride, with tetrachloroethylene (PCE) being released as a by-product[4]. In 1989, the United States Environmental Protection Agency (EPA) established a maximum contaminant level (MCL) on TCE and several methods have been employed for remediation, including soil stripping, activated carbon adsorption and bioremediation. Spills of this volatile organic compound (VOC) result in "plumes" of pollutant which can sink into the groundwater and form dense, non-aqueous phase liquids or DNAPLs, which pose a significant remediation challenge[5]. The high toxicity and low solubility of TCE and other CAHs (<1g/L) can allow the contaminant to persist for decades without treatment[5,6]. TCE also has a high affinity for soil and organic matter, prolonging its residence time in the environment[1]. TCE is currently listed as number sixteen on the Agency for Toxic Substances and Disease Registry (ATSDR) substance priority list for contaminant remediation[7]. The current drinking water maximum contaminant level (MCL) for TCE is only 5 ppb. As typical wastewater treatment has little effect on CAH degradation, contaminants are often treated *in situ*, downstream from the source plume where concentration is lower.

A Brief History of TCE:

Trichloroethylene was first produced in Germany in 1864 and came into industrial use as a degreasing agent in the 1920s[8]. During World War I, the USA confiscated German patents following the Trading-with-the-Enemy Act in 1917. Production increased quickly and TCE became a common industrial chemical used in defense, dry-cleaning, electronics, and railroads. TCE was considered safe with no regulations on disposal, even seeing use for a time as general

anesthetic for out-patient surgeries[9] and veterinary procedures[10]. Production continued to climb throughout the first half of the Cold War; at one point 55 gallons of TCE per month were used to clean the X15 rocket plane engines[11] at a single Air Force Base. The solvent also became a standard degreasing agent for use in nuclear power plants.

The toxicity of TCE and PCE began to be understood starting in the 1960s. Unfortunately, by this time hundreds of millions of pounds of TCE were being used every year in the United States. Lack of toxicological information and regulation over the past four decades resulted in unmeasured tons of carcinogenic chemical being released to the environment. As a result, many water supply wells have been shut down in states such as New York and Massachusetts[1,12].

CAHs such as PCE, TCE, and DCE are denser than water and can remain in groundwater for decades. Spills can form DNAPLs at the bottom of aquifers which slowly dissolve into surrounding water. The low solubility, high toxicity, and inability of many naturally occurring microbes to degrade these chemicals make contamination a persistent remediation challenge. Heavy soil contamination of TCE can cause vapor intrusion[13] where TCE and other CAHs volatilize from the soil and contaminate air in crawl spaces and dwelling places. Such contamination has resulted in evacuation of some residential and commercial buildings around factories[14]. Much research has been conducted to determine methods for CAH remediation[15–17].

1.2 Current Methods of Remediation

Air Strippers:

Perhaps the simplest method of eliminating CAHs from groundwater is air stripping, where groundwater is pumped above ground, forcing air through the groundwater, and capturing discharged solvents within an air stream[18]. The large Henry's constant (low solubility, high volatility) of TCE allows fast elimination from water, though this contaminates the air and

does not degrade the carcinogen. Packed towers are typically used for air stripping and are successful at lowering CAH concentrations but at high cost[19].

Activated Carbon Adsorption:

This method involves pumping groundwater into an adsorption bed of activated carbon[20]. Organic solvents are accumulated in the bed, and effluent is pumped back into the water table. This method is attractive, as many contaminants including PCE, can be simultaneously removed. However, this treatment is rarely used due to the high cost of pumping and background organic matter (BOM) saturating the activated carbon faster than CAHs. In many systems, these naturally occurring organic materials are present at concentrations orders of magnitude higher than TCE. Furthermore, the diffusion of organic solvents to adsorption binding sites makes the process time-consuming, though contaminants diffuse faster in activated carbon fibers compared to granular activated carbon[21].

Soil Venting:

Soil venting is another option for TCE remediation[12]. The technology is essentially air stripping which uses the soil as an *in situ* packed column. For plumes in the vadose zone or near the surface, air can be pumped into the soil or below the soil/groundwater interface. The vapor then carries organic solvents to the atmosphere or a withdrawal well. This method is useful for a variety of CAHs as they tend be highly volatile[22]. Treatment of air at the surface may be necessary to meet air quality regulations and perhaps for this reason it is rarely employed.

Thermal Treatment:

Thermal treatment is most useful in situations where contaminant penetration is limited to the vadose zone. Heat addition to the groundwater by steam injection, electrode voltage, or combustion of fuels can volatilize or even combust CAHs. In the former case, an extraction well is surrounded by heat injection sites and contaminants are removed by a vacuum. The

Henry's law constant for TCE increases by a factor of twenty between 10 and 95ºC[23]. In thermal treatment, large amounts of heat may be added, raising the subsurface temperature to 500ºC and combusting pollutants *in situ*[24]. Massive capital is needed for thermal treatment, and soil properties may be drastically altered in the process. Additionally, high groundwater flow rates (>1 ft/day) can limit thermal treatment efficacy and increase costs.

Bioremediation:

Perhaps the most cost-effective method of CAH degradation is reductive dechlorination by anaerobic microbes belonging to genera such as such as *Geobacter* and *Dehalococcoides*[25]. Normally these microbes are not naturally present and must be added to contaminated groundwater. Bioremediation, specifically bioaugmentation, is the only method which does not require movement of soil or pumping groundwater. This 'unconventional' methodology may significantly decrease the estimated cost of total USA contaminant remediation of $1.7 trillion[26]. In bioaugmentation, a consortium of microbes is anaerobically injected into groundwater in wells downstream of the source plume. One particular consortium initially isolated by Duhamel et al. is KB-1[27], which is used extensively in scientific studies[26–30]. Several years ago, the Moberly lab used KB-1 encapsulated in hydrogel membranes to prove the biobead concept[31]. Degradation of TCE is a multi-step process which sequentially yields dichloroethylene (DCE), highly toxic vinyl chloride (VC), and finally harmless ethylene as microbes shift their metabolic processes to degrade the most chlorinated solvent present. The three-step degradation process is shown in **Figure 1.1**. The KB-1 consortium only degrades TCE to the 'cis-1,2-' isomer of DCE (cDCE). cDCE is then degraded to VC, which is mutagenic and highly carcinogenic. The MCL for drinking water as defined by the EPA is 5 ppb for TCE, 70 ppb for cDCE, and 2 ppb for VC[32]. Incomplete degradation can therefore significantly increase the overall toxicity of contamination.

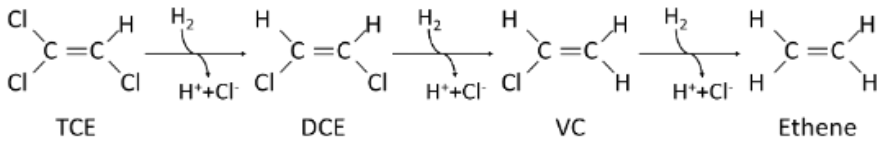

Figure 1.1*: Sequential degradation of TCE to cDCE, VC and finally ethene*

Biodegradation of TCE and cDCE is inhibited at high solute concentrations. TCE degradation with KB-1 is completely inhibited at concentrations above 2 mM[30]. For this reason, bioremediation is generally conducted downstream of the source plume where the contaminant is dilute. In addition, the rate of reaction decreases for each sequential CAH by-product. Batch experiments with initial concentrations of 0.3 mM TCE show that cDCE requires approximately 30 days to completely degrade while TCE is effectively eliminated after less than ten days[30]. VC degradation is significantly slower than cDCE, so for a planktonic system the most toxic by-product[30] has the longest residence time in the environment. VC is also less dense than water and highly volatile, increasing the risk of vapor intrusion from groundwater or soil. VC is listed as number four on the current ATSDR's Substance Priority List.

With each degradation step, hydrochloric acid is released to the immediate environment. In poorly buffered groundwater the increase in solution acidity can cause a massive drop in viable cells and leave the system with a high concentration of hazardous by-products. Inhibition[33] of consortium starts at pH 5.5 and complete inhibition is observed around pH 4.5. Such systems are termed "stuck", as further remediation of carcinogens is halted. As can be seen in **Figure 1.2**, inhibitory pH levels are reached in unbuffered groundwater when less than 150 ppb TCE is mineralized to ethylene. Addition of buffering groups and substrate with microbes produces better results but also significantly increases the cost of bioremediation. This thesis explores the feasibility of encapsulating microbial consortia in pH-buffered hydrogel membranes, providing a safe environment for long-term degradation of TCE.

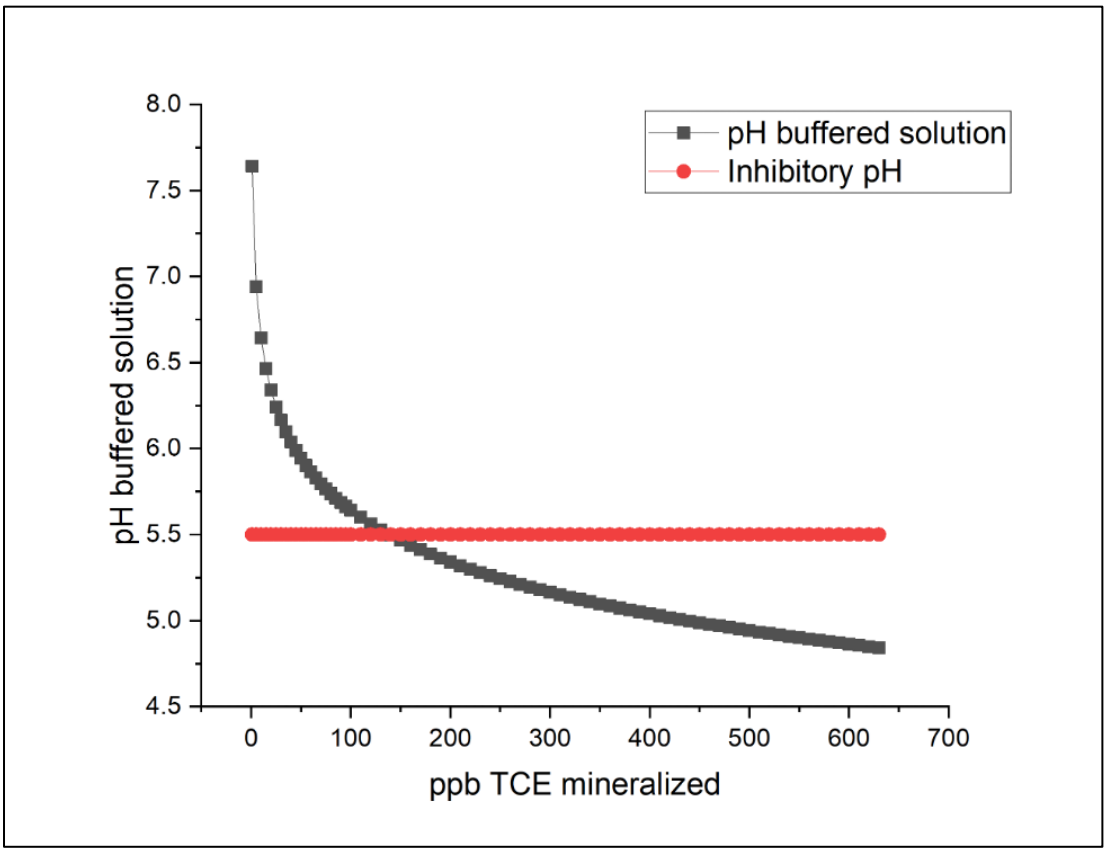

Figure 1.2: *pH vs TCE degradation for unbuffered system*

1.3 Biodegradation in Hydrogel Beads

This research investigates protection of microbes by mimicking the bacterial adaptation of biofilm formation. In nature, biofilms protect embedded cells from rapid environmental changes, and limit competition with other species. In some cases, microbes are capable of complete cell encapsulation, while others merely produce exo-polysaccharides which partially shield them from the local environment[34]. In addition, close contact with members of the same species/consortium allows a communal system of living[35]. Artificial polymer membranes saturated with water can serve as synthetic biofilms, offering a characterizable, homogeneous environment for cells. Encapsulation of microbes in hydrogel matrices can promote cell metabolism, limit replication, and protect cells from non-optimal environments. In addition, the polymer type and concentration can be selected so as to achieve optimal diffusion of key nutrients and byproducts to and from cells. Much research has been conducted for hydrogel

use as both medical implants and drug delivery[36–40]. Non-toxic polymers and non-fouling membranes are especially researched for biomedical applications. Due to their hydrophilic nature, synthetic hydrogels are often employed to diffuse substances dissolved in water in a controlled manner. They have also been used as artificial biofilms for bacteria, including impregnating with yeast for ethanol production[41,42].

Artificial biofilms are primarily composed of water, which is trapped by crosslinked polymer chains[43]. These hydrogels are hydrophilic and tend to swell in water or aqueous environments, carrying fluid in pores or 'packets'. Hydrogels are applied in a wide range of fields including separations[44], fuel cells[45], biomedical implants[46], and microbial encapsulations for fermentation[47]. Common polymers used in hydrogels are poly(vinyl alcohol) (PVA), sodium alginate (SA) (**Figures 1.3** and **1.4**), agarose, κ-carrageenan, and poly(ethylene oxide).

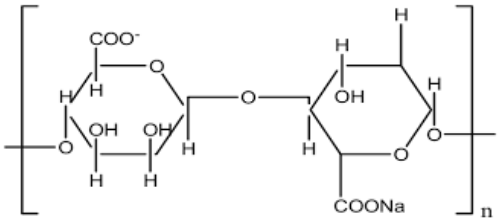

Figure 1.3: *Sodium alginate polymer*[48]

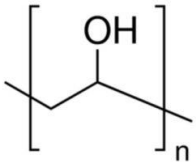

Figure 1.4: *poly(vinyl alcohol) polymer structure*[49]

Among these, alginate systems are particularly well researched for use in artificial biofilms, as the molecule is synthesized in natural biofilms by *Pseudomonas aeruginosa*[50]. This thesis is mainly concerned with poly(vinyl alcohol), sodium alginate mixture (PVA/SA) hydrogels and membranes crosslinked by boric acid/calcium chloride solutions or repeated freeze/thaw cycles (**Figure 1.5**).

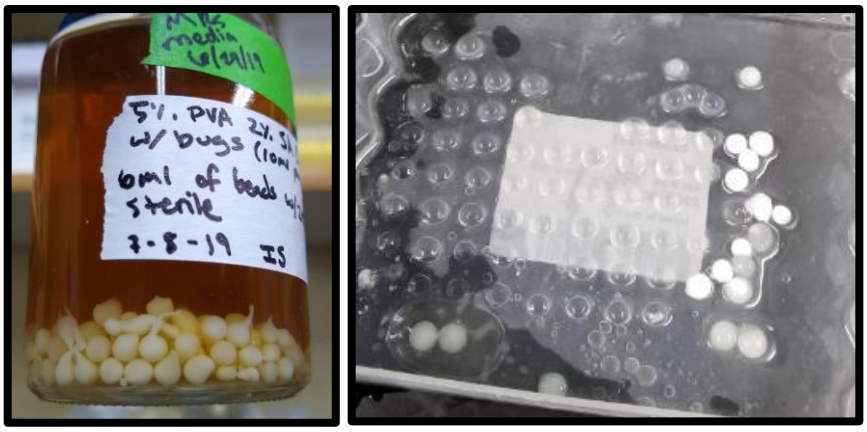

Figure 1.5: *Chemically crosslinked 10% PVA 2% SA (left) and physically crosslinked 10% PVA (right) membrane beads*

Encapsulation of microbial consortia for TCE degradation may shield cells from inhibitory concentrations of CAHs, allowing deployment closer to the source plume. Inclusion of buffering groups in the membrane can protect microbes from acid released by the degradation steps. The water saturated hydrogel may also prevent contact with naturally occurring bacterial species, eliminating competition and forming a symbiotic microbial community. This property of encapsulated bacteria has been seen in several medical studies where hydrogel encapsulation prevents immune rejection of foreign cells *in vivo*.[51(p)] In the biobead system, the tight polymer matrix excludes outside microbes from entering and effectively immobilizes encapsulated cells. In a TCE degrading biobead, such a system would result in several layers of bead with distinct microbial populations, each targeting a specific CAH species. Thus, a "biobead" system achieves simultaneous degradation of TCE, cDCE, and VC across a spatial volume while the "direct push" method degrades sequentially. Biobeads may also be deployed closer to the plume source, as diffusion and biodegradation can keep CAHs below inhibitory levels within the bead (**Figure 1.6**).

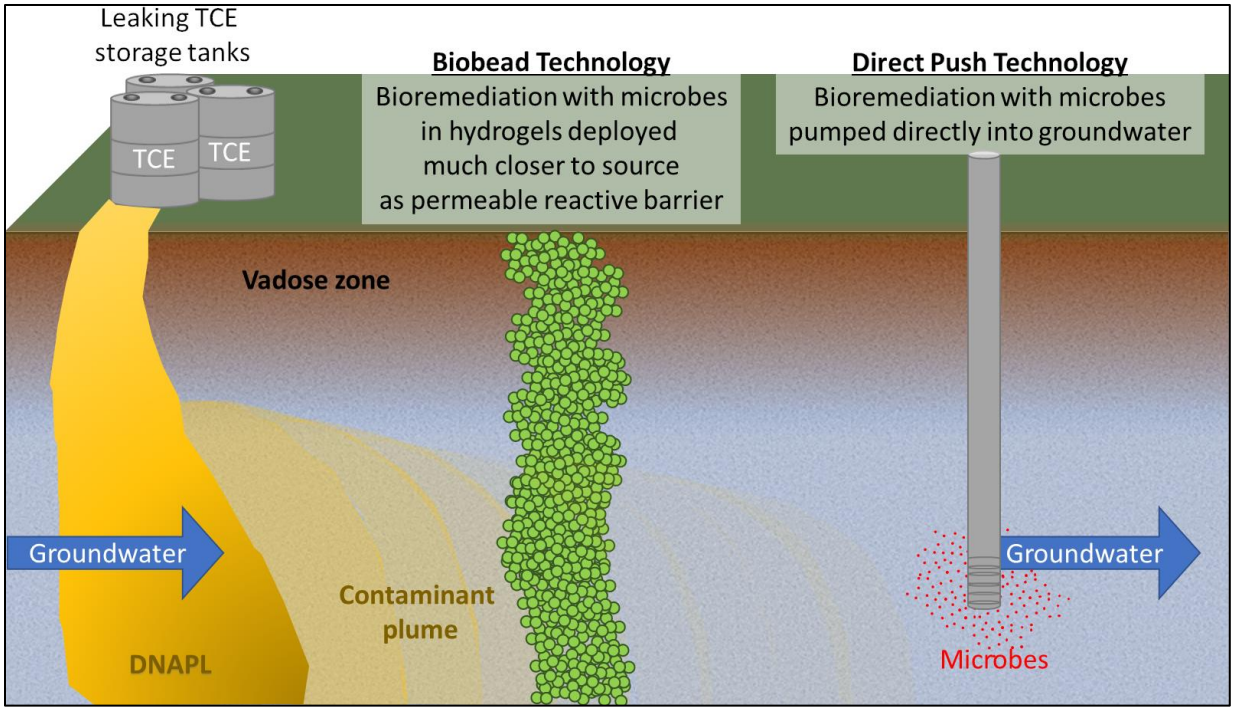

Figure 1.6: *Comparison of Direct Push Tech. (current methods) and Biobeads*

Biobeads may be deployed closer to the contaminant source plume, as the polymer matrix slows migration of CAHs, keeping concentrations low enough for cells to function. In situations where contamination is near the ground surface, a permeable reactive barrier (PBR) impregnated with biobeads may be used. Some breakdown products, including highly toxic VC will diffuse from the bead and into surrounding groundwater. A conjugated system combining biobeads and current methods (Direct Push Technologies) downstream would eliminate large amounts of TCE close to the source plume, and further degrade breakdown products as they flow through the aquifer.

Crosslinking and polymers:

Dissolved hydrophilic polymer in water forms a three-dimensional network, which continues to expand when more water is added[52]. Crosslinking between polymer chains increases mechanical strength and prevents hydrogel dissolution[53]. Crosslinking can be achieved with chemical, radioactive, or physical agents such as freezing and thawing cycles. Common chemical crosslinking agents include glutaraldehyde[53], calcium chloride[54], iron chloride[55],

boric acid[56] and bis(ß-hydroxyethyl) sulfone[52]. Ionic crosslinking is especially common with alginate membranes, as the negative charges on guluronate groups from different polymer chains bind to divalent cations[57]. Crosslinks may also form from chemical bonding between chains and chemical agents as in the case of PVA crosslinking by boric acid.

As hydrogels are often researched for biomedical applications, a crosslinking mechanism which does not involve reagents which are toxic to humans is desirable. One such mechanism is the thermo-reversible crosslinking of PVA by repeated freezing and thawing cycles. This process results in a mechanically strong hydrogel which remains insoluble at common biological temperatures, as the hydroxyl groups in PVA align and are held together by hydrogen bonding. Repeated freeze/thaw cycles cause the interacting regions to expand, resulting in both amorphous and dense, crystalline domains[58].

1.4 Diffusion Mechanisms

Diffusion is the movement of particles from areas of high to low concentration or potential. The diffusivity or diffusion coefficient for a solute through a solvent can be used to model solute migration through porous media. Movement of simple solutes in water is known as aqueous diffusion, which can be estimated using the Wilke Chang or Hayduk Laudie correlation[59]. Although hydrogels are primarily composed of water, diffusion through hydrogels is more complex[60] as solutes generally move only through the small volumes of water surrounded by polymer chains. These polymer chains pose a physical obstruction and increase the tortuosity of travel for diffusing species[61]. In certain situations (such as non-polar particles and polymers) solutes may diffuse through the polymer chains themselves, or interact/react with polymers[62]. To model the biobead system, diffusive parameters are needed for each chemical species involved.

Fickian vs Non-Fickian Flux:

The simplest type of diffusion is that in which the pseudo-steady state concentration gradient across a diffusive layer is proportional to the flux. Such a scenario is described as Fickian diffusion[63]. Flux in these systems can be easily described mathematically using Fick's first law of diffusion[64] (**Equation 1.1**).

$$J = -D\,\frac{dC}{dZ}$$

Equation 1.1: *Where J is flux in mol/area time, D is diffusion coefficient, and* $\frac{dC}{dZ}$ *is concentration gradient over distance.*

An important distinction must be made with Fick's first law regarding the $\frac{dC}{dZ}$ term. If only the interior concentration of the membrane is considered, the diffusive term (D) is called the diffusion coefficient or diffusivity. If the concentration gradient is measured by the concentration of the aqueous phase on each side of the membrane (exterior), the diffusive term is the effective diffusivity or D_e[59,65]. D can be considered the diffusivity *within* the membrane, while D_e is that *through* the membrane,[65] including solute adsorption and desorption (**Figure 1.7**).

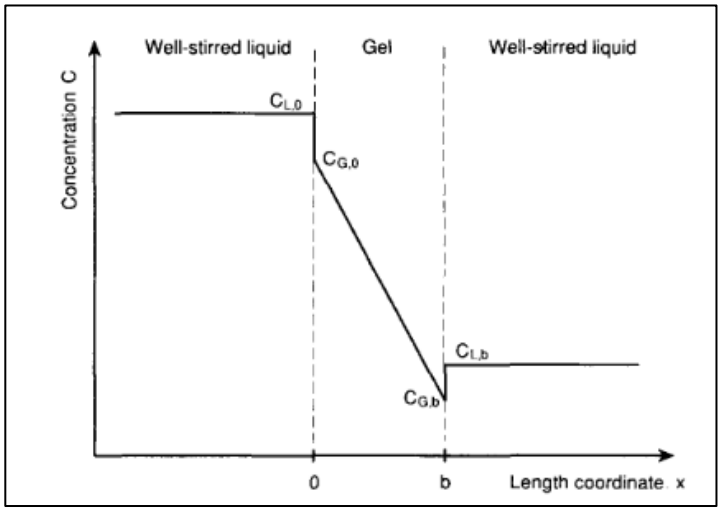

Figure 1.7: *D_e is based on dC_L, while D is based on dC_G. Figure is from 'Diffusion in Gels Containing Immobilized Cells – A Critical Review' by Westrin and Axelsson*

Effective diffusivity incorporates partitioning effects, interactions, and wall collisions within the system. Biochemical engineers prefer the D_e term, as measurements are simpler and directly apply to systems where solutes diffuse into or out of a membrane[65]. Effective diffusivity has also been shown to change with membrane cell concentration while diffusivity may not[57].

Systems in which the diffusive layer experiences significant shrinking or swelling may not have a linear relationship between flux and concentration gradient; these systems are simply called non-Fickian[66]. Diffusion through heterogeneous media[67] and systems exhibiting interaction or reaction may also result in non-Fickian behavior. To accurately model bioremediation of CAHs in cell-encapsulating hydrogels, the diffusion coefficient of each chemical species through the hydrogel must be estimated. In diffusion tests, TCE, cDCE, and VC exhibit Fickian behavior while proton adsorption in membranes causes a noticeable lag period (no acid breakthrough into sink) prior to Fickian flux.

Aqueous Diffusion:

Aqueous diffusion (D_{aq}) is the molecular transport of solutes in water or other solvents without convection or applied potential. Aqueous diffusion is Fickian by definition, depending only on hydrodynamic forces and interactions between solute and solvent[68]. Stokes and Einstein modelled solutes in water as solid spheres which did not interact with solvent. Their model assumes solute molecules are larger than solvent[69], and that movement is a result of osmotic pressure differences (given by Van't Hoff) and is resisted by hydrodynamic drag (Stoke's Law). Both Hayduk and Laudie[70] (**Equation 1.2)** and Wilke and Chang[71] (**Equation 1.3**) developed their own correlations which relate D_{aq} to parameters such as solvent viscosity, temperature, and solute size. Estimates using such correlations are generally within 90% of experimental values and for simple solutes may even be substituted for D_e in hydrogels[72].

$$D_{AB} = \frac{13.26x10^{-5}}{n_w^{1.14} V_B^{0.589}}$$

Equation 1.2: *Hayduk Laudie Equation, where D_{AB} is diffusivity of solute A in water (cm^2/sec), n is water viscosity at a specified temperature in cP, and V_B is solute molar volume*

$$D_{AB} = \frac{7.4x10^{-8}(\emptyset_B M_B)^{\frac{1}{2}} T}{\mu_B V_A^{0.6}}$$

Equation 1.3: *Wilke Chang Equation, where D_{AB} is diffusivity of solute A in solvent B (cm^2/sec), $\emptyset_B$ is an association parameter, M_B is molecular weight of solvent, T is temperature in K, μ_B is solvent viscosity, and V_A is molecular volume ($cm^3/mole$)*

Pore Size, Charge, and Other Effects:

Diffusion through hydrogels includes the hydrodynamic effects discussed in aqueous diffusion with additional restrictions on solute movement caused by physical obstructions. Hydrogels are three dimensional matrixes of polymer and entrapped water. Generally, solutes are assumed to have negligible diffusivity in the organic polymer phase and only travel through the entrapped water packets or "pores". Water can either be "free" or "freezable", having the properties of liquid water or "bound" to the polymer[73,74]. As the volume fraction of these pores increases, the effective diffusivity of chemical species approaches the free aqueous diffusivity (D_{aq}), where diffusing molecules are only impeded by their size and solvent interactions[60]. In simple hydrogel systems with negligible interaction, diffusion may be predicted by considerations of the polymer volume fraction, physical obstruction, and hydrodynamic drag[75].

Simple models which describe diffusing solutes as hard spheres in rigid (low mobility) polymer systems are common in the literature[76,60,77], but always encounter limitations as the solute size and volume fraction of polymer increase. In practice, these models are not reliable predictors of most diffusing systems as physical, chemical, geometric, and electrostatic effects of both solute and polymer influence diffusivity. The mobility of polymer fibers is another important factor in diffusion[60]. Rigid polymer fibers constitute heterogeneous hydrogels, while homogenous gels have mobile polymer fibers and increase solute diffusivity. Crosslinking density, whereby polymer chains are interconnected to form the 3D hydrogel, decreases pore size and promotes interaction with solute. Even the penetrant's shape can influence diffusion, as smaller (lower molecular radii) isomers of xylene show decreased diffusivity in polyethylene polymers[78]. Finally, some solutes preferentially bind to hydrogel polymers, allowing little or no efflux until the binding sites are saturated[79,80].

A common technique in aqueous diffusion measurements was the use of hydrogels to approximate dilute solute diffusion in water[81]. For small solutes in non-adsorbing systems, it was common to observe only a 5-10% difference between D_{aq} and diffusivity in a hydrogel. A modified version of Fick's first law proposed by Westrin and Axelsson[65] assumed that only physical obstruction of the polymer slowed solute movement (**Equation 1.4**).

$$J = -D\,(1 - øß)\,\frac{dC}{dZ}$$

Equation 1.4: *Where D is aqueous diffusivity, ß is a constant related to obstruction shape and orientation, and ø is the volume fraction of the obstruction*

Aqueous diffusivity values for many solutes have been estimated, either using modified high performance liquid chromatography[82] or a theoretical model such as the Wilke Chang correlation. However as previously stated, **Equation 1.3** does not apply for adsorbing systems or those with solute/solvent interactions. Electrochemical interactions, charge effects and even the shape of solutes profoundly affect flux, sometimes causing great deviation from theoretical models[83]. The author is not aware of any model which accurately predicts hydrogel diffusivity based on solute size, shape, interactions and charge. Experimental analysis is the only reliable method to estimate diffusion coefficients especially for solutes with potential for interaction or reaction.

Diffusion coefficients for TCE, cDCE, VC, and protons are measured using the diaphragm cell method with a chemically crosslinked 10%PVA 2%SA membrane as the diaphragm. Additional tests for protons are run for PVA, PVA/chitosan, and partially phosphorylated PVA membranes. To elucidate the effects of charge on effective diffusivity, three compounds of differing charge and the same molecular weight (194 g/mol) are also tested within 10% PVA 2% SA membranes: caffeine, saccharine, and a cinnamaldehyde derivative: (E)-*N*,*N*,*N*-trimethyl-3-prop-2-en-1-aminium iodide, which will be referred to simply as cinnamon.

1.5 Diaphragm Cell Measurements:

The diaphragm cell method is employed to estimate the effective diffusivity or effective diffusion coefficient. Unlike the simple diffusion coefficient, this value reflects more than diffusivity due to porosity and tortuosity, and is influenced by polymer mobility, electrochemical effects, chemical interactions, and surface transport effects[84,85]. D may be considered as the diffusivity *in* the system while D_e is *through* the system.

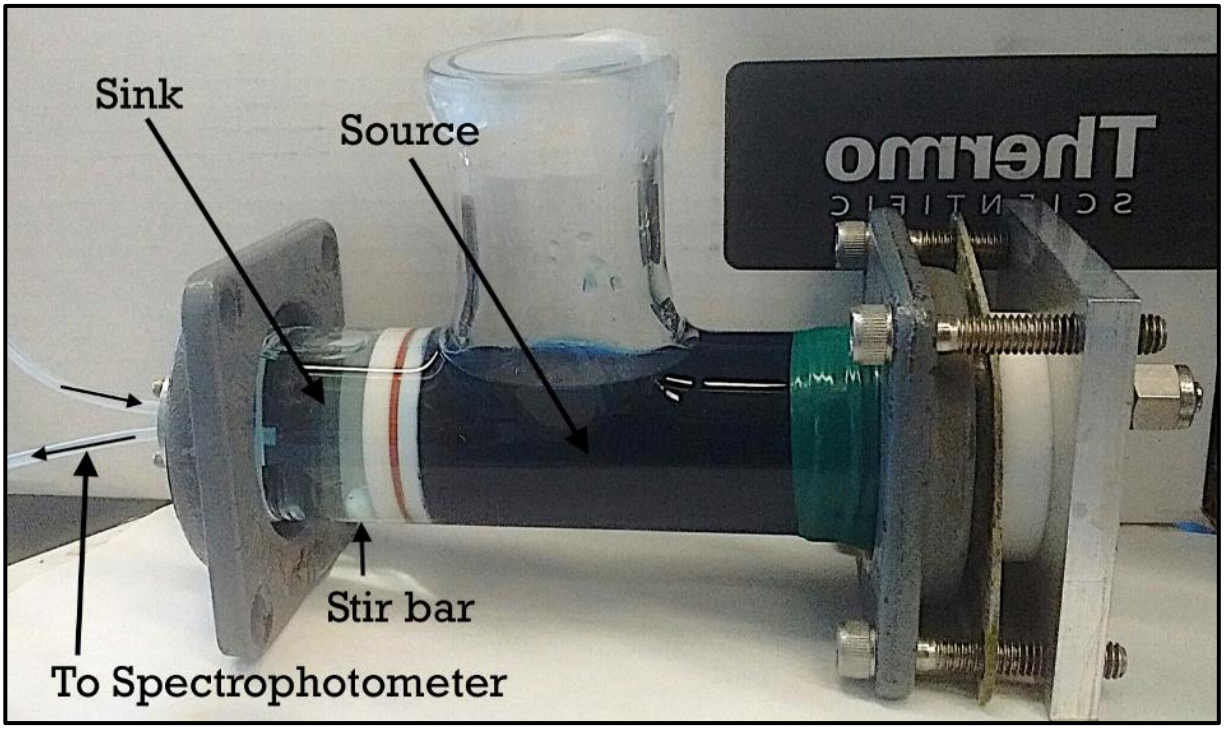

Figure 1.8: *A diaphragm cell – note that both sink and source are stirred*

The diaphragm 'cell' is composed of two compartments separated by a diaphragm which is permeable to the component of interest (**Figure 1.8**). One side (termed the "source") of the cell contains a relatively high concentration of the diffusing species dissolved in a solvent. The other ("sink") side initially contains only the solvent. Both source and sink are stirred to maintain uniform concentration and minimize mass transfer effects at the interface of solvent and diaphragm. For most systems, flux into the sink is sufficiently low and the source concentration sufficiently high to assume constant source concentration. Concentration of the solute in the sink is measured with time, and flux through the membrane is calculated using

Equation 1.5. Sink concentration is continuously measured by pumping solution through a spectrophotometer blanked with pure solvent.

$$J = \frac{C_{t1} - C_{t0}}{t\ Z}$$

Equation 1.5: *Where J is flux in* $\frac{mol}{Area*Time}$, C_{t0} *is initial sink concentration,* C_{t1} *is concentration at a later time, t is the time between measurements, and Z is membrane thickness*

Equation 1.5 can be substituted into **Equation 1.1**, and the only unknowns remaining are effective diffusivity and concentration gradient within the membrane ($\frac{dC}{dZ}$). This value can be estimated by assuming negligible sink concentration compared to source concentration. The result is simply $\frac{C_{source}}{Z}$. This final assumption results in **Equation 1.6**.

$$D_e = \frac{(Z)\frac{dC}{dt}(V_{sink})}{(Area)\ C_{source}}$$

Equation 1.6: *Where* $\frac{dC}{dt}$ *is in (M/sec),* V_{sink} *is sink Volume in mL and Area is cross sectional membrane area in* cm^2

1.6 Modelling and Prediction:

The purpose of estimating CAH D_e is to model solute transport within hydrogel membranes and pair this with a kinetic model to determine optimal biobead size and cell density. As the KB-1® microbial consortium uses CAHs as terminal electron acceptors, the cells need a near-constant supply to survive. Substrate supply by flux in and waste product removal by efflux are major concerns to address when maintaining a productive immobilized consortium[25]. Encapsulated cells must be constantly supplied with nutrients, as they are unable to move to more favorable microenvironments. By modelling transport using Fick's first law and effective diffusion coefficients coupled with kinetic degradation parameters, a proper bead size and cell concentration for optimal TCE biodegradation and minimal VC release is estimated.

The model used in this study is a non-steady state, finite difference method approach with CAH degradation parameters obtained by Haest et al.[30]. The kinetic study used a batch system of non-encapsulated cells in broth, and rate constants may be different for immobilized cells. However, to model the general optimal size and cell concentration this study assumes the kinetic parameters are identical. Further discussion on the biobead degradation model is found in Chapter 3.

Chapter 2: Charge Effects on Diffusion

2.1 Charged Particle Diffusion

Diffusion of solutes through hydrogel membranes is affected by physical obstruction posed by the polymer chains, chemical reactions or interactions with the polymer, and electrostatic interactions between the polymer and solute[86]. Generally, organic solutes do not undergo appreciable chemical reactions with the polymer, and physical limitations from solute size and effective pore radius of the gel are the primary influencing factors. However, electrostatic interactions can greatly influence diffusion, as dipole moments and charge of solute can cause substantial interactions[87]. Even solute shape can significantly change effective diffusion coefficients for different solute isomers in polymer membranes[78].

To elucidate the effects of charge on diffusive properties, effective diffusivity can be estimated in a highly ionic system. Comparing similarly sized particle diffusion through identical membrane types allows determination of the approximate effect of different charges. Neutral compounds can also be tested to create a baseline where only physical obstruction effects are present. The solutes used in this study are caffeine (neutral), saccharine (negative), and a derivative of cinnamaldehyde, (E)-*N*,*N*,*N*-trimethyl-3-prop-2-en-1-aminium iodide, (referred to as "cinnamon") (positive) as each has a comparable molecular weight (176-194 g/mol). In addition, diffusion coefficients for sodium metanil yellow (negative, 376.4 g/mol) and methylene blue (positive, 319.85 g/mol) are measured.

Diffusing Solute	Molecular Weight (g/mol)	Charge
Caffeine	194.2	0
Saccharin	183.2	-1
Cinnamon	176.3	+1
Methylene blue	319.9	+1
Metanil yellow	376.4	-1
Hydronium ion	19.0	+1

Table 2.1: Solute molecular weights and charge

Materials and Methods:

The polymer hydrogel used to determine diffusion rates is made as follows: 10g of PVA (MW: 146-186kg/mol from Sigma Aldrich) and 2g SA (Sigma Aldrich) are placed in a beaker with 100mL DI water. The mixture is covered and submerged in a water bath at 80^{o}C to provide uniform heating. The mixture is stirred at 550 RPM with a one-inch Teflon coated stir bar and a smaller stir bar. The smaller stir bar is propelled by the larger one around the edge of the beaker, mixing the system well. After approximately one hour the polymers are dissolved and the solution reaches a visibly uniform consistency. Membranes composed of only PVA and water are also prepared, and other polymers such as chitosan may be substituted for alginate.

The molten gel is then cooled in the water bath to 40^{o}C and slowly poured into the top of circular stainless steel, PVC, or Teflon® molds with care taken to not entrap air bubbles. Filled pucks are then placed in the freezer at -20^{o}C for at least one hour to solidify with a weight on top to prevent membrane leakage. Frozen membranes are then immersed in a beaker of crosslinking solution (saturated boric acid, 2% (w/v) $CaCl_2$). The beaker is then placed in the refrigerator at 4^{o}C for 4 ½ hours which allows the membranes to slowly thaw and simultaneously crosslink while maintaining a flat surface. After 4 ½ hours, the crosslinking solution is decanted and membranes well rinsed with deionized water. The membranes are then placed in DI water to equilibrate and swell for at least one hour, at which point thickness is measured and they are placed in a diffusion cell. Membranes continue to swell for several days in deionized water, increasing in volume by nearly 30%. However the effects of swelling on effective diffusivity measurements are negligible.

An alternative to the chemical crosslinker is a physical crosslink via repeated cycles of freezing and thawing. After the first freeze at -20^{o}C, the membranes are removed to room temperature and allowed to thaw for one hour. At this point, they are frozen again for one hour. The process is repeated for five total freezes and thaws, and the membranes are allowed to swell in deionized water for at least one hour. Five measurements of membrane thickness are taken using calipers prior to experimentation, providing an average value for calculations. The membrane is then inserted into the diaphragm cell.

A leak check is performed for ten minutes by filling the source compartment with water and monitoring for water seepage around the membrane sides. Then the source is emptied and the sink is also leak checked. Finally, solute solution is added to the source compartment and pure solvent to the sink. Both sides are mixed by stir bars after placing the diaphragm cell on a stir plate, and the sink volume is pumped through a ThermoFisher Evolution 60S UV-Vis Spectrophotometer. Absorbance readings are taken every 5-10 minutes at a wavelength predetermined by calibrations.

Statistical Analysis:

Three independent data points for solute diffusivity are collected at a minimum. The mean value for D_e estimates is reflected by each data point. Statistical analysis is conducted using one-way analysis of variance (ANOVA), and results were considered as statistically significant at 95% confidence interval ($p < 0.05$). Statistical analysis is conducted using Origin Lab b9.5.5409 (OriginLab Corporation, MA).

Neutral solutes and dipoles:

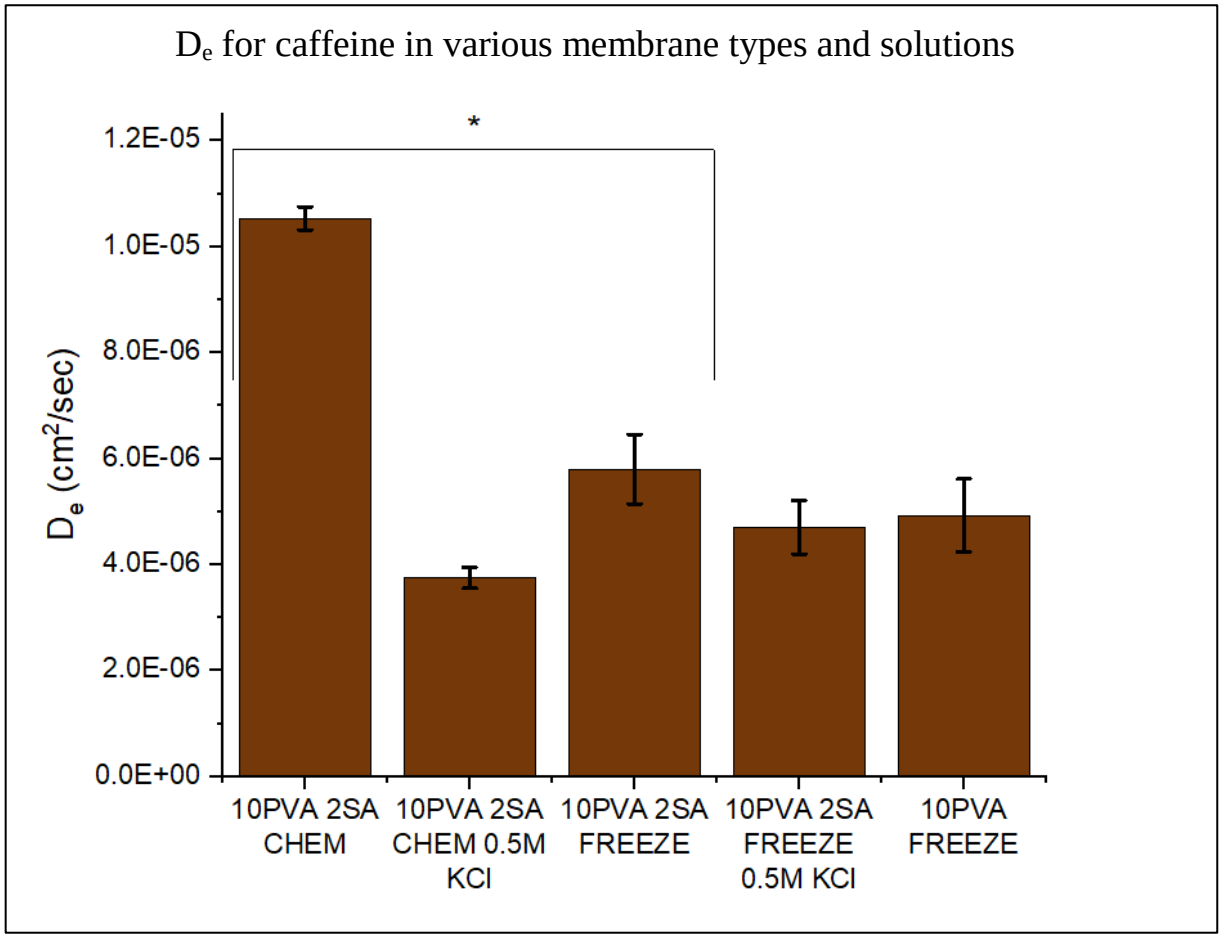

Figure 2.1: *De for caffeine in various membranes/systems '10PVA 2SA' indicates 10% PVA 2% SA membrane. 'FREEZE' indicates physical and 'CHEM' chemical crosslink. An asterisk denotes statistically different values.*

Caffeine is a nearly ideal solute for measuring diffusion, having a unique absorbance spectrum, compact shape, and no formal charge. The standard error associated with caffeine diffusivity measurements is often quite low (< 5%). Initially, caffeine diffusion was assumed to only be influenced by physical obstruction of polymer chains, however, ionic solutions (0.5M KCl) cause a significant drop on effective diffusivity (**Figure 2.1**). This indicates that the dipole moment within caffeine molecules may be affected by ionic strength of solution. Initially, it was suspected that caffeine was forming complexes with chlorine ions from the KCl. The absorbance spectrum of natural organic matter (NOM) has been known to change in chlorine

or salt solutions[74,88]. However, spectrophotometric analysis of caffeine and KCl solutions shows no significant change in absorbance, confirming the measured D_e values.

A study on solute release from non-fouling hydrogels shows that caffeine release from gels is not influenced by ionic strength of surrounding solution[42]. However, these tests only studied release from hydrogels, and did not include adsorption effects of caffeine from solution to membrane. Also, the membranes were zwitterionic, possessing both positive and negative charges which were largely shielded by disodium phosphate ions. As functional groups on caffeine are electronegative, the solute may experience greater electrostatic repulsion in PVA/SA membranes, which possess negatively charged carboxylate groups but no positive charges. This repulsion is limited by cation shielding in highly ionic solutions, possibly causing the large drop in D_e. This is an example of the risks associated with assuming diffusion is only influenced by physical size effects.

Effective diffusivity of caffeine was also heavily influenced by crosslinking type. Chemically crosslinked PVA/SA membranes allowed roughly twice the flux of caffeine compared to physically crosslinked (Freeze/Thaw) membranes. It is hypothesized that the difference is mainly caused by pore size restrictions and lower polymer mobility in physically crosslinked gels. A similar drop in D_e is observed using 10% PVA Freeze/Thawed membranes which possess no formal charge, and 10% PVA 2%SA membranes physically crosslinked in ionic solution. It is therefore concluded that physical crosslinking restricts effective pore size in hydrogels without having a profound effect on the electrochemical characteristics of the membrane. Physically crosslinked PVA hydrogels form dense, hydrogen bonded polymer regions[58]. Crosslinked polymer chains may be held further apart by crosslinking agents, increasing the hydrogel effective pore size.

Positive solutes:

PVA/SA membranes have negatively charged carboxylate groups which electrostatically attract positively charged solutes, potentially slowing diffusion. This causes positively charged methylene blue to have a D_e similar to larger, negatively charged metanil yellow. This

attractive electrostatic force is also evidenced by the steep concentration gradient of methylene blue within the PVA/SA membranes, as seen in **Figure 2.2**. Additionally, the membranes are significantly weaker on the source side after diffusion indicating that methylene blue may be substituting for calcium chloride crosslinker due to its positive charge. The monovalent dye is incapable of linking two alginate chains, decreasing the crosslinking density and mechanical strength.

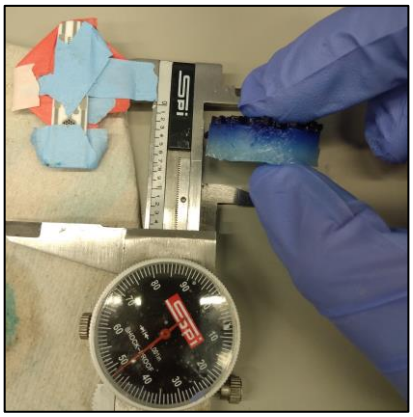

Figure 2.2: *A PVA/SA membrane (chemically crosslinked) after diffusion of methylene blue.*

The effective diffusivity of methylene blue increases by 31% in highly ionic solutions, as the carboxylate groups in SA are shielded by the potassium ions in 0.5 M KCl (**Figure 2.3**). This increase was also observed with positively charged solutes such as protons. The increase in D_e using ionic solutions is not repeated with positively charged cinnamon (MW: 176g/mol), as the D_e decreases by more than 50%. This may be due to complexation between salts and solute giving an inaccurate spectrophotometer reading.

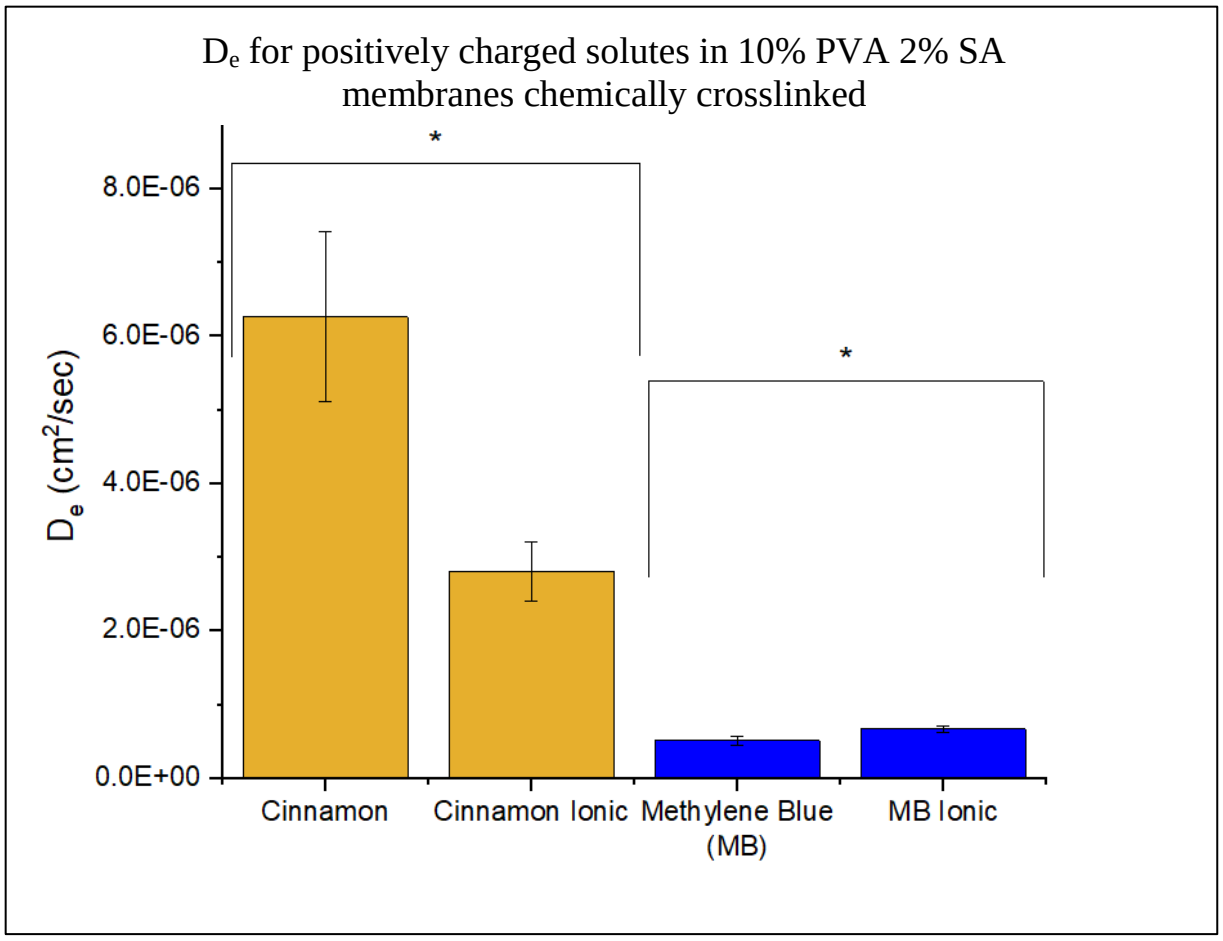

Figure 2.3: *De for various organic solutes in 10% PVA 2% SA Chemically Crosslinked with deionized or ionic solvent*

Hydronium ions are tested as a charged solute with a unique diffusive mechanism termed "proton hopping"[89] or the Grotthuss mechanism[90]. Effects of ionic solution on diffusion are more pronounced than either cinnamon or methylene blue. When charge effects are shielded by KCl solutions, hydronium ions display a two-fold increase in flux compared to deionized solutions (**Figure 2.4**). This trend is repeatable for membranes composed of only PVA and water, which have no formal charge. We therefore conclude that ions in solution can shield dipole moments, hydrogen bonding, and charge for simple solutes[91]. Ionic disruption of hydrogen bonding between water and PVA increases the number of water molecules available for proton hopping.

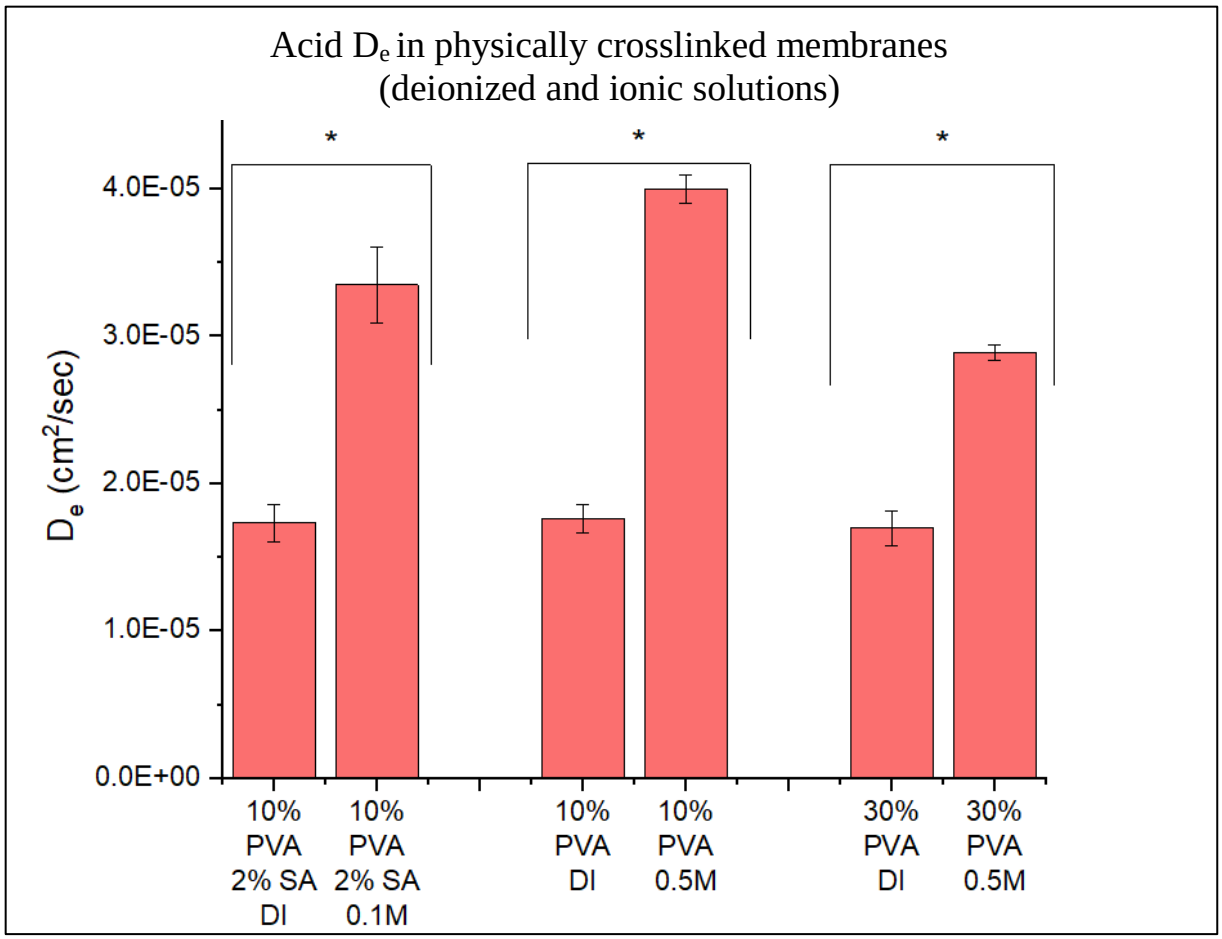

Figure 2.4: *Effective Diffusivity (cm^2/s) of hydronium ions in deionized (DI) and ionic (molarity shown) systems. Membranes are physically crosslinked. An asterisk denotes statistical difference.*

Negatively charged solutes:

Saccharin (MW: 183.2 g/mole) and metanil yellow (376.4 g/mole) are used as negative solutes in the diaphragm cell. In chemically crosslinked 10% PVA 2% SA membranes, saccharin has a similar D_e to caffeine, and a similar drop in diffusivity in an ionic solution (0.5M KCl). Metanil yellow has a very low D_e due to its large hydrodynamic radius. Metanil yellow has shown a decrease in release rate from hydrogel membranes in ionic solutions as the repulsive force between negative charges in solute and polymer are shielded[92]. However, in this study no significant difference in D_e was observed for metanil yellow in deionized and ionic solutions. Flux through diffusive membranes is similar to smaller methylene blue, although

the visible concentration gradient is less pronounced, likely due to the aforementioned repulsion effects (**Figure 2.5**).

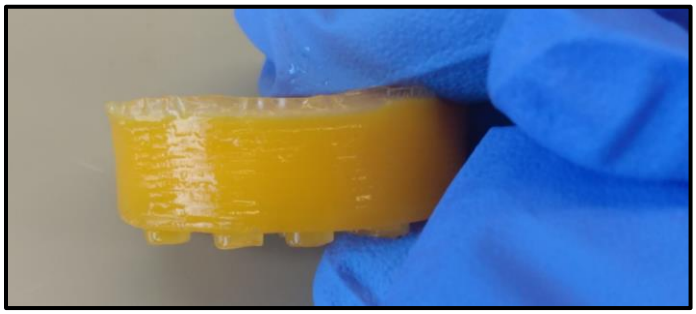

Figure 2.5: *A 10% PVA 2%SA membrane (chemically crosslinked) after metanil yellow diffusion*

Saccharin diffusivity is similar to caffeine in chemically crosslinked membranes, and D_e drops sharply in ionic solutions. This drop is likely due to a decrease in repulsive force between solute and polymer caused by shielding of negatively charged carboxylate sites in alginate. No statistically significant difference was found between D_e values for cinnamon, saccharin, and caffeine in chemically crosslinked 10% PVA 2% SA membranes within deionized solutions.

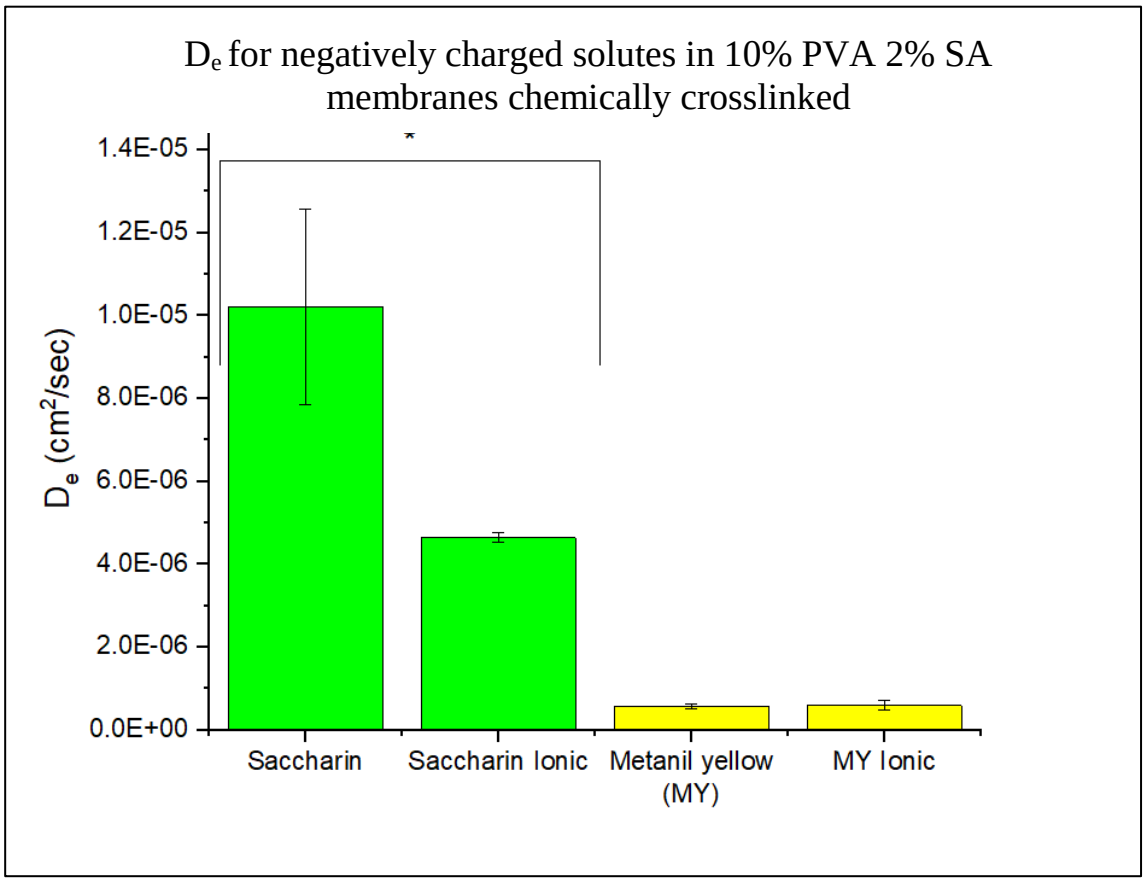

Figure 2.6: *Negative solute diffusivity in deionized and ionic (0.5 M KCl) solutions with chemically crosslinked 10% PVA 2% SA membranes. An asterisk denotes statistical difference.*

As the stated goal of charged solute research is to develop a correlation relating charge, solute size, and effective diffusivity much more work is needed. Effective diffusivity can be greatly influenced by charge and polymer chain mobility. Obviously a simple correlation between polymer volume fraction and D_e is not sufficient for reliable predictions, especially in environments where solvent properties may change[87]. Furthermore the effect of charge may diminish as the solute size increases, and the physical obstruction posed by polymer chains grows. Large molecules may also shield their own charge by nearby functional groups or steric effects.

2.2: Proton Diffusion

Adsorption of Protons:

Diffusion of protons through PVA membranes shows a considerable lag period of approximately 5 hours. This period extends to ~10 hours for PVA/SA membranes and ~60 hours for PVA/chitosan membranes (**Figure 2.7**). For a small solute, only electrostatic and chemical effects could cause such a lag. During this period, it is hypothesized that hydronium ions saturate the PVA/SA polymer, as the pKa of carboxylate sites in alginate is 3.24[93]. Chitosan membranes have a longer lag time as the amine group has a pKa of around 6 depending on degree of deacetylation[94]. Once all the carboxylate sites are fully protonated, linear flux of protons ensues. In the first few hours of lag period the pH of solution in both sink and source increase slightly, as acid protonates the polymer. Hydronium ions may also substitute for calcium ions in chemically crosslinked membranes, although no concomitant decrease in mechanical strength is observed in PVA/SA gels. Many data sets were needed to determine diffusivity of protons for a variety of membranes, and this need for a large quantity of experiments lead to the development of the GellipHish.

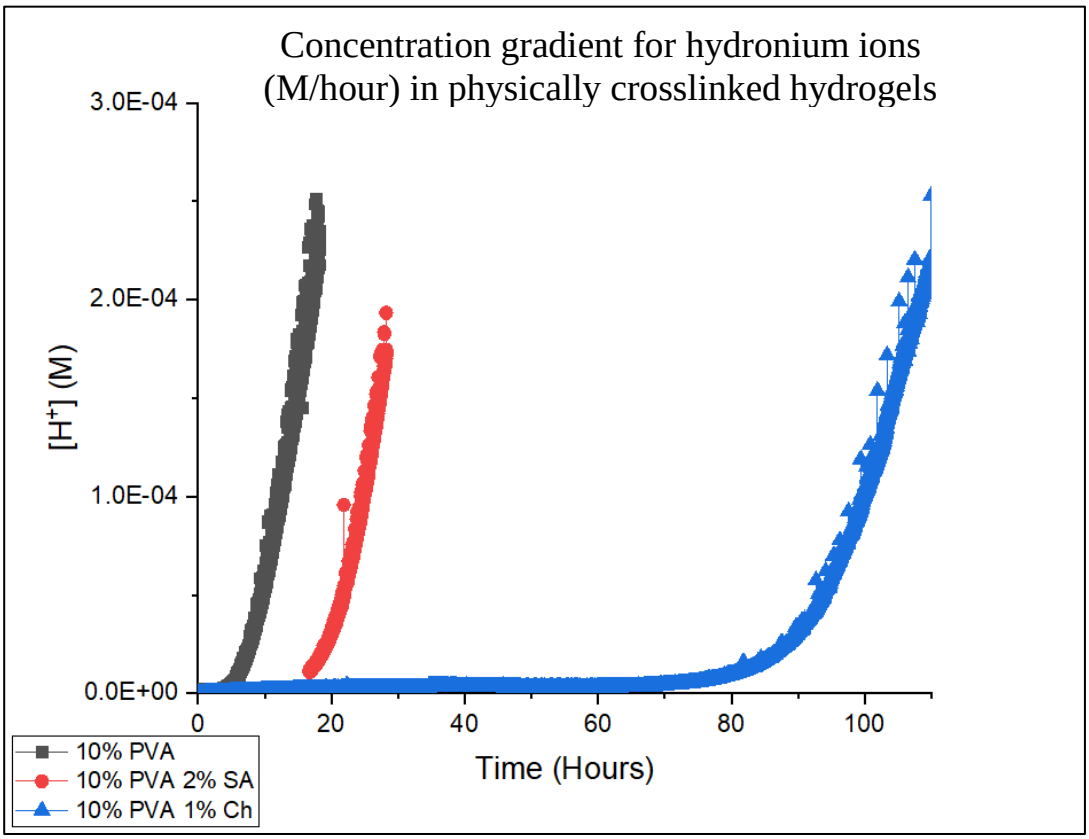

Figure 2.7: *Concentration gradient of hydronium ions in sink showing lag times. 'Ch' denotes chitosan.*

GellipHish Diffusion Measurements:

Proton diffusion is most accurately measured by a pH probe. Initial experiments estimated proton flux using pH indicator dye and spectroscopic analysis. This approach was abandoned as the buffered pH indicator solution may result in an overestimation of free proton concentration and concentration of protonated buffering species could not be measured. To obtain large quantities of accurate proton diffusion data, a multiplexed diffusion cell with integrated pH probes (Oakton double-junction gel probes: 35816-77) was constructed. This custom diffusion cell is called the 'GellipHish'.

The GellipHish is composed of four PVC tubes with 1 1/2" nominal OD and a PVC cross coupling. Three of the tubes are diffusion sinks, fitted with PVC membrane molds or 'pucks'. The fourth tube is considerably longer and serves as the proton source, the pH of which is measured throughout the run. A large volume of source maintains a near-constant proton

concentration (<10% drop). The final measured pH value for the source is used in diffusion calculations, as the initial value would include hydronium ions which have not yet adsorbed to the membrane. Both sinks and source are stirred with magnetic Teflon coated stir bars. The pH probes are connected to a Raspberry Pi and monitor pH over a 15-53 hour period, taking readings every 32 seconds. A single GellipHish run produces a triplicate data set with identical source conditions for each membrane. Multiple GellipHish are now employed in undergraduate labs in the University of Idaho Chemistry Dept. to serve as both educational and data acquisition devices.

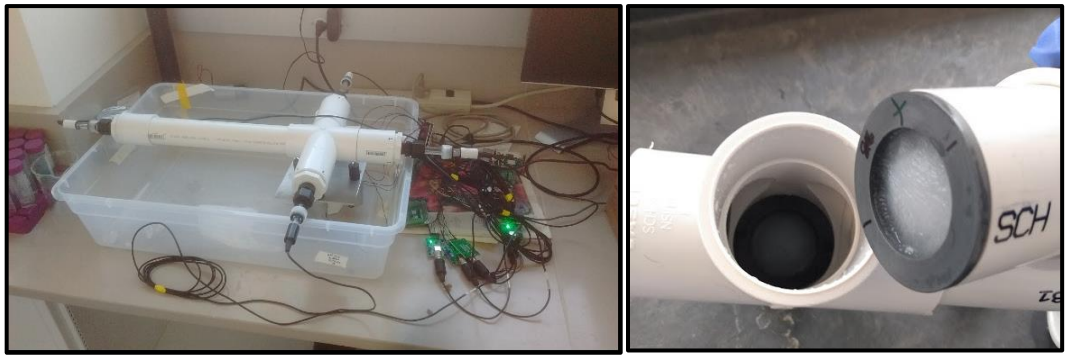

Figure 2.8: *A fully and partially assembled GellipHish*

GellipHish Materials and Methods:

There are two connected systems comprising a GellipHish: a triple-sink diaphragm cell made of Sch. 40 1 ½" PVC pipe with couplings and a cross coupling, and Raspberry Pi integrated with 4 to 16 Oakton pH probes. Each probe connects to a BNC connector, which obtains power from and delivers signal to a breadboard. The breadboard draws power from the raspberry pi, or from a 5V external power supply. This power supply can also power a series of 5V motors, which are fitted with Neodymium magnets and serve as stirrers. Alternatively the cross coupling of the GellipHish can be centered on a regular laboratory stir plate, which results in vigorous stirring for both source and sinks.

The Raspberry pi runs on a version of Python; code was provided by Dr. Macpherson and Thomas Christensen II. Membranes are prepared by the same methods used for CAH diffusion and fitted into the 1 ½" diameter (2 ¾" long) PVC pipes which serve as sinks. A 1 ½" reduced

bushing (Lasco D2466) with a coupling is fitted to the other sink end. Chemically crosslinked membranes shrink within the PVC GellipHish molds allowing convective rather than diffusive flux. Diffusive measurements with these membranes are conducted with Teflon molds in a glass diffusion cell normally used for CAH diffusion with a custom pH probe adapter.

Diffusion of Protons:

Biodegradation of CAHs produces both a chloride and hydronium ion with each dechlorinating step. While diffusivity of CAHs in aqueous and artificial biofilm environments may be roughly estimated by considerations of solute size and polymer volume fraction, transport of hydronium ions is more complex as it occurs often at the subatomic level[89]. Such movement of protons without physical diffusion of either oxygen or hydrogen is called "proton hopping" or the Grotthuss mechanism. This mechanism results in a four-fold increase in aqueous diffusivity of hydronium compared to the similarly sized sodium cation[95].

Diffusion of protons in hydrogels, like diffusion of CAHs is influenced by size considerations (including volume fraction of polymer), chemical effects, and electrostatic interactions. Protons are assumed to not diffuse through the physical polymer chains and instead tunnel between water molecules and hydrogen bonded clusters of water namely H_5O_2, the Zundel cation and H_9O_4, the Eigen cation. These temporary molecular clusters form due to increased hydrogen bonding of water around the hydronium ion. A free proton is transferred within the cluster after a hydrogen bond in the second solvation shell breaks, decreasing the distance between adjacent oxygens (see **Figure 2.9**). These clusters of water and hydronium form and break on the femtosecond scale, shuttling charge much faster than physical diffusion alone.

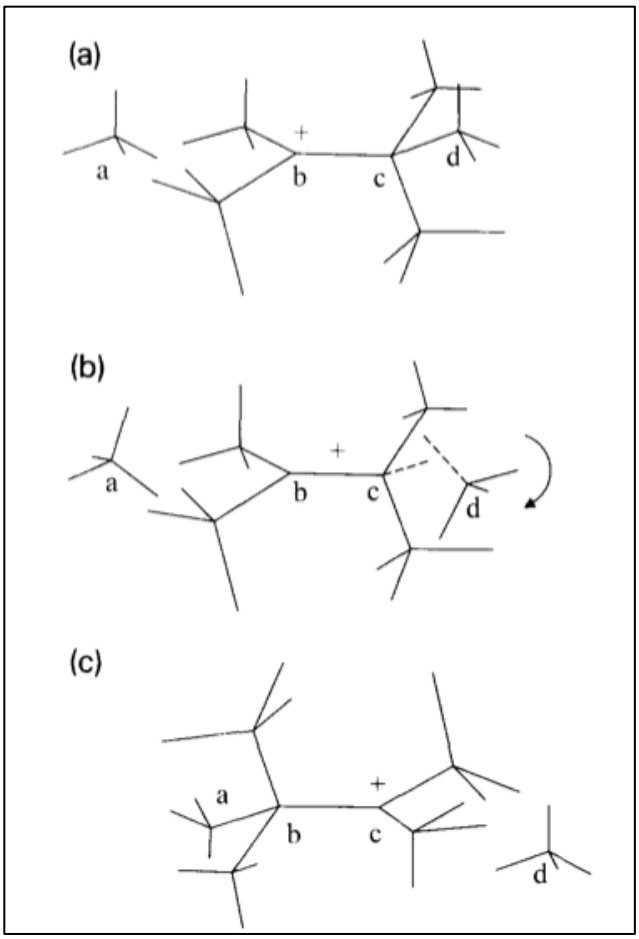

Figure 2.9: *The Grotthuss mechanism where intersections represent O and ends represent H*[90].

For physically crosslinked PVA membranes, a linear relationship is found between polymer volume fraction and diffusivity of sodium and water[74]. Thus in an uncharged PVA polymer, electrostatic interactions are minimized and obstruction effects limit diffusivity. However, volume fraction of polymer in hydrogels appears to have negligible effect on effective proton diffusivity. As seen in **Figure 2.10**, no statistically significant difference ($p = 0.4$) in proton D_e is observed with variations in PVA concentration for F/T membranes. Inclusion of partially phosphorylated PVA also has negligible influence on D_e. The highest PVA volume fraction tested was 30% (30g PVA in 100mL water), using a lower molecular weight polymer (31 kDa). It is possible that diffusivity changes caused by lower molecular weight are offset by increased polymer volume fraction in this case.

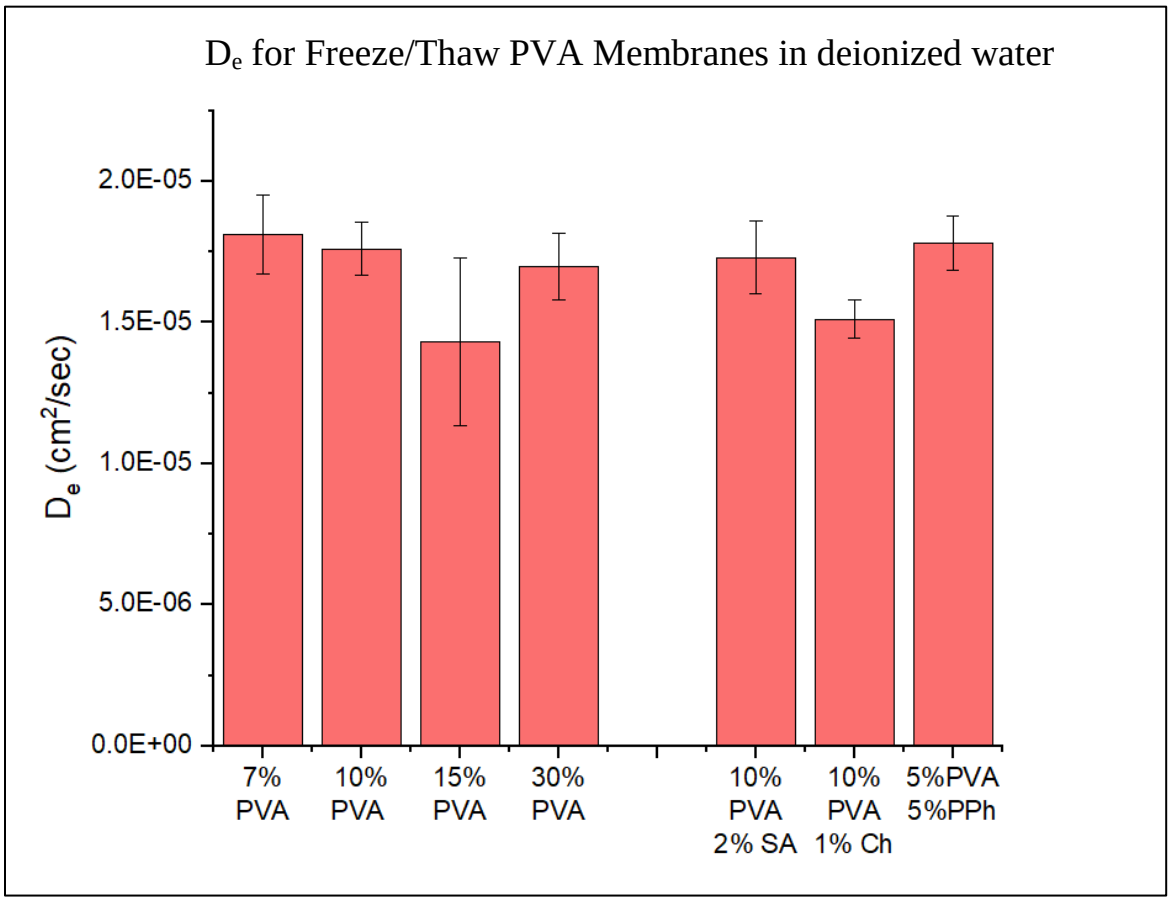

Figure 2.10: Effective diffusivities for acid in physically crosslinked membranes. *7-15% PVA was 146-186 kDa while 30% PVA was 31-51 kDa. Ch is chitosan, PPh is partially phosphorylated PVA. Membranes were frozen (-20°C, 1hr) and thawed (room temp, 1hr) five times*

Effect of Chitosan on Proton Diffusion:

The lag period for PVA/SA membranes is considerable as the ~1cm thick hydrogels can block acid flow from a pH 2.3 source to a neutral sink for up to 20 hours. This high capacity for proton adsorption is useful in maintaining neutral pH within CAH degrading biobeads, where acid is continually being generated. An even more promising polymer for proton adsorption is chitosan, where the lag period may extend for more than 48 hours.

Chitosan is a linear polymer found in nature in the cell walls of certain fungi[94]. It is produced industrially by acetylation of chitin, a polymer present in the exoskeletons of shellfish. Chemically, chitosan is a repeating chain of units of D-glucosamine and *N*-acetyl-D-

glucosamine which are connected by glycosidic ß bonds. The pKa of chitosan is about 6.5, though it depends to some extent on the degree of acetylation. The primary amine in D-glucosamine can be protonated, therefore chitosan is considered a polycation[96] and serves as a buffering agent in acidic solutions. In a laboratory test, we find that 1.0 g of chitosan powder raises the pH of 500mL of a hydrochloric acid/water mixture from 2.35 to 4.31. More than 99% of free hydronium ions are adsorbed by the chitosan in this solution.

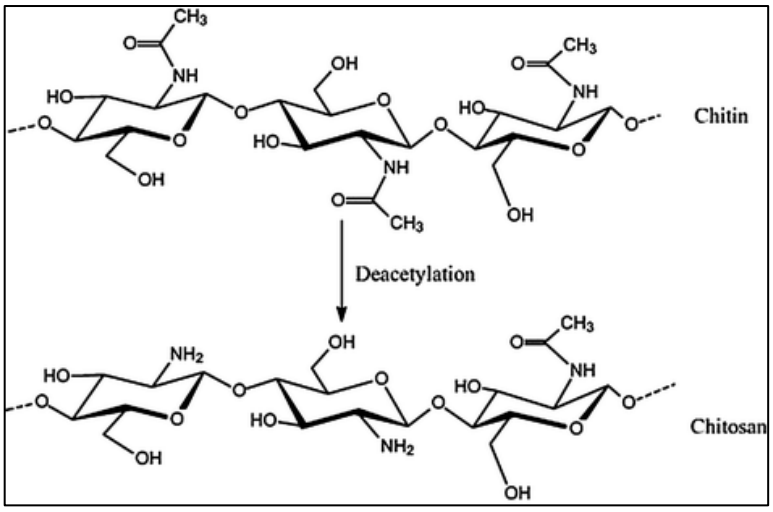

Figure 2.11: *Molecular structure of chitosan and chitin*[97]

Chitosan is insoluble in water and alkaline solutions, though it does achieve solubility below pH 6.3. It has seen use in wastewater treatment[98], cell encapsulation[99], medical supplements[100], and as a clarifying agent for brewing[101]. Diffusion of hydronium was effectively blocked for over 48 hours by freeze/thawed (F/T) 10% PVA 1% chitosan membranes, more than 20 hours longer than any other membrane without chitosan. The ability to buffer near the pH range of neutrophils makes chitosan a very intriguing polymer for cell encapsulation. The polymer is known to have a broad and high antibacterial activity, perhaps due to the amino group interfering with cell growth by adsorbing to the cell surface[96]. However, such effects are ameliorated by chitosan's low solubility and crosslinking when used for cell encapsulation.

Chitosan is a common primary component in hydrogel membranes for a variety of encapsulation applications. It has also been researched for adsorption of heavy metals, dyes, and drinking water contaminants such as fulvic acid[102]. Yi et al. determined that chitosan

improved the thermal stability and activity of enzymes by increasing covalent bonds between enzyme and nanofibers[103]. However, due to the harsh crosslinking conditions needed, we do not work with pure chitosan membranes and instead include it as a secondary additive in PVA hydrogels. Chitosan in biobeads provides an additional layer of buffering for near neutral conditions. The high adsorption capacity of chitosan also extends the period of time a biobead remains in the viable pH range while degrading CAHs.

2.3 Conclusions and Applications:

Many papers in literature recommend a simplified approach to estimating solute diffusivity in hydrogels, considering only physical obstruction, hydrodynamic effects, and free volume reduction. Others consider charge effects[104], shape of solute[78], and mobility of crosslinked polymer chains[75]. For some charged species, repulsion and attraction between polymer and solute influence diffusivity, although this is not predictable based on charge alone. In the case of DGT, certain charged metal ions interact strongly with membranes while others do not[87]. As shown previously, D_e may increase (cinnamon) or decrease (methylene blue) with ionic strength of solution for positive solutes in hydrogels. As no model can accurately predict D_e based on solute, solvent, and polymer properties, the diaphragm cell method is recommended for estimating effective diffusivity.

Proton diffusivity through hydrogels has applications in tissue engineering[105], environmental remediation, and drug delivery[36]. Hydronium ions in hydrogel membranes can react with polymer functional groups or diffuse via the Grotthuss mechanism through aqueous domains. In situations where near neutral pH must be maintained such as biological applications, incorporation of polymers with neutral pKa can eliminate excess hydronium ions. Acid may also diffuse away from the system, especially when ionic strength of solution is increased. Polymer formulations may be tuned to limit acidity in hydrogels by both reaction and diffusion. Additionally, flux of unwanted organic solutes may be slowed by increasing polymer volume fraction with minimal influence on hydronium diffusivity.

Chapter 3: Hydrogels Applied to TCE Degradation

3.1 Diffusion of CAHs:

The ultimate goal of biobeads is to achieve maximum degradation of TCE with minimal release of highly toxic VC. Biobeads should also adsorb or emit acid as it is generated to prevent inhibitory pH levels and promote long term degradation. Though hydrogel beads impregnated with microbes have been used extensively[106–108] and even tested for anaerobic TCE degradation[31], it would be beneficial to model the biodegradation of CAHs to ensure adequate transport of waste products (acid) and minimal efflux of highly toxic VC from the biobead. This reaction/diffusion model requires D_e values for each species in the hydrogel membrane. Experiments using a diaphragm cell were conducted to determine these transport properties for TCE, DCE, and VC in 10% PVA 2% SA membranes which are chemically crosslinked in a saturated boric acid, 2% (w/v) $CaCl_2$ solution for 4.5 hours. Hydrogel membranes are also swollen in deionized water for at least one hour prior to experimentation. Standard measure of error is used to determine standard error between triplicate data samples.

Materials and Methods:

As CAHs can be both carcinogenic and mutagenic in the case of VC, proper safety is exercised with PPEs and engineering controls. All work with open containers of CAHs is conducted in the fume hood with goggles, splash coats, and double gloves. Syringes, containers, and diffusion cells are constructed of glass or metal whenever possible to avoid sorption and keep CAHs dissolved in aqueous phase. The diffusion cell is constructed of a glass tube with Teflon® end caps and membrane puck. As TCE and DCE are obtained as pure solvents, serial dilutions are performed in glass serum bottles before addition to the source compartment. Dilutions are sonicated for one hour prior to use to ensure dissolution. VC is obtained as a 2000 ppm standard in methanol and is directly injected into the source compartment.

TCE is known to have an affinity for Teflon®, so a solid puck was used as a diaphragm to measure diffusion through the puck material. After 48 hours of continuous stirring on both sides of the membrane, no solute breakthrough was observed. However, after collecting diffusive data, spectroscopic analysis of the source side indicates that the TCE concentration drops for several hours by more than 22 ppm per hour. Absorbance values for calibration solutions also decrease over time, indicating volatilization during calibrations. These methodological problems are solved by reconstructing the diffusion cell with 1½" stainless steel (304, Sch 80) tubing with threaded endcaps and a metal pump. The 1/8" plastic tubing between pump and spectrophotometer is also replaced with 1/16" stainless steel tubing. The new diffusion cell's increased volume requires a larger volume of CAH addition. This decreases the number of serial dilutions needed for calibration, and completely eliminates the need for serial dilutions for TCE and cDCE diffusion runs (instead direct injection of pure CAHs). Teflon® coated stir bars will be replaced with glass stir bars to eliminate sorption from the aqueous phase. At the time of this manuscript's publication, the diffusive experiments have not been redone and previously determined values are used for modelling.

Concentration of CAHs in the sink is monitored by a closed-loop, continually measuring spectrophotometric system. The sink volume is stirred and continually pumped through a spectrophotometer, which measures sample absorbance every 5-10 minutes for a 24 hour period. Beer-Lambert's Law is used to determine the molar absorption coefficient for each CAH. Serial dilutions of TCE, DCE, and VC are scanned spectrophotometrically from 190-1100 nm. The wavelength of greatest linearity for a curve of absorbance vs concentration is 200 nm for TCE, 200 nm for DCE, and 202 nm for VC.

At such low absorbances, every chemical species involved in the system has a significant molar extinction coefficient (**Figure 3.1**). Running a diffusion experiment with no solute in the source (water on both side of the membrane) we found that the absorbance of the sink increases with time for the first 24 hours, at which point it approaches a stable value. This is likely due to some crosslinking calcium ions leaching from the membrane. Gradual calcium loss from crosslinked hydrogels has also been noted by Chandy et al[109]. Dissociation of PVA and SA from the hydrogel is unlikely as the polymers are crosslinked. Spectrophotometer calibrations

will be repeated using the new diaphragm cell. Use of a wavelength greater than 215 nm would be optimal to exclude absorbance of calcium ions. However, this is contingent on a suitable wavelength being found which results in a CAH absorbance proportional to concentration.

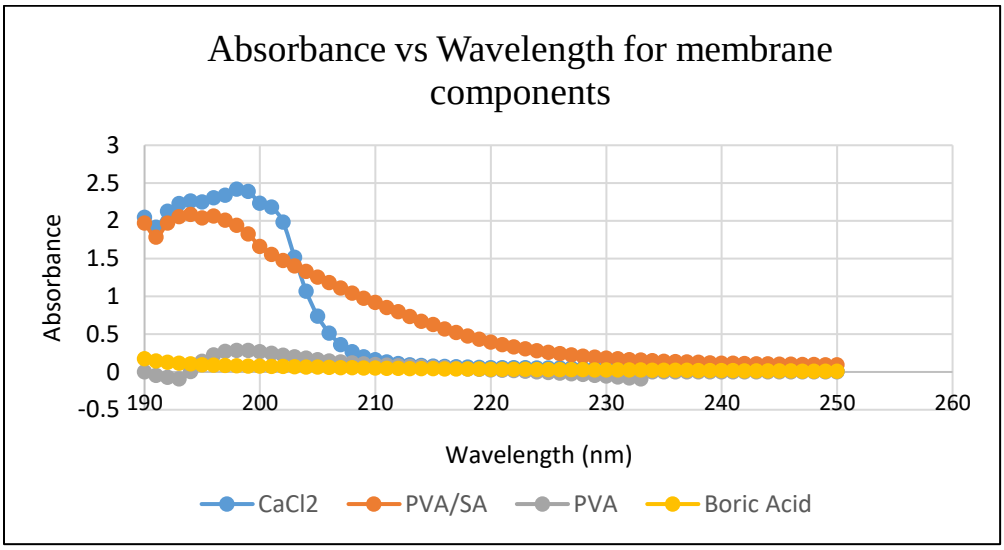

Figure 3.1: *Absorbance values at different wavelengths for membrane components. Spectrophotometer was blanked with deionized water. Calcium ions have significant absorbance at wavelengths used for CAH diffusion.*

To eliminate the diffusion of calcium from our absorbance measurements, the system is stirred and approaches steady-state for approximately 24 hours before source solute addition. A concentration profile for a VC sink is shown in **Figure 3.2**, where the system was equilibrated for 19 hours prior to VC addition. Future diffusion runs will use only physically crosslinked membranes to prevent crosslinker leaching. These membranes also have a higher effective diffusivity for protons, making them more suitable for CAH degrading biobeads.

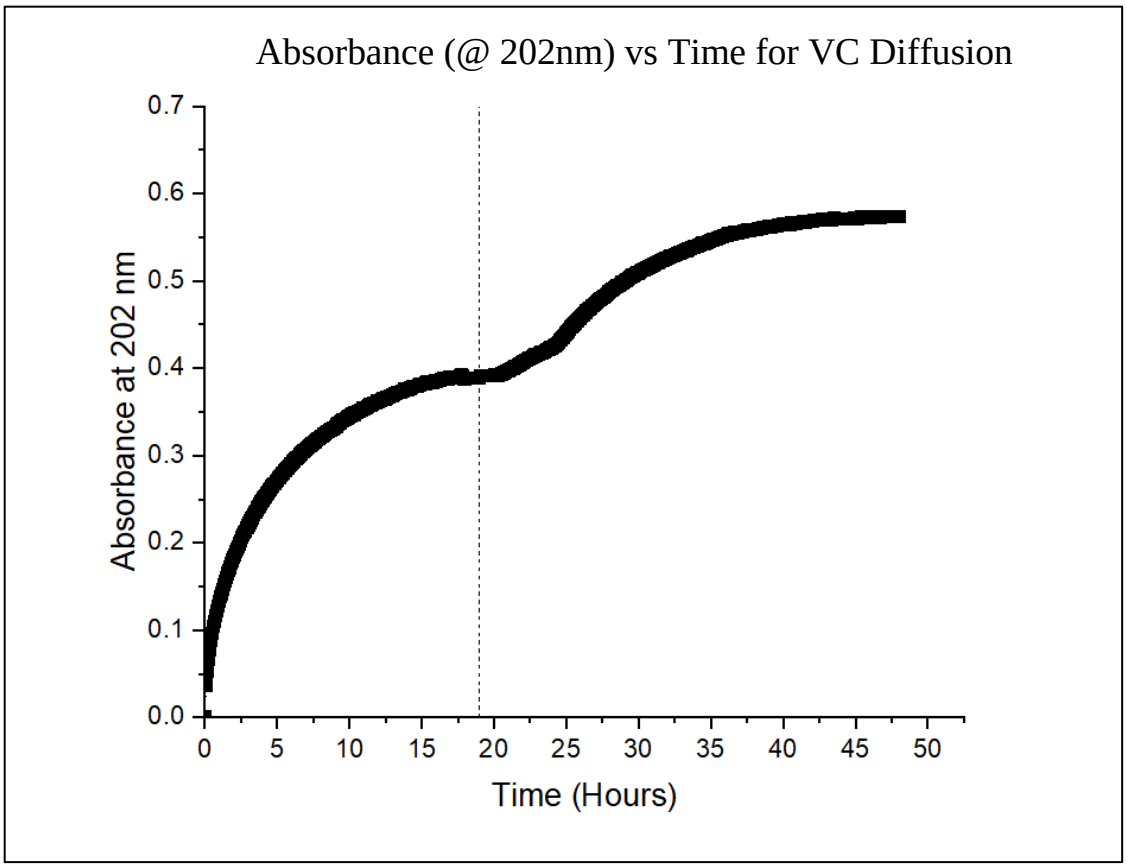

Figure 3.2: *Absorbance at 202 nm for VC diffusion run – VC was added at 19 hours (red line), initial absorbance is due to calcium leaching from membrane.*

Estimated D_e values

After triplicate data collection for every chlorinated aliphatic hydrocarbon (CAH) species, **Equation 1.6** is used to determined D_e. Effective diffusivities (cm^2s^{-1}) are $11.0 \pm 1.46\times10^{-6}$ for TCE, $6.90 \pm 0.68\times10^{-6}$ for cDCE and $4.04 \pm 1.27\times10^{-6}$ for VC (**Figure 3.3**). An unexpected trend was found between CAH size and D_e, as TCE diffuses fastest and VC slowest. Simple understanding of diffusive mechanisms would indicate that the largest solute would diffuse slowest. It is hypothesized that significant dipole moments in the case of cDCE and VC increase interactions with membrane components and decrease diffusivity. However, after the discovery of methodological problems the measured D_e values are suspect. As the improved diffusion cell is not completed at the time of publication, the determined diffusive parameters are used in the reaction/diffusion model.

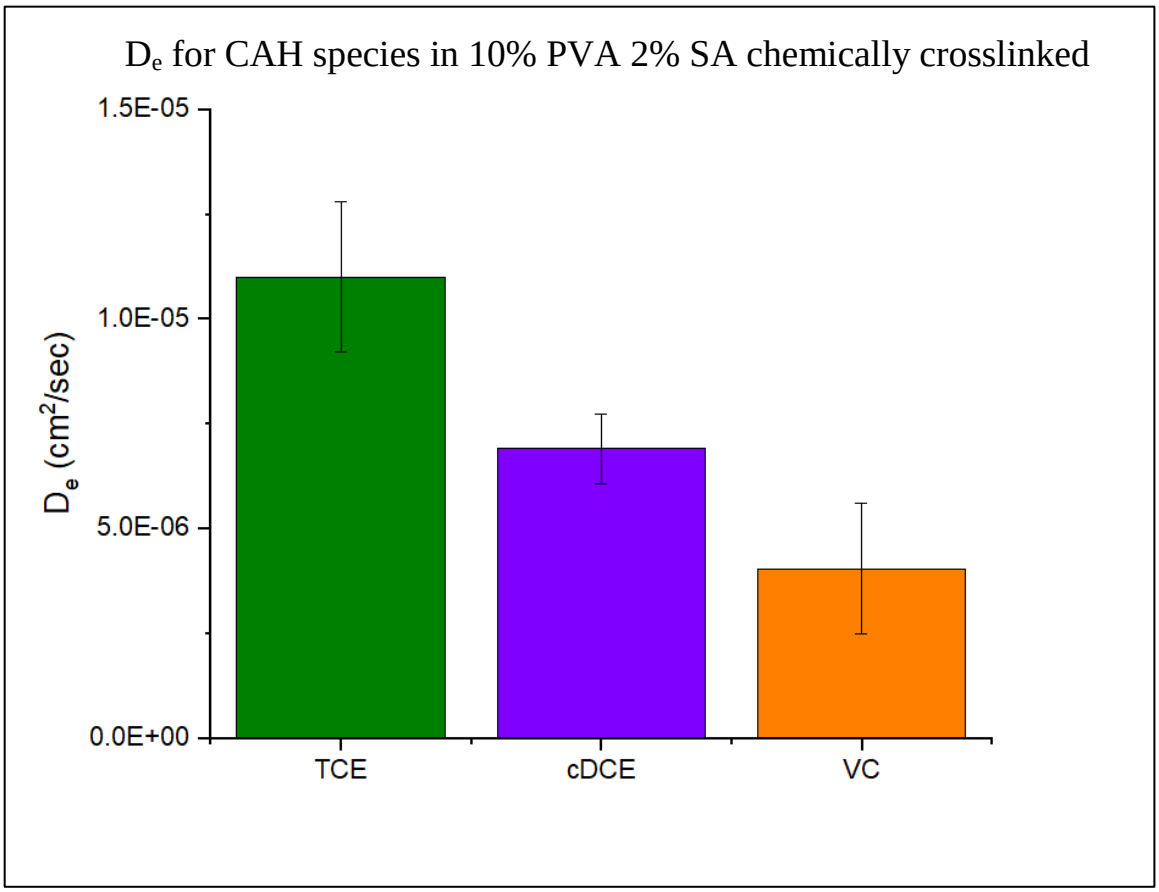

Figure 3.3: *D_e values for all CAH species tested in 10% PVA 2% SA chemically crosslinked. Only D_e values for TCE and VC are statistically different.*

3.1 Kinetics of Biodegradation:

Measurements of the effective diffusivities of CAHs allow accurate modelling of diffusion through hydrogels of various sizes and shapes. However, the biobead system is not a purely diffusing system; chlorinating solvents enter the hydrogel, react, and transform to other species which can diffuse further into or out of the bead. In order to model the biobead and optimize its size and cell concentration, reaction rates for the various CAHs are needed. However, to the best of the author's knowledge, there is currently no kinetic data for encapsulated TCE reducing bacteria. Instead, we assume identical reaction rates between cells in planktonic or encapsulated systems. There are likely differences between rates of reaction for these different cultures, but for purposes of modelling they are assumed negligible.

Much work has been done to determine the reaction rate for microbial TCE degradation, especially when modelled a function of both CAH and cell concentrations[110–112]. A commonly used model is Michaelis-Menten kinetics[113,114], designed for enzyme kinetics where a single substrate is converted to product. This model assumes that the substrate (S) first binds to an enzyme (E), forming an intermediate complex (ES) which dissociates, yielding the final product (P) and an enzyme (**Equation 3.1**). A first order Michaelis-Menten reaction has a rate expressed by **Equation 3.2**.

$$E + S \leftrightarrow ES \leftrightarrow E + P$$

Equation 3.1: *Reaction mechanism for Michaelis-Menten where E is enzyme, S is substrate, and P is product*

$$Rate = \frac{V_{max}\,[S]}{K_m + [S]}$$

Equation 3.2: *Where [S] is substrate concentration, V_{max} is the reaction rate for saturated S, and K_m is the Michaelis-Menten constant*

Michaelis-Menten can also be applied to microbial growth with the Monod equation. However, additional terms must be added for systems with substrate inhibition. For KB-1, CAH saturated conditions do not lead to V_{max}, but complete inhibition of degradation. Additionally, degradation of DCE is heavily inhibited in the presence of TCE, and VC degradation is inhibited by both TCE and DCE. To reflect these competitive and self-inhibitions and include the impacts of cell density in solution, a more complex model is needed.

Kinetic parameters for TCE reduction by the planktonic anaerobic bacterial consortium K-B1 (Sirem™) are employed as determined by Haest et al..[30] An EC50 inhibition model accounts for self-inhibition of TCE and DCE, as well as complete inhibition of TCE degradation at concentrations greater than 2.2 mM. In the model, the EC50 term is placed within a logarithm inside of an exponential term, which quickly dampens reaction rate as inhibitory concentrations are reached for TCE, and cDCE. Our reaction/diffusion model assumes non-steady state degradation with a constant concentration of cells, constant bulk

CAH concentration, and one-dimensional transport. Reaction rates as taken from literature are shown in **Equations 3.3-3.5**.

$$Rate_{TCE} = \frac{k_{max,TCE}\, X_m\, [TCE]}{\left[K_{s,TCE} + [TCE]\right] \cdot \left[1 + \exp\left(b_{TCE} \times \log\left(\frac{[TCE]}{EC_{50,TCE}}\right)\right)\right]}$$

Equation 3.3: *EC50 rate equation where [TCE] is concentration of TCE (mM), Xm is cell concentration in cells/L,*

$$Rate_{DCE} = \frac{k_{max,DCE}\, X_m\, [DCE]}{\left[K_{s,DCE}\left(1 + \frac{[TCE]}{K_{CI,TCE}}\right) + [DCE]\right] \cdot \left[1 + \exp\left(b_{DCE} \times \log\left(\frac{[DCE]}{EC_{50,DCE}}\right)\right)\right]}$$

Equation 3.4: *EC50 rate equation with optimized parameters for DCE degradation*

$$Rate_{VC} = \frac{k_{max,VC}\, X_m\, [VC]}{\left[K_{s,VC}\left(1 + \frac{[TCE]}{K_{CI,TCE}} + \frac{[DCE]}{K_{CI,DCE}}\right) + [VC]\right]}$$

Equation 3.5: *EC50 rate equation with manually fitted parameters for VC degradation. VC degradation has not been observed to be self-inhibited and therefore the EC50 term is not applicable. (Haest et al.)*

3.3 Finite Difference Method:

Simultaneous reaction/diffusion systems are common transport problems. The solution begins with a general mass balance. The full form is shown in **Equation 3.6**. This can then be reduced for a spherical system where the concentration only varies radially. The Material balance reduces to **Equation 3.7**.

$$\frac{\partial C}{\partial t} = D_e \nabla^2 C - Rate$$

Equation 3.6: *Where C is concentration, t is time and D_e is effective diffusivity*

$$\frac{\partial C}{\partial t} = D_e \left(\frac{2}{r} \frac{\partial C}{\partial r} + \frac{\partial^2 C}{\partial r^2} \right) - Rate$$

Equation 3.7: *Where r is bead radius*

At this point, the system can be numerically solved using the finite-difference method, which divides the system into a matrix of space and time steps. By this method, the concentration of each species in the biobead can be modelled at unsteady state and for many spatial points within the gel. Other geometries of cell encapsulating hydrogels can be modelled by a repeated derivation starting from **Equation 3.6** into rectangular coordinates. **Equations 3.8**, **3.9**, and **3.10** show the delineation of the partial differentials of **Equation 3.7** into finite difference form.

$$\frac{\partial C}{\partial r} = \frac{C_{i+1,j} - C_{i,j}}{h}$$

Equation 3.8: *Delineation of the partial differential of concentration with radius. C is concentration at space step 'i' and time step 'j'. h is the space step distance.*

$$\frac{\partial^2 C}{\partial r^2} = \frac{C_{i+1,j} - 2C_{i,j} + C_{i-1,j}}{h^2}$$

Equation 3.9: *Delineation of the partial second derivative of concentration with radius.*

$$\frac{\partial C}{\partial t} = \frac{C_{i,j+1} - C_{i,j}}{k}$$

Equation 3.10: *Delineation of the partial differential of concentration with time. C is concentration at space step 'i' and time step 'j'. k is the time step distance.*

Upon establishing an initial condition, the system property under consideration (concentration) can be solved one time step into the future. Thus, the array of space steps becomes a row in a matrix of concentrations. Each additional time step creates another row, and time continues to increase until steady state concentration values are achieved (unchanging values with each new row). A basic diagram showing this method is shown in **Figure 3.4**.

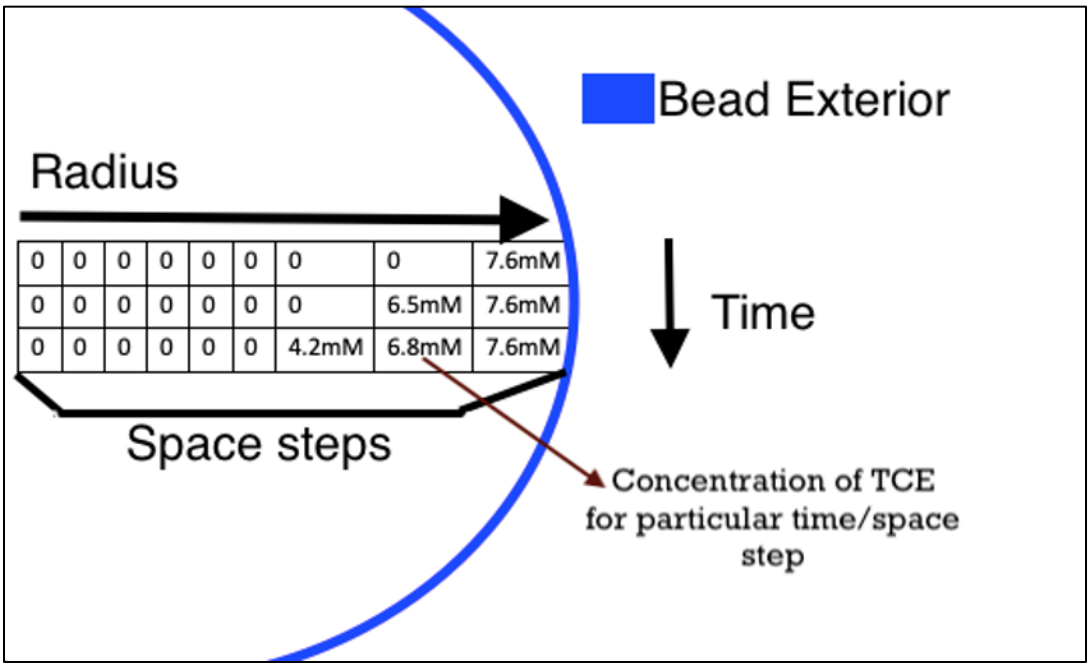

Figure 3.4: *Diagram Explaining the Finite Difference Method for Spherical System*

One purpose for modelling the biobead system was to determine optimal bead size and cell concentration to achieve maximum conversion of TCE while emitting minimal toxic VC to the environment. Degradation of by-product CAHs (cDCE and VC) is inhibited by the presence of their parent products. In a small bead, TCE may not be fully degraded and all by-products will simply diffuse into the surrounding groundwater. The opposite extreme is a large bead which achieves rapid conversion of CAHs near the bead surface, where they are likely to diffuse rapidly out of the system.

3.4 Results and Discussion:

TCE is rapidly degraded by KB-1 consortium at concentrations below 2.2 mM. For this reason, direct push technologies inject the culture downstream of the contaminant plume where concentration is lower. TCE degradation is self-inhibited at high concentration, and the presence of TCE also inhibits conversion of cDCE and VC. Furthermore, the reaction rate decreases as the number of chlorine atoms per molecule decreases. In pilot systems of

anaerobic degradation, conversion of TCE is often evidenced by the presence of cDCE and VC[2,115–117].

Using a 10% PVA 2% SA biobead system, higher levels of cDCE and VC degradation can be achieved compared to direct push methods. Since the effective diffusivity of a molecule decreases with the number of chlorine atoms, the by-products have a longer residence time in the bead, facilitating improved degradation. Furthermore, the biobead provides several regions for targeted degradation of by-products. TCE degrades near the surface of the bead, while cDCE degrades at a deeper level where no TCE is present. In a correctly sized biobead, VC degradation will occur near the center (**Figure 3.5**).

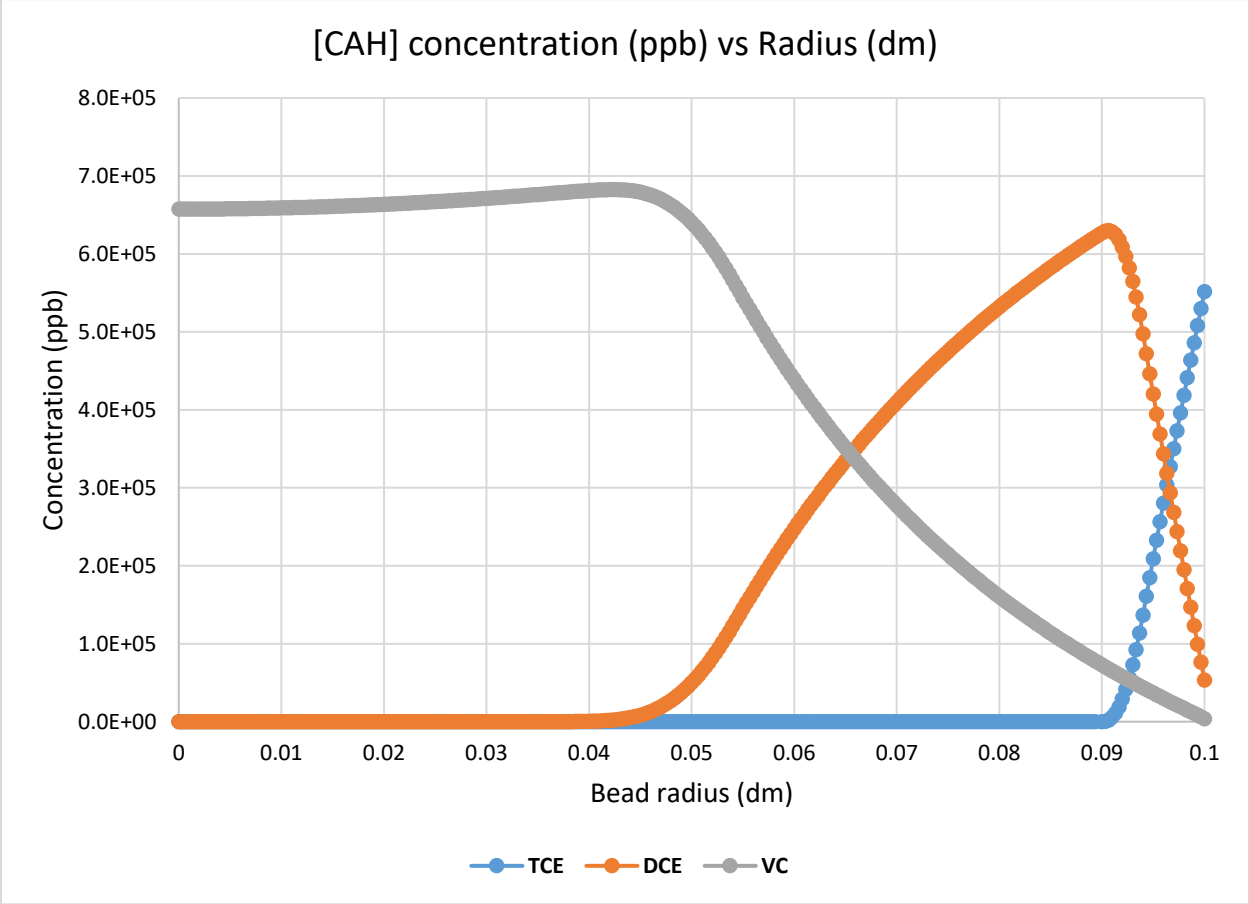

Figure 3.5: *Concentration gradient of CAHs in simulated biobead. Exterior TCE concentration is 4mM.*

Additionally, the 10% PVA 2% SA biobead system can operate at TCE concentrations far greater than planktonic microbes. At TCE concentrations above 2.2 mM, unencapsulated KB-

1 consortium is incapable of biodegradation. With the diffusion limitation introduced by the hydrogel, the effective concentration of TCE in the majority of the bead is kept below inhibitory levels. Biobeads which have been modelled using the finite difference method and EC50 reaction kinetics show steady state degradation of TCE to ethylene at environmental CAH concentrations above 5mM. Unlike traditional biodegradation using direct push technologies, a biobead system may be used very close to the source – perhaps even directly at the source if sufficiently high concentrations of cells are achieved (1E11 cells per cm^3 biobead).

The ultimate goal of a biobead system is to achieve long term CAH degradation by adsorption of protons, simultaneously degrade TCE and breakdown products, and minimize efflux of highly toxic VC. To determine optimal performance, the system was simulated for a variety of biobead sizes and cell densities. The primary concern was to maximize the ratio of VC degraded to VC formed in the bead. As can be seen in **Figure 3.6**, a maximum of 30% VC degradation to formation is achieved for cell concentrations ranging from 3E8 to 1E11 cells per cm^3 of biobead.

As the D_e values for CAHs in the system need to be re-estimated, the modelled concentration gradients at steady state may be inaccurate. However, the ratio of steady state VC degradation to formation is constant, regardless of diffusivities. Substitution of the aqueous diffusivity values for TCE, DCE, and VC produced no difference in optimal VC ratio. At steady state, there is no accumulation within the bead, and the rate of solute flux and degradation is constant regardless of diffusivity. Solutes may move away from or toward the bead center, and the direction of travel is affected by geometry and not D_e.

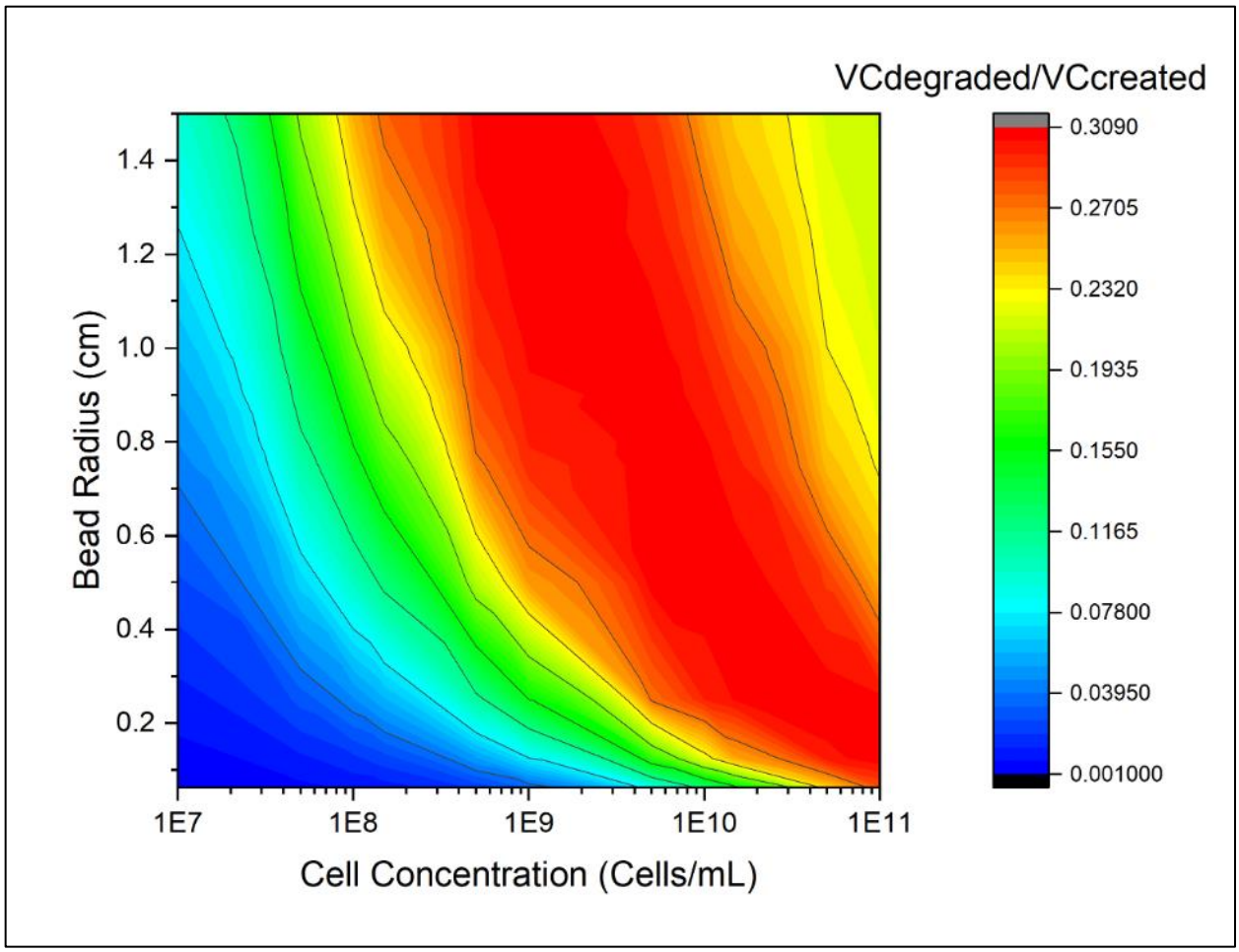

Figure 3.6: *Concentration plots of simulated biobeads in an infinite 1500ppm TCE groundwater source*

As biobeads have potential for use at the contaminant source and efflux of VC is significant, a large number of biobeads should be employed. In this manner, VC leaving one bead is likely to diffuse into a neighboring bead facilitating further degradation. Alternatively, a combination of the biobead system and direct push technologies may deliver the best results. Biobeads can significantly reduce the contaminant level at the source plume, while bioaugmentation further downstream can eliminate the remnant by-products. Different shapes of biobeads, such as straw shaped or slab to form a permeable reactive barrier may further improve remediation.

Chapter 4: Future Work

4.1 Model Improvements:

Cell concentration relation to D_e

Effective diffusivity has been known to change in membranes with varying cell concentrations[57]. Solute sorption and physical obstruction caused by biomass can significantly slow transport. A linear relationship between D_e and cell concentration is anticipated but is yet to be shown experimentally. Future testing may use dead KB-1 microbial consortium to prevent CAH degradation and estimate effective diffusivity. The relationship between cell concentration and D_e can then be used in the finite difference model to achieve more accurate results.

Determination of biodegradation parameters for immobilized cells

In the biobead model presented, degradation parameters for TCE, cDCE, and VC are assumed to be identical to KB-1 microbial consortium in broth media. Kinetic biodegradation parameters may be significantly different when microbes are encapsulated[118]. The EC50 kinetic model shown by Haest et al. will likely be used as it accurately decreases degradation rates as TCE and DCE approach inhibitory concentrations. However, the rate constants will likely change for immobilized cells. Elucidating the kinetic parameters experimentally will require estimates of solute flux from the biobead into surrounding solution. Accurate D_e values for each solute involved must be determined before a kinetic model can be proposed.

Creating a model relating charge to D_e

The work presented in Chapter 2 was initially done to develop a model relating solute charge and dipole moment to diffusivity. The small scope of data collected provides a starting point for this model, but more work is needed before a confident correlation can be established. A

survey of the relevant literature shows that D_e is affected by solute charge, shape, size, and electronegativity as well as hydrogel mobility, volume fraction, and ionic strength of solution. Future work should be limited to one membrane type to avoid these latter influences.

trans-DCE diffusion

Effective diffusivity is influenced by dipole moments and solute shape; isomers can have significantly different D_e values. DCE is the only CAH tested that has an isomer, and trans-1,2-dichloroethylene (tDCE) testing should be conducted. Comparing the values obtained with the biologically relevant cis-1,2-dichloroethylene will show the effect of dipole moment on DCE diffusion. tDCE is not produced by KB-1 consortium[30] and will not be used in the biobead degradation model.

4.2 Cell Viability

Cell viability with different membranes/crosslinkers

Modelling of the biobead system assumes a constant cell density of biodegrading microbes. In practice, formation of biobeads and the crosslinking process kills a large number of microorganisms. Estimates of cell viability in chemically and physically crosslinked 10% PVA 2% SA membranes will provide a correction factor for future models.

Cell viability should also be estimated for membranes incorporating chitosan polymers. Chitosan is the most promising molecule for proton adsorption in membranes but it is known to be a biocidal agent in some cases. A chitosan polymer with lower degree of deacetylation will be safer for bacteria due to a reduction in charge and proton transfer in and around cells. If cell viability is especially low in chitosan membranes, a biobead may be constructed with a sterile chitosan core for proton adsorption coated with biologically active PVA/SA hydrogel.

Cell viability should be estimated for a variety of biobead deployment times, as carcinogen degradation for KB-1 is correlated with cell reproduction. Experiments conducted by a senior design team using ethanol producing yeast cells encapsulated in SA beads crosslinked with calcium chloride showed a large increase in viable cells with time. Eventually, biobeads were so saturated with biomass that they swelled and tore apart. A similar result using KB-1 consortium could invalidate the model presented here, as cell concentrations and bead size are assumed to be constant.

4.3 Hydrogel Improvements

Zwitterionic membrane proton diffusion

As demonstrated in the proton diffusion experiments shown in Chapter 2, ionic strength of solution has a profound influence on effective diffusivity. Although ionic solutions show heightened flux of protons, the salt concentrations used are not conducive to bacterial growth. Zwitterionic polymers may be useful in shielding proton charge while allowing the microbial consortium to remain in a salt-free environment. Some work has been conducted using 10% PVA 1% SA 1% chitosan freeze/thaw membranes as a preliminary test. Chitosan has a pKa of 6.5[119] and will protonate before alginate, leading to a positive charge. Negatively charged carboxylate groups on alginate have a pKa of 3.24. This could lead to a zwitterionic effect locally after chitosan is protonated and until the alginate is saturated with protons. No significant difference in proton D_e was observed compared to regular 10% PVA 2% SA freeze/thaw membranes. A true zwitterionic copolymer will maintain countering charges throughout pseudo-steady state flux, potentially influencing the effective diffusivity.

PVA-glycerol "freeze-less" membranes

Both chemically (boric acid and calcium chloride) and physically (freeze/thaw) crosslinked PVA/SA membranes are expected to have low cell viability. A less harsh method of crosslinking which does not involve toxic chemicals or rapid shifts in temperature is the

gelation of PVA dissolved in water with glycerol. A mixture of 10 g PVA in 50 mL glycerol and 50 mL water is heated, dissolved, and cooled. Bacteria are added to this molten gel, which sets at room temperature over several days forming a tough, crosslinked hydrogel. Proton diffusion through this type of membrane results in similar D_e values compared to regular 10% PVA when freeze/thawed. An alternative membrane type is PVA/SA membranes with added glycerol physically crosslinked by the freeze/thaw procedure. Glycerol addition in frozen hydrogels has been shown to increase cell viability[34].

References

1. Russell HH, Matthews JE, Sewell GW. TCE Removal from Contaminated Soil and Ground Water 1. In: Boulding JR, ed. *Epa Environmental Engineering Sourcebook*. 1st ed. Routledge; 2019:87-99. doi:10.1201/9780203756720-6

2. Pant P, Pant S. A review: Advances in microbial remediation of trichloroethylene (TCE). *J Environ Sci*. 2010;22(1):116-126. doi:10.1016/S1001-0742(09)60082-6

3. US EPA O. Superfund: National Priorities List (NPL). US EPA. https://www.epa.gov/superfund/superfund-national-priorities-list-npl. Published August 17, 2015. Accessed September 18, 2019.

4. perc.pdf. https://www3.epa.gov/ttn/chief/le/perc.pdf. Accessed April 23, 2020.

5. Parker BL, Cherry JA, Chapman SW. Field study of TCE diffusion profiles below DNAPL to assess aquitard integrity. *J Contam Hydrol*. 2004;74(1):197-230. doi:10.1016/j.jconhyd.2004.02.011

6. Matthieu DE, Brusseau ML, Guo Z, Plaschke M, Carroll KC, Brinker F. Persistence of a Groundwater Contaminant Plume after Hydraulic Source Containment at a Chlorinated-Solvent Contaminated Site. *Groundw Monit Remediat*. 2014;34(4):23-32. doi:10.1111/gwmr.12077

7. Substance Priority List | ATSDR. https://www.atsdr.cdc.gov/spl/index.html. Published January 27, 2020. Accessed April 27, 2020.

8. History Associates. A Historical Survey of the Use and Regulation of TCE. Law presented at the: 09:44:25 UTC. https://www.slideshare.net/HistoryAssociates/history-associatesabameetingtechnical-roundtable101113. Accessed September 30, 2019.

9. ATSDR - Public Health Statement: Trichloroethylene (TCE). https://www.atsdr.cdc.gov/phs/phs.asp?id=171&tid=30. Accessed April 23, 2020.

10. Sykes MK, Arnot RN, Jastrzebski J, Gibbs JM, Obdrzalek J, Hurtig JB. Reduction of hypoxic pulmonary vasoconstriction during trichloroethylene anesthesia. *J Appl Physiol*. 1975;39(1):103-108. doi:10.1152/jappl.1975.39.1.103

11. McCarty PL, Goltz MN, Hopkins GD, et al. Full-Scale Evaluation of In Situ Cometabolic Degradation of Trichloroethylene in Groundwater through Toluene Injection. *Environ Sci Technol*. 1998;32(1):88-100. doi:10.1021/es970322b

12. Boulding JR. *EPA Environmental Engineering Sourcebook*. Routledge; 2019.

13. Microfabricated Gas Chromatograph for On-Site Determinations of TCE in Indoor Air Arising from Vapor Intrusion. 2. Spatial/Temporal Monitoring | *Environmental Science*

& Technology. https://pubs.acs.org/doi/abs/10.1021/es204625w. Accessed April 23, 2020.

14. Poison vapor evacuations increase as old chemical threats resurface. mlive. https://www.mlive.com/news/2017/02/michigan_vapor_intrusion_deq.html. Published February 26, 2017. Accessed March 13, 2020.

15. Lendvay JM, Löffler FE, Dollhopf M, et al. Bioreactive Barriers: A Comparison of Bioaugmentation and Biostimulation for Chlorinated Solvent Remediation. *Environ Sci Technol*. 2003;37(7):1422-1431. doi:10.1021/es025985u

16. Stroo HF, Leeson A, Marqusee JA, et al. Chlorinated Ethene Source Remediation: Lessons Learned. *Environ Sci Technol*. 2012;46(12):6438-6447. doi:10.1021/es204714w

17. Stroo HF, Ward CH. *In Situ Remediation of Chlorinated Solvent Plumes*. Springer Science & Business Media; 2010.

18. Amy GL, Narbaitz RM, Cooper WJ. Removing VOCs From Groundwater Containing Humic Substances by Means of Coupled Air Stripping and Adsorption. *J - AWWA*. 1987;79(8):49-54. doi:10.1002/j.1551-8833.1987.tb02893.x

19. Document Display | NEPIS | US EPA. https://nepis.epa.gov/Exe/ZyNET.exe/2000BC6O.txt?ZyActionD=ZyDocument&Client=EPA&Index=1991%20Thru%201994&Docs=&Query=&Time=&EndTime=&SearchMethod=1&TocRestrict=n&Toc=&TocEntry=&QField=&QFieldYear=&QFieldMonth=&QFieldDay=&UseQField=&IntQFieldOp=0&ExtQFieldOp=0&XmlQuery=&File=D%3A%5CZYFILES%5CINDEX%20DATA%5C91THRU94%5CTXT%5C00000004%5C2000BC6O.txt&User=ANONYMOUS&Password=anonymous&SortMethod=h%7C-&MaximumDocuments=1&FuzzyDegree=0&ImageQuality=r75g8/r75g8/x150y150g16/i425&Display=hpfr&DefSeekPage=x&SearchBack=ZyActionL&Back=ZyActionS&BackDesc=Results%20page&MaximumPages=1&ZyEntry=2&slide. Accessed November 19, 2019.

20. Miyake Y, Sakoda A, Yamanashi H, Kaneda H, Suzuki M. Activated carbon adsorption of trichloroethylene (TCE) vapor stripped from TCE-contaminated water. *Water Res*. 2003;37(8):1852-1858. doi:10.1016/S0043-1354(02)00564-X

21. Sakoda A, Kawazoe K, Suzuki M. Adsorption of tri- and tetra-chloroethylene from aqueous solutions on activated carbon fibers. *Water Res*. 1987;21(6):717-722. doi:10.1016/0043-1354(87)90084-4

22. Nielsen Frands, Olsen Erik, Fredenslund Aage. Henry's Law Constants and Infinite Dilution Activity Coefficients for Volatile Organic Compounds in Water by a Validated Batch Air Stripping Method. *Environ Sci Technol*. 1994;28(12):2133-2138. doi:10.1021/es00061a022

23. Heron G, Christensen TH, Enfield CG. Henry's Law Constant for Trichloroethylene between 10 and 95 °C. *Environ Sci Technol*. 1998;32(10):1433-1437. doi:10.1021/es9707015

24. US EPA O. In Situ Thermal Treatment Technologies: Lessons Learned. US EPA. https://www.epa.gov/remedytech/situ-thermal-treatment-technologies-lessons-learned. Published June 24, 2015. Accessed March 30, 2020.

25. Perelo LW. Review: In situ and bioremediation of organic pollutants in aquatic sediments. *J Hazard Mater*. 2010;177(1):81-89. doi:10.1016/j.jhazmat.2009.12.090

26. Dixon B. *Bioremediation Is Here to Stay*. amer soc microbiology 1325 massachusetts avenue, nw, washington, dc 20005-4171; 1996.

27. Duhamel M, Edwards EA. Microbial composition of chlorinated ethene-degrading cultures dominated by Dehalococcoides. *FEMS Microbiol Ecol*. 2006;58(3):538-549. doi:10.1111/j.1574-6941.2006.00191.x

28. Heffernan B, Murphy CD, Casey E. Comparison of Planktonic and Biofilm Cultures of Pseudomonas fluorescens DSM 8341 Cells Grown on Fluoroacetate. *Appl Environ Microbiol*. 2009;75(9):2899. doi:10.1128/AEM.01530-08

29. Peale JGD, Mueller J, Molin J. Successful ISCR-enhanced bioremediation of a TCE DNAPL source utilizing EHC® and KB-1®. *Remediat J*. 2010;20(3):63-81. doi:10.1002/rem.20251

30. Haest PJ, Springael D, Smolders E. Dechlorination kinetics of TCE at toxic TCE concentrations: Assessment of different models. *Water Res*. 2010;44(1):331-339. doi:10.1016/j.watres.2009.09.033

31. Hillyer, K. E. *Bioremediation of Trichloroethylene by Use of Polymer Bio-Beads and Quantification of Diffusion of Trichloroethylene Through Various Polymer Membranes*; University of Idaho, 2016.

32. US EPA O. National Primary Drinking Water Regulations. US EPA. https://www.epa.gov/ground-water-and-drinking-water/national-primary-drinking-water-regulations. Published November 30, 2015. Accessed October 31, 2019.

33. Yang Y. *Exploring anaerobic reductive dechlorination at low pH environments*. 2012.

34. Vidhyalakshmi R. Encapsulation "The Future of Probiotics"-A Review. In: ; 2009.

35. What drives bacteria to produce a biofilm? | FEMS Microbiology Letters | Oxford Academic. https://academic.oup.com/femsle/article/236/2/163/535288. Accessed September 26, 2019.

36. Chen S-C, Wu Y-C, Mi F-L, Lin Y-H, Yu L-C, Sung H-W. A novel pH-sensitive hydrogel composed of N,O-carboxymethyl chitosan and alginate cross-linked by genipin

for protein drug delivery. *J Controlled Release*. 2004;96(2):285-300. doi:10.1016/j.jconrel.2004.02.002

37. Kashyap N, Kumar N, Kumar MNVR. Hydrogels for Pharmaceutical and Biomedical Applications. *Crit Rev Ther Drug Carr Syst*. 2005;22(2). doi:10.1615/CritRevTherDrugCarrierSyst.v22.i2.10

38. A smart hydrogel-based time bomb triggers drug release mediated by pH-jump reaction - IOPscience. https://iopscience.iop.org/article/10.1088/1468-6996/13/6/064202/meta. Accessed June 28, 2019.

39. Hydrogels in drug delivery: Progress and challenges | Elsevier Enhanced Reader. https://reader.elsevier.com/reader/sd/pii/S0032386108000487?token=E4C995ED9C91C0825EA8C1F8028FDEC9F370ADA42E158E9A1F43796553D94F057023882109891055717F1C7F8D9BDE23. Accessed February 26, 2020.

40. Moffat KL, Marra KG. Biodegradable poly(ethylene glycol) hydrogels crosslinked with genipin for tissue engineering applications. *J Biomed Mater Res B Appl Biomater*. 2004;71B(1):181-187. doi:10.1002/jbm.b.30070

41. Peppas N. Hydrogels in pharmaceutical formulations. *Eur J Pharm Biopharm*. 2000;50(1):27-46. doi:10.1016/S0939-6411(00)00090-4

42. Characterizing Drug Release from Nonfouling Polyampholyte Hydrogels | Langmuir. https://pubs.acs.org/doi/abs/10.1021/acs.langmuir.5b03597. Accessed March 6, 2020.

43. Lee HB, Jhon MS, Andrade JD. Nature of water in synthetic hydrogels. I. Dilatometry, specific conductivity, and differential scanning calorimetry of polyhydroxyethyl methacrylate. *J Colloid Interface Sci*. 1975;51(2):225-231. doi:10.1016/0021-9797(75)90107-1

44. Castellanos A, DuPont SJ, Heim AJ, et al. Size-Exclusion “Capture and Release” Separations Using Surface-Patterned Poly(N-isopropylacrylamide) Hydrogels. *Langmuir*. 2007;23(11):6391-6395. doi:10.1021/la700338p

45. Yang C-C, Lee Y-J. Preparation of the acidic PVA/MMT nanocomposite polymer membrane for the direct methanol fuel cell (DMFC). *Thin Solid Films*. 2009;517(17):4735-4740. doi:10.1016/j.tsf.2009.03.138

46. Composite hydrogels for implants - L Ambrosio, R De Santis, L Nicolais, 1998. https://journals.sagepub.com/doi/abs/10.1243/0954411981533863. Accessed April 29, 2020.

47. Öztop HN, Öztop AY, Karadağ E, Işikver Y, Saraydin D. Immobilization of Saccharomyces cerevisiae on to acrylamide–sodium acrylate hydrogels for production of ethyl alcohol. *Enzyme Microb Technol*. 2003;32(1):114-119. doi:10.1016/S0141-0229(02)00244-2

48. (PDF) Effect of lecithin and calcium chloride solution on the Microencapsulation process yield of calcium alginate beads. ResearchGate. https://www.researchgate.net/publication/228632739_Effect_of_lecithin_and_calcium_chloride_solution_on_the_Microencapsulation_process_yield_of_calcium_alginate_beads. Accessed April 29, 2020.

49. USP Monographs: Polyvinyl Alcohol. http://ftp.uspbpep.com/v29240/usp29nf24s0_m66990.html. Accessed April 29, 2020.

50. Hassett DJ. Anaerobic production of alginate by Pseudomonas aeruginosa: alginate restricts diffusion of oxygen. *J Bacteriol*. 1996;178(24):7322-7325. doi:10.1128/jb.178.24.7322-7325.1996

51. Nanocellulose-alginate hydrogel for cell encapsulation | Elsevier Enhanced Reader. doi:10.1016/j.carbpol.2014.07.059

52. Kumeta K, Nagashima I, Matsui S, Mizoguchi K. Crosslinking of Poly(vinyl alcohol) via Bis(β-hydroxyethyl) Sulfone. *Polym J*. 2004;36(6):472-477. doi:10.1295/polymj.36.472

53. Figueiredo KCS, Alves TLM, Borges CP. Poly(vinyl alcohol) films crosslinked by glutaraldehyde under mild conditions. *J Appl Polym Sci*. 2009;111(6):3074-3080. doi:10.1002/app.29263

54. Uchiyama H, Oguri K, Nishibayashi M, Kokufuta E, Yagi O. Trichloroethylene degradation by cells of a methane-utilizing bacterium, Methylocystis sp. M, immobilized in calcium alginate. *J Ferment Bioeng*. 1995;79(6):608-613. doi:10.1016/0922-338X(95)94756-H

55. Swamy BY, Yun Y-S. In vitro release of metformin from iron (III) cross-linked alginate–carboxymethyl cellulose hydrogel beads. *Int J Biol Macromol*. 2015;77:114-119. doi:10.1016/j.ijbiomac.2015.03.019

56. Wu K-YA, Wisecarver KD. Cell immobilization using PVA crosslinked with boric acid. *Biotechnol Bioeng*. 1992;39(4):447-449. doi:10.1002/bit.260390411

57. Determination of effective diffusion coefficients in calcium alginate gel plates with varying yeast cell content | SpringerLink. https://link.springer.com/article/10.1007/BF02930828. Accessed January 31, 2020.

58. L. Holloway J, M. Lowman A, R. Palmese G. The role of crystallization and phase separation in the formation of physically cross-linked PVA hydrogels. *Soft Matter*. 2013;9(3):826-833. doi:10.1039/C2SM26763B

59. Axelsson A, Persson B. Determination of effective diffusion coefficients in calcium alginate gel plates with varying yeast cell content. *Appl Biochem Biotechnol*. 1988;18(1):231-250. doi:10.1007/BF02930828

60. Amsden B. Solute Diffusion within Hydrogels. Mechanisms and Models. *Macromolecules*. 1998;31(23):8382-8395. doi:10.1021/ma980765f

61. Galgoczy R, Pastor I, Colom A, Giménez A, Mas F, Alcaraz J. A spectrophotometer-based diffusivity assay reveals that diffusion hindrance of small molecules in extracellular matrix gels used in 3D cultures is dominated by viscous effects. *Colloids Surf B Biointerfaces*. 2014;120:200-207. doi:10.1016/j.colsurfb.2014.05.017

62. Fergg F, J. Keil F. Diffusion and reactions of multicomponent electrolytes in poly(vinyl alcohol) hydrogels — modeling and experiment. *Chem Eng Sci*. 2001;56(4):1305-1315. doi:10.1016/S0009-2509(00)00353-5

63. Tyrrell HJV. The origin and present status of Fick's diffusion law. *J Chem Educ*. 1964;41(7):397. doi:10.1021/ed041p397

64. Comyn J. Introduction to Polymer Permeability and the Mathematics of Diffusion. In: Comyn J, ed. *Polymer Permeability*. Dordrecht: Springer Netherlands; 1985:1-10. doi:10.1007/978-94-009-4858-7_1

65. Westrin BA, Axelsson A. Diffusion in gels containing immobilized cells: A critical review. *Biotechnol Bioeng*. 1991;38(5):439-446. doi:10.1002/bit.260380502

66. Kim SW, Bae YH, Okano T. Hydrogels: Swelling, Drug Loading, and Release. *Pharm Res*. 1992;9(3):283-290. doi:10.1023/A:1015887213431

67. Levy M, Berkowitz B. Measurement and analysis of non-Fickian dispersion in heterogeneous porous media. *J Contam Hydrol*. 2003;64(3):203-226. doi:10.1016/S0169-7722(02)00204-8

68. Mason TG. Estimating the viscoelastic moduli of complex fluids using the generalized Stokes–Einstein equation. *Rheol Acta*. 2000;39(4):371-378. doi:10.1007/s003970000094

69. Northrop JH, Anson ML. A Method for the Determination of Diffusion Constants and the Calculation of the Radius and Weight of the Hemoglobin Molecule. *J Gen Physiol*. 1929;12(4):543-554. doi:10.1085/jgp.12.4.543

70. Hayduk W, Laudie H. Prediction of diffusion coefficients for nonelectrolytes in dilute aqueous solutions. *AIChE J*. 1974;20(3):611-615. doi:10.1002/aic.690200329

71. Wilke CR, Chang P. Correlation of diffusion coefficients in dilute solutions. *AIChE J*. 1955;1(2):264-270. doi:10.1002/aic.690010222

72. Takenaka S, Pitts B, Trivedi HM, Stewart PS. Diffusion of Macromolecules in Model Oral Biofilms. *Appl Environ Microbiol*. 2009;75(6):1750-1753. doi:10.1128/AEM.02279-08

73. Hatakeyema T, Yamauchi A, Hatakeyema H. Studies on bound water in poly(vinyl alcohol). Hydrogel by DSC and FT-NMR. *Eur Polym J*. 1984;20(1):61-64. doi:10.1016/0014-3057(84)90223-4

74. Spherulitic membranes of alkylated polyvinylalcohol: Water and salt transport in relation to their structure and to the state of swelling water - ScienceDirect. https://www.sciencedirect.com/science/article/abs/pii/0014305778900666. Accessed January 23, 2020.

75. Amsden B, Turner N. Diffusion characteristics of calcium alginate gels. *Biotechnol Bioeng*. 1999;65(5):605-610. doi:10.1002/(SICI)1097-0290(19991205)65:5<605::AID-BIT14>3.0.CO;2-C

76. Masaro L, Zhu XX. Physical models of diffusion for polymer solutions, gels and solids. *Prog Polym Sci*. 1999;24(5):731-775. doi:10.1016/S0079-6700(99)00016-7

77. Evaluation of effective diffusion coefficient and intrinsic kinetic parameters on azo dye biodegradation using PVA-immobilized cell beads - Chen - 2003 - Biotechnology and Bioengineering - Wiley Online Library. https://onlinelibrary.wiley.com/doi/abs/10.1002/bit.10730. Accessed January 2, 2020.

78. Saleem M, Asfour A-FA, Kee DD, Harrison B. Diffusion of organic penetrants through low density polyethylene (LDPE) films: Effect of size and shape of the penetrant molecules. *J Appl Polym Sci*. 1989;37(3):617-625. doi:10.1002/app.1989.070370303

79. Chen X, Stewart PS. Chlorine Penetration into Artificial Biofilm Is Limited by a Reaction−Diffusion Interaction. *Environ Sci Technol*. 1996;30(6):2078-2083. doi:10.1021/es9509184

80. Xiaoming X, Stewart P, Chen X. "Transport limitation of chlorine disinfection of Pseudomonas aeruginosa entrapped in alginate beads." *Biotechnology and Bioengineering* 49.1 (1996): 93-100.https://onlinelibrary.wiley.com/doi/epdf/10.1002/%28SICI%291097-0290%2819960105%2949%3A1%3C93%3A%3AAID-BIT12%3E3.0.CO%3B2-C. Accessed March 22, 2020.

81. Northrop J, Anson M. "*a method for the determination of diffusion constants and the calculation of the radius and weight of the hemoglobin molecule" The Journal of General Physiology* 12.4 (1929): 543-554 https://rupress.org/jgp/article/12/4/543/26644/A-METHOD-FOR-THE-DETERMINATION-OF-DIFFUSION. Accessed January 3, 2020.

82. Rossi F, Cucciniello R, Intiso A, Proto A, Motta O, Marchettini N. Determination of the trichloroethylene diffusion coefficient in water. *AIChE J*. 2015;61(10):3511-3515. doi:10.1002/aic.14861

83. Bierbrauer F. Hydrogel Drug Delivery: Diffusion Models. :31. (2005)

84. Zhang TC, Bishop PL. Evaluation of tortuosity factors and effective diffusivities in biofilms. *Water Res*. 1994;28(11):2279-2287. doi:10.1016/0043-1354(94)90043-4

85. Bishop PL, Zhang TC, Fu Y-C. Effects of biofilm structure, microbial distributions and mass transport on biodegradation processes. *Water Sci Technol*. 1995;31(1):143-152. doi:10.1016/0273-1223(95)00162-G

86. Akalp U, Chu S, Skaalure SC, Bryant SJ, Doostan A, Vernerey FJ. Determination of the polymer-solvent interaction parameter for PEG hydrogels in water: Application of a self learning algorithm. *Polymer*. 2015;66:135-147. doi:10.1016/j.polymer.2015.04.030

87. Davison W. *Diffusive Gradients in Thin-Films for Environmental Measurements*. 1st ed. University Printing House, Cambridge CB2 8BS, UK: Cambridge University Press; 2016. https://lccn.loc.gov/2016017704.

88. Strichartz GR, Chance B. Absorbance changes at 520 nm caused by salt addition to chloroplast suspensions in the dark. *Biochim Biophys Acta BBA - Bioenerg*. 1972;256(1):71-84. doi:10.1016/0005-2728(72)90164-8

89. Wraight CA. Chance and design—Proton transfer in water, channels and bioenergetic proteins. *Biochim Biophys Acta BBA - Bioenerg*. 2006;1757(8):886-912. doi:10.1016/j.bbabio.2006.06.017

90. Agmon N. The Grotthuss mechanism. *Chem Phys Lett*. 1995;244(5-6):456-462. doi:10.1016/0009-2614(95)00905-J

91. Fatin-Rouge N, Milon A, Buffle J, Goulet RR, Tessier A. Diffusion and Partitioning of Solutes in Agarose Hydrogels: The Relative Influence of Electrostatic and Specific Interactions. *J Phys Chem B*. 2003;107(44):12126-12137. doi:10.1021/jp0303164

92. Barcellona MN, Johnson N, Bernards MT. Characterizing Drug Release from Nonfouling Polyampholyte Hydrogels. *Langmuir*. 2015;31(49):13402-13409. doi:10.1021/acs.langmuir.5b03597

93. Kalis EJJ, Davis TA, Town RM, Leeuwen HP van. Impact of pH on CdII partitioning between alginate gel and aqueous media. *Environ Chem*. 2009;6(4):305-310. doi:10.1071/EN09060

94. Chapter 4.2 - Chitosan | Elsevier Enhanced Reader. doi:10.1016/B978-0-12-812491-8.00064-3

95. Volumes of aqueous hydrogen and hydroxide ions at 0 to 200 °C: The Journal of Chemical Physics: Vol 137, No 15. https://aip.scitation.org/doi/full/10.1063/1.4758071. Accessed March 24, 2020.

96. Liu XF, Guan YL, Yang DZ, Li Z, Yao KD. Antibacterial action of chitosan and carboxymethylated chitosan. *J Appl Polym Sci*. 2001;79(7):1324-1335. doi:10.1002/1097-4628(20010214)79:7<1324::AID-APP210>3.0.CO;2-L

97. Chitin and Chitosan Based Blends, Composites and Nanocomposites | SpringerLink. https://link.springer.com/chapter/10.1007/978-3-642-20940-6_3. Accessed April 29, 2020.

98. Hassan MA, Li TP, Noor ZZ. Coagulation and flocculation treatment of wastewater in textile industry using chitosan. *J Chem Nat Resour Eng*. 2009;4(1):43-53.

99. A. Zielinski B, Aebischer P. Chitosan as a matrix for mammalian cell encapsulation. *Biomaterials*. 1994;15(13):1049-1056. doi:10.1016/0142-9612(94)90090-6

100. The effect of the dietary supplement, Chitosan, on body weight: a randomised controlled trial in 250 overweight and obese adults | International Journal of Obesity. https://www.nature.com/articles/0802693. Accessed April 27, 2020.

101. Gassara F, Antzak C, Ajila CM, Sarma SJ, Brar SK, Verma M. Chitin and chitosan as natural flocculants for beer clarification. *J Food Eng*. 2015;166:80-85. doi:10.1016/j.jfoodeng.2015.05.028

102. Wang S-G, Sun X-F, Liu X-W, Gong W-X, Gao B-Y, Bao N. Chitosan hydrogel beads for fulvic acid adsorption: Behaviors and mechanisms. *Chem Eng J*. 2008;142(3):239-247. doi:10.1016/j.cej.2007.11.025

103. Ye P, Xu Z-K, Wu J, Innocent C, Seta P. Nanofibrous poly(acrylonitrile-co-maleic acid) membranes functionalized with gelatin and chitosan for lipase immobilization. *Biomaterials*. 2006;27(22):4169-4176. doi:10.1016/j.biomaterials.2006.03.027

104. Effect of charge and size of diffusing probe on the diffusion thr...: Ingenta Connect. https://www.ingentaconnect.com/content/govi/pharmaz/2007/00000062/00000012/art00006. Accessed April 25, 2020.

105. Analysis of pH Gradients Resulting from Mass Transport Limitations in Engineered Heart Tissue | SpringerLink. https://link.springer.com/article/10.1007/s10439-007-9360-4. Accessed April 4, 2020.

106. Wadhawan T, McEvoy J, Prüβ BM, Khan E. Assessing tetrazolium and ATP assays for rapid in situ viability quantification of bacterial cells entrapped in hydrogel beads. *Enzyme Microb Technol*. 2010;47(4):166-173. doi:10.1016/j.enzmictec.2010.05.003

107. Park JK, Chang HN. Microencapsulation of microbial cells. *Biotechnol Adv*. 2000;18(4):303-319. doi:10.1016/S0734-9750(00)00040-9

108. Entrapment of microbial cells within polyurethane hydrogel beads with the advantage of low toxicity | SpringerLink. https://link.springer.com/article/10.1007/BF02447818. Accessed April 29, 2020.

109. Evaluation of Modified Alginate-Chitosan-Polyethylene Glycol Microcapsules for Cell Encapsulation - Chandy - 1999 - Artificial Organs - Wiley Online Library.

https://onlinelibrary.wiley.com/doi/full/10.1046/j.1525-1594.1999.06244.x. Accessed November 22, 2019.

110. Saiyari DM, Chuang H-P, Senoro DB, et al. A review in the current developments of genus Dehalococcoides, its consortia and kinetics for bioremediation options of contaminated groundwater. *Sustain Environ Res*. 2018;28(4):149-157. doi:10.1016/j.serj.2018.01.006

111. Comparative Evaluation of Chloroethene Dechlorination to Ethene by Dehalococcoides-like Microorganisms | Environmental Science & Technology. https://pubs.acs.org/doi/abs/10.1021/es049965z. Accessed April 29, 2020.

112. Mustafa NA. Numerical simulation of anaerobic reductive dechlorination of CAHs in continuous flow systems. (2011)

113. Duba AG, Jackson KJ, Jovanovich MC, Knapp RB, Taylor RT. TCE Remediation Using In Situ, Resting-State Bioaugmentation. *Environ Sci Technol*. 1996;30(6):1982-1989. doi:10.1021/es950730k

114. Fennell DE, Nelson YM, Underhill SE, White TE, Jewell WJ. TCE degradation in a methanotrophic attached-film bioreactor. *Biotechnol Bioeng*. 1993;42(7):859-872. doi:10.1002/bit.260420711

115. Freedman DL, Gossett JM. Biological reductive dechlorination of tetrachloroethylene and trichloroethylene to ethylene under methanogenic conditions. *Appl Environ Microbiol*. 1989;55(9):2144-2151.

116. Mohn WW, Tiedje JM. Microbial reductive dehalogenation. *Microbiol Mol Biol Rev*. 1992;56(3):482-507.

117. Murray WD, Richardson M. Progress toward the biological treatment of C1 and C2 halogenated hydrocarbons. *Crit Rev Environ Sci Technol*. 1993;23(3):195-217. doi:10.1080/10643389309388451

118. Kirdponpattara S, Phisalaphong M. Bacterial cellulose–alginate composite sponge as a yeast cell carrier for ethanol production. *Biochem Eng J*. 2013;77:103-109. doi:10.1016/j.bej.2013.05.005

119. Sano H, Shibasaki K-I, Matsukubo T, Takaesu Y. Effect of Rinsing with Phosphorylated Chitosan on Four-Day Plaque Regrowth. *Bull Tokyo Dent Coll*. 2001;42(4):251-256. doi:10.2209/tdcpublication.42.251

Appendix A: Computational Modelling

The finite difference method was used to model TCE, cDCE, and VC concentration with time for a variety of membrane bead sizes (radii) and cell concentrations. The following MATLAB code was called as a function with inputted bead size and cell concentration. This non-steady state approach can be modified to view the concentrations within the bead as a function of time, however it currently saves only the necessary numbers, overwriting the previous data to save computational time. The MATLAB file outputs a csv file with the steady-state flux of CAHs, and steady state concentrations along the radius.

```
% Jonathan 'Jonny' Counts 10/17/19
% Modified version of 'beadfine'
% set to run on uidaho supercomputer as a function
% It will be called with a series of bead radii and cell concentrations
% The function allows input of a bead radius (in dm) and runs 150 space
% steps (or whatever m is set as) and 400000 time steps (or whatever n is
% set as) for a bead of radius R (as input by user). The cell concentration is also input by the user
% it is (unit*10^pwr) cells/mL. Function outputs a
% csv file of radius, concentrations, and degradation rates. The csv file
% will also contain fluxes of CAHs into/out of the bead

% The mMTCE etc. matrices are also pre-allocated for this version
% This should be the fastest version to date.

function riff = beaddeg(R,unit,pwr)
%DeTCE = (11E-6)*3600*24*.01;   % TCE diffusivity convert from cm^2/s to dm^2/day
%DeDCE = (6.90E-6)*3600*24*.01; % DCE diffusivity convert from cm^2/s to dm^2/day
%DeVC = (4.04E-6)*3600*24*.01;  % VC diffusivity convert from cm^2/s to dm^2/day

DeTCE = (10.63E-6)*3600*24*.01;   % TCE diffusivity (Wilke Chang) convert from cm^2/s to dm^2/day
DeDCE = (12E-6)*3600*24*.01;      % DCE diffusivity (Wilke Chang) convert from cm^2/s to dm^2/day
DeVC = (13.96E-6)*3600*24*.01;    % VC diffusivity (Wilke Chang) convert from cm^2/s to dm^2/day
% These will be substituted with experimental values when they are determined with confidence
%% Sizing of Concentration matrices/ size and number of time/space steps
m = 300;
nodes = m+1; % Number of nodes where concentration is calculated

dr = R/m;    % radius step size in dm
stability = 0.49;
dt = (stability*dr*dr)/DeTCE;   % Stability criteria set for lambda
% dt is the time step in days (should be much less than one day)
%n = 250000;
n = 620000;   % n is the number of time steps to be iterated

% TCE Parameters from Haest et al.
ktce = 1.56E-10;    % kmax,tce (mM/cell*day)
```

```
Kstce = 4.19E-3;    % Ks,tce (mM)
Kitce = 37E-2;      % KCI,tce (mM)
EC50tce = 1.01;     % EC 50,tce (mM)
btce = 8.83;        % b,tce (exponential constant for inhibition)
Ytce = 9E8;         % yield,tce (cells/mM TCE)
kdtce = .029;       % kd,tce (1/days)
%XmL = 1e11;         % (cells/mL)
cellsmL = 10^pwr;
Xm = cellsmL*unit*1000;      % (cells/L)

Tcesat=.011415;        % concentration of TCE (mM) = 1500ppb in the aquifer mentioned in 'Full-
Scale Evaluation of In Situ Cometabolic Degradation of
                    % Trichloroethylene in Groundwater through Toluene Injection'
                    % Paper by McCarty et al. 1998
TCEdw=3.805*10^-8;  % drinking water standard for TCE is 5ppb (mM)

%% DCE Parameters
kdce = 2.08E-11;    % kmax,dce (mM/cell*day)
Ksdce = 99.7E-3;    % Ks,dce (mM)
Kidce = 4.79E-3;    % KCI,dce (mM)
EC50dce = 1.27;     % EC 50,dce (mM)
bdce = 10.4;        % b,dce (exponential constant for inhibition)
Ydce = 1.56E10;     % yield,dce (cells/mM TCE)
kddce = .05;        % kd,dce (1/days)

%% VC Parameters (Some parameters are from Heurst et al. some are repeated values from DCE)
kvc = 5E-13;          % kmax,dce (mM/cell*day)
Ksvc = 2.6E-3;    % Ks,vc (mM)
Kivc = 4.79E-3;    % KCI,vc (mM)
% There is no EC50 term for VC degradation, as no inhibition at high
% concentrations was observed experimentally by Haest et al. (personal
% communication). The same goes for the bvc term
Yvc = 2E11;           % yield,vc (cells/mM TCE)
kdvc = .05;        % kd,vc (1/days)


% Next establish FD matrix which is the matrix of concentrations using
% radius from 0 to R for rows, and Time from 0 to T for columns
TCE = zeros(1,nodes);
TCE(1,:) = 0;       % First row is all zeros except for when r = R
rateTCE = TCE;
TCE(1,nodes)=Tcesat;
Volume = zeros(1,nodes);                % zeroing the matrices for volume/flux/concentration
FluxTCE = zeros(n,1);
FluxDCE = zeros(n,1);
FluxVC = zeros(n,1);

DCE = zeros(1,nodes);
```

```
rateDCE = zeros(1,nodes);
VC = DCE;
rateVC = rateDCE;
% The concentration at radius R is the saturation concentration of TCE,
% so all the elements of the last column are set to this value. (TCE
% matrix) The first row is known (t=0,[TCE]=0) so we start calculating [TCE] at t=1
% This is the second row.

% For DCE and VC matrices, initial concentrations are set to zero.
% They will increase with degradation of TCE and DCE
%% ----------------------TCE LOOP-------------------------------------
%---------------------------------------------------------------------
for rws=2:n

for clmn=1:nodes
   % The FD matrix will have its elements iterated column by column and
   % then row by row. The first row is zeros except for where r=R where
   % the concentration column will be TCE saturated.

   r = dr*(clmn-1);   % r goes from zero to R, making m+1 nodes
   % If r is zero at the center (t=0), the whole equation blows up!
   if (r == 0)
      r = .00000001;
   end

   % rw picks the row above the element to be selected. These elements are
   % used to calculate the concentration one time step into the future
   % (one row below)
   rw = rws-1;

      if(TCE(1,clmn)<=0)
      rate = 0;         % If concentration is zero, the rate is zero
      else
    rate =(ktce*Xm*TCE(1,clmn)/((Kstce+TCE(1,clmn))*(1+exp(btce*log(TCE(1,clmn)/EC50tce))))) ;  % rate is in mmol/(L*day)
      end          % If concentration is not zero, rate can be calculated (has a log term)

 if(clmn == 1)                          %The first column doesn't have an FD(rw,clmn-
1) element, so we give it FD(rw,clmn+1) instead (different side of the center)
    T = TCE(1,clmn)+ (dt*(DeTCE*(((2/r)*((TCE(1,clmn+1)-TCE(1,clmn+1))/(2*dr)))+((TCE(1,clmn+1)-
2*TCE(1,clmn)+TCE(1,clmn+1))/(dr^2)))));   % TCE is in mmol/L
    S = -dt*rate;
 elseif (clmn == nodes)
    T = Tcesat;   % at r=R, the concentration is the saturation limit of TCE
    S = 0;
 else
    T = TCE(1,clmn)+ (dt*(DeTCE*(((2/r)*((TCE(1,clmn+1)-TCE(1,clmn-1))/(2*dr)))+((TCE(1,clmn+1)-
2*TCE(1,clmn)+TCE(1,clmn-1))/(dr^2)))));
    S = -dt*rate;
```

```
 end             % This is the regular calculation procedure for Concentration of TCE, based on the previous time step's concentr
ations

 if(T >=0)
    TCE(1,clmn) = T+S;   % Filling the FD matrix with concentration values one element at a time.  TCE is concentration of TC
E in mmol/mL or uM
 else
    TCE(1,clmn) = 0;
 end
 rateTCE(1,clmn)=rate;              % Rate of TCE at each space and time step
 Volume(1,clmn) = (4/3)*pi*r^3;       % Volume increasing with each dr addition

 FluxTCE(rws,1) = (-DeTCE*((TCE(1,nodes-1)-TCE(1,nodes))/dr))/1000;              % Flux TCE in mmol/cm^2*day

 if(clmn<2)
   molTCErxted(rws,clmn) = (rate/1000)*(Volume(1,clmn))*dt;                    % mMoles of TCE reacted within a given sliver of m
embrane
 else                                                    % This is equal to TCE rate of sliver*Volumesliver*time step
   molTCErxted(rws,clmn) = (rate/1000)*(Volume(1,clmn)-Volume(1,clmn-1))*dt;
 end




  if(DCE(1,clmn)<=0)
  rateDCE = 0;         % If concentration is zero, the rate is zero
  else
  rateDCE =((kdce*Xm*DCE(1,clmn)/((Ksdce*(1+(TCE(1,clmn)/Kitce))+DCE(1,clmn))*(1+exp(bdce*log(DCE(1,clmn)/EC50dce)
)))));   % rate is changed from mM/day to mmol/(mL*day)
  end              % If concentration is not zero, rate can be calculated (has a log term)


 rateDCE2 = rateDCE-
rateTCE(1,clmn); % rateDCE2 is the total rate of DCE (generated by TCE, and consumed by cells) *this is a negative number

 if(clmn == 1)     % The first column doesn't have an FD(rw,clmn-
1) element, so we give it FD(rw,clmn+1) instead (different side of the center)
    D = DCE(1,clmn)+ (dt*(DeDCE*(((DCE(1,clmn+1)-2*DCE(1,clmn)+DCE(1,clmn+1))/(dr^2)))-rateDCE2));
 elseif (clmn == nodes)
    D = DCE(1,clmn)+ (dt*(DeDCE*(((2/r)*((0.575*DCE(1,clmn)-DCE(1,clmn-1))/(2*dr)))+((0.575*DCE(1,clmn)-
2*DCE(1,clmn)+DCE(1,clmn-1))/(dr^2)))-rateDCE2)); % DCE concentration one step past surface is assumed zero
 else
    D = DCE(1,clmn)+ (dt*(DeDCE*(((2/r)*((DCE(1,clmn+1)-DCE(1,clmn-1))/(2*dr)))+((DCE(1,clmn+1)-
2*DCE(1,clmn)+DCE(1,clmn-1))/(dr^2)))-rateDCE2));
 end             % This is the regular calculation procedure for Concentration of TCE, based on the previous time step's concentr
ations

 if(D<=0)
```

```
    D = 0;
 end

 DCE(1,clmn)=D;   % Filling the FD matrix with concentration values one element at a time
 rateDCEdeg(1,clmn) = rateDCE;
 %rategenDCE(rws,clmn) = realrateDCE;
 rateDCEmatrix(1,clmn) = rateDCE2;
 FluxDCE(rws,1) = (DeDCE*((DCE(1,nodes-1)-DCE(1,nodes))/dr))/1000;       % Flux of DCE in mmol/cm^2*day

 if(clmn<2)
      molDCErxted(rws,clmn) = (rateDCE/1000)*(Volume(1,clmn))*dt;            % mMoles of DCE reacted within a given sliver o
f membrane
 else                                                  % This is equal to TCE rate of sliver*Volumesliver*time step
      molDCErxted(rws,clmn) = (rateDCE/1000)*(Volume(1,clmn)-Volume(1,clmn-1))*dt;
 end




 if(VC(1,clmn)<=0)
       rateVC = 0;         % If concentration is zero, the rate is zero
     else
       rateVC =((kvc*Xm*VC(1,clmn)/((Ksvc*(1+(DCE(1,clmn)/Kidce)+(TCE(1,clmn)/Kitce))+VC(1,clmn)))));   % rate is change
d from mM/day to mmol/(mL*day)
     end              % If concentration is not zero, rate can be calculated (has a log term)
     %realrateDCE = real(rateDCE);
     realrateVC = real(rateVC);
     rateVC2 = realrateVC-
rateDCEdeg(1,clmn); % rateDCE2 is the total rate of DCE (generated by TCE, and consumed by cells) *this is a negative numb
er

     if(clmn == 1)     % The first column doesn't have an FD(rw,clmn-
1) element, so we give it FD(rw,clmn+1) instead (different side of the center)
       V = VC(1,clmn)+ (dt*(DeVC*(((VC(1,clmn+1)-2*VC(1,clmn)+VC(1,clmn+1))/(dr^2)))-rateVC2));
     elseif (clmn == nodes)
       V = VC(1,clmn)+ (dt*(DeVC*(((2/r)*((0.289*VC(1,clmn)-VC(1,clmn-1))/(2*dr)))+((0.289*VC(1,clmn)-
2*VC(1,clmn)+VC(1,clmn-1))/(dr^2)))-rateVC2)); % DCE concentration one step past surface is assumed zero
     else
       V = VC(1,clmn)+ (dt*(DeVC*(((2/r)*((VC(1,clmn+1)-VC(1,clmn-1))/(2*dr)))+((VC(1,clmn+1)-2*VC(1,clmn)+VC(1,clmn-
1))/(dr^2)))-rateVC2));
     end              % This is the regular calculation procedure for Concentration of TCE, based on the previous time step's conc
entrations

     if(V<=0)
       V = 0;
     end
```

```
        VC(1,clmn)=V;   % Filling the FD matrix with concentration values one element at a time
        rateVCdeg(1,clmn) = rateVC;
        %rategenDCE(rws,clmn) = realrateDCE;
        rateVCmatrix(1,clmn) = rateVC2;
        FluxVC(rws,1) = (DeVC*((VC(1,nodes-1)-VC(1,nodes))/dr))/1000;   % mmoles of VC to leave per day

    if(clmn<2)
    molVCrxted(rws,clmn) = (rateVC/1000)*(Volume(1,clmn))*dt;    % Moles of TCE reacted within a given sliver of membrane
    else                                                         % This is equal to TCE rate of sliver*Volumesliver*time step
    molVCrxted(rws,clmn) = (rateVC/1000)*(Volume(1,clmn)-Volume(1,clmn-1))*dt;
    end

end
end




TCEss = sum(molTCErxted(n,:)) ;   % Rate of TCE degradation at steady state in mmoles per time step
DCEss = sum(molDCErxted(n,:));
VCss = sum(molVCrxted(n,:));

FluxTCEss = FluxTCE(n);
FluxDCEss = FluxDCE(n);
FluxVCss = FluxVC(n);


%% Plotting of Concentrations
ar = [0:dr:R];  % ar is the array of radius values from 0 to R stepping by dr

tceppb = TCE*131400;     % converting mM concentrations to ppb for semilog plot
dceppb = DCE*96940;      % same for DCE
vcppb = VC*62498;        % and for VC

% Flux of TCE and such into/out of the system
molTCEin=dt*4*pi*(R-dr)^2*FluxTCEss;
molDCEout=dt*4*pi*(R-dr)^2*FluxDCEss;
molVCout=dt*4*pi*(R-dr)^2*FluxVCss;        % mMoles per time step leaving/entering bead
% Degradation of TCE and others in the bead


TCEf = tceppb(1,:);
DCEf = dceppb(1,:);
VCf = vcppb(1,:);
TCEfin = TCEf';
DCEfin = DCEf';
```

```
VCfin = VCf';
arfin = ar';

mMTCE = zeros(nodes,1);
mMDCE = zeros(nodes,1);
mMVC = zeros(nodes,1);

Vol = zeros(1,m);
for(x = 1:m)
   r = dr*(x-1);

if(r==0)
r = .000001;
end

   Vol(x) = (4/3)*pi*r*r*r;

   if(x<2)
   mMTCE(x) = TCE(1,x)*Vol(x);
   mmDCE(x) = DCE(1,x)*Vol(x);
   mmVC(x) = VC(1,x)*Vol(x);
   else
    mMTCE(x) = TCE(1,x)*(Vol(x)-Vol(x-1));
    mMDCE(x) = DCE(1,x)*(Vol(x)-Vol(x-1));
    mMVC(x) = VC(1,x)*(Vol(x)-Vol(x-1));
   end
end

ssmolTCE = sum(mMTCE);      % total mMoles of TCE in bead at SS
ssmolDCE = sum(mMDCE);      % total mMoles of DCE in bead at SS
ssmolVC = sum(mMVC);        % total mMoles of VC in bead at SS


extra = zeros(1,m+1);  % extra is moles in, moles degraded, moles present
extra(1) = molTCEin; extra(2) = molDCEout; extra(3)=molVCout;
extra(4) = TCEss; extra(5) = DCEss; extra(6)=VCss;
extra(7)=ssmolTCE; extra(8)=ssmolDCE; extra(9)=ssmolVC;
extra(9) = pwr;
finicky = [arfin,TCEfin,DCEfin,VCfin,extra',rateTCE',rateDCEdeg',rateVCdeg'];  % Write all these variables to one variable

filename = ['R is' num2str(R) 'dm with' num2str(unit) 'e' num2str(pwr) 'cells.xlsx'];  % The radius is R cm
xlswrite(filename,finicky);
end
```

This function was called by an additional MATLAB file, which input several cell concentrations and bead radii.

```
r = [1 1 1 1 1 0.5 0.5 0.5 0.5 0.5]*0.1;  % 0.1 factor is to convert cm to dm
unit = [1 1 1 1 1 1 1 1 1 1];                              % unit and power of cell concentration
pwr = [7 8 9 10 11 7 8 9 10 11];            % This will be unitx10^(power)


parfor i = 1:length(r)
   beaddegAq_Theory(r(i), unit(i), pwr(i));
end
```

Degradation rates for a variety of biobead sizes and cell concentrations are shown:

R is 1.5 cm		R is 1.5 cm		R is 1.5 cm		R is 1.5 cm		R is 1.5 cm	
XmL = 1e7 cells/mL		XmL = 5e7 cells/mL		XmL = 1e8 cells/mL		XmL = 1.5e8 cells/mL		XmL = 5e8 cells/mL	
mmoles per day		mmoles per day		mmoles per day		mmoles per day		mmoles per day	
TCE in	3.3022E-06	TCE in	7.4516E-06	TCE in	1.0411E-05	TCE in	1.2597E-05	TCE in	2.155E-05
DCE out	2.9912E-06	DCE out	6.3466E-06	DCE out	8.586E-06	DCE out	1.0149E-05	DCE out	1.5571E-05
VC out	2.8153E-07	VC out	8.8507E-07	VC out	1.3632E-06	VC out	1.7719E-06	VC out	4.1577E-06
TCE degraded	3.457E-06	TCE degraded	8.2277E-06	TCE degraded	1.1964E-05	TCE degraded	1.4927E-05	TCE degraded	2.9318E-05
DCE degraded	3.1111E-07	DCE degraded	1.1109E-06	DCE degraded	1.8434E-06	DCE degraded	2.481E-06	DCE degraded	6.1751E-06
VC degraded	2.9272E-08	VC degraded	2.1967E-07	VC degraded	4.6233E-07	VC degraded	6.7642E-07	VC degraded	1.8266E-06
R is 1.25 cm		R is 1.25 cm		R is 1.25 cm		R is 1.25 cm		R is 1.25 cm	
XmL = 1e7 cells/mL		XmL = 5e7 cells/mL		XmL = 1e8 cells/mL		XmL = 1.5e8 cells/mL		XmL = 5e8 cells/mL	
mmoles per day		mmoles per day		mmoles per day		mmoles per day		mmoles per day	
TCE in	2.2707E-06	TCE in	5.1872E-06	TCE in	7.2854E-06	TCE in	8.8456E-06	TCE in	1.5346E-05
DCE out	2.0843E-06	DCE out	4.4837E-06	DCE out	6.1164E-06	DCE out	7.2788E-06	DCE out	1.1563E-05
VC out	1.7184E-07	VC out	5.8328E-07	VC out	9.0553E-07	VC out	1.1657E-06	VC out	2.6481E-06
TCE degraded	2.3601E-06	TCE degraded	5.6363E-06	TCE degraded	8.184E-06	TCE degraded	1.0194E-05	TCE degraded	1.9841E-05
DCE degraded	1.8637E-07	DCE degraded	7.0619E-07	DCE degraded	1.1774E-06	DCE degraded	1.5826E-06	DCE degraded	3.8796E-06
VC degraded	1.4434E-08	VC degraded	1.2012E-07	VC degraded	2.6337E-07	VC degraded	4.0116E-07	VC degraded	1.138E-06
R is 1.0 cm		R is 1.0 cm		R is 1.0 cm		R is 1.0 cm		R is 1.0 cm	
XmL = 1e7 cells/mL		XmL = 5e7 cells/mL		XmL = 1e8 cells/mL		XmL = 1.5e8 cells/mL		XmL = 5e8 cells/mL	
mmoles per day		mmoles per day		mmoles per day		mmoles per day		mmoles per day	
TCE in	1.4288E-06	TCE in	3.3182E-06	TCE in	4.6887E-06	TCE in	5.7188E-06	TCE in	1.006E-05
DCE out	1.3319E-06	DCE out	2.9176E-06	DCE out	4.0129E-06	DCE out	4.8078E-06	DCE out	7.886E-06
VC out	9.106E-08	VC out	3.4454E-07	VC out	5.474E-07	VC out	7.0683E-07	VC out	1.5432E-06
TCE degraded	1.4744E-06	TCE degraded	3.548E-06	TCE degraded	5.1487E-06	TCE degraded	6.4104E-06	TCE degraded	1.2362E-05
DCE degraded	9.6907E-08	DCE degraded	4.0153E-07	DCE degraded	6.7898E-07	DCE degraded	9.1433E-07	DCE degraded	2.2141E-06
VC degraded	5.832E-09	VC degraded	5.5943E-08	VC degraded	1.2804E-07	VC degraded	2.0075E-07	VC degraded	6.3212E-07
R is 0.75cm		R is 0.75cm		R is 0.75cm		R is 0.75cm		R is 0.75cm	
XmL = 1e7 cells/mL		XmL = 5e7 cells/mL		XmL = 1e8 cells/mL		XmL = 1.5e8 cells/mL		XmL = 5e8 cells/mL	
mmoles per day		mmoles per day		mmoles per day		mmoles per day		mmoles per day	
TCE in	7.785E-07	TCE in	1.8542E-06	TCE in	2.6409E-06	TCE in	3.2335E-06	TCE in	5.7841E-06
DCE out	7.3852E-07	DCE out	1.6658E-06	DCE out	2.3117E-06	DCE out	2.7865E-06	DCE out	4.7117E-06
VC out	3.8231E-08	VC out	1.6845E-07	VC out	2.8037E-07	VC out	3.6803E-07	VC out	7.86E-07
TCE degraded	7.976E-07	TCE degraded	1.951E-06	TCE degraded	2.8348E-06	TCE degraded	3.5247E-06	TCE degraded	6.7549E-06
DCE degraded	3.9922E-08	DCE degraded	1.886E-07	DCE degraded	3.3004E-07	DCE degraded	4.4885E-07	DCE degraded	1.085E-06
VC degraded	1.6978E-09	VC degraded	1.9892E-08	VC degraded	4.852E-08	VC degraded	7.8888E-08	VC degraded	2.8657E-07

R is 0.5cm		R is 0.5cm		R is 0.5cm		R is 0.5cm		R is 0.5cm	
XmL = 1e7 cells/mL		XmL = 5e7 cells/mL		XmL = 1e8 cells/mL		XmL = 1.5e8 cells/mL		XmL = 5e8 cells/mL	
mmoles per day		mmoles per day		mmoles per day		mmoles per day		mmoles per day	
TCE in	3.2189E-07	TCE in	8.0611E-07	TCE in	1.1628E-06	TCE in	1.4332E-06	TCE in	2.615E-06
DCE out	3.1138E-07	DCE out	7.4579E-07	DCE out	1.0492E-06	DCE out	1.2738E-06	DCE out	2.2173E-06
VC out	1.0235E-08	VC out	5.6177E-08	VC out	1.0224E-07	VC out	1.3991E-07	VC out	3.1517E-07
TCE degraded	3.2742E-07	TCE degraded	8.3465E-07	TCE degraded	1.2202E-06	TCE degraded	1.5194E-06	TCE degraded	2.9025E-06
DCE degraded	1.0496E-08	DCE degraded	6.0323E-08	DCE degraded	1.1367E-07	DCE degraded	1.5962E-07	DCE degraded	4.0005E-07
VC degraded	2.6676E-10	VC degraded	4.1264E-09	VC degraded	1.1292E-08	VC degraded	1.9406E-08	VC degraded	8.2413E-08
R is 0.25cm		R is 0.25cm		R is 0.25cm		R is 0.25cm		R is 0.25cm	
XmL = 1e7 cells/mL		XmL = 5e7 cells/mL		XmL = 1e8 cells/mL		XmL = 1.5e8 cells/mL		XmL = 5e8 cells/mL	
mmoles per day		mmoles per day		mmoles per day		mmoles per day		mmoles per day	
TCE in	6.1105E-08	TCE in	1.843E-07	TCE in	2.7541E-07	TCE in	3.4484E-07	TCE in	6.5264E-07
DCE out	6.0346E-08	DCE out	1.7744E-07	DCE out	2.6049E-07	DCE out	3.2211E-07	DCE out	5.8403E-07
VC out	7.4983E-10	VC out	6.6554E-09	VC out	1.4205E-08	VC out	2.1356E-08	VC out	6.0897E-08
TCE degraded	6.1739E-08	TCE degraded	1.8779E-07	TCE degraded	2.8249E-07	TCE degraded	3.5552E-07	TCE degraded	6.8851E-07
DCE degraded	7.5763E-10	DCE degraded	6.8533E-09	DCE degraded	1.4905E-08	DCE degraded	2.2707E-08	DCE degraded	6.8692E-08
VC degraded	8.456E-12	VC degraded	2.0089E-10	VC degraded	6.7545E-10	VC degraded	1.3141E-09	VC degraded	7.6327E-09
R is 0.125cm		R is 0.125cm		R is 0.125cm		R is 0.125cm		R is 0.125cm	
XmL = 1e7 cells/mL		XmL = 5e7 cells/mL		XmL = 1e8 cells/mL		XmL = 1.5e8 cells/mL		XmL = 5e8 cells/mL	
mmoles per day		mmoles per day		mmoles per day		mmoles per day		mmoles per day	
TCE in	8.6629E-09	TCE in	3.6462E-08	TCE in	5.9667E-08	TCE in	7.7328E-08	TCE in	1.5596E-07
DCE out	8.6322E-09	DCE out	3.5921E-08	DCE out	5.8216E-08	DCE out	7.4899E-08	DCE out	1.4652E-07
VC out	3.0501E-11	VC out	5.3368E-10	VC out	1.4182E-09	VC out	2.3616E-09	VC out	8.9188E-09
TCE degraded	8.7387E-09	TCE degraded	3.6864E-08	TCE degraded	6.0512E-08	TCE degraded	7.8623E-08	TCE degraded	1.604E-07
DCE degraded	3.063E-11	DCE degraded	5.4003E-10	DCE degraded	1.4484E-09	DCE degraded	2.4251E-09	DCE degraded	9.4234E-09
VC degraded	1.5527E-13	VC degraded	6.7998E-12	VC degraded	2.7301E-11	VC degraded	5.9003E-11	VC degraded	4.8927E-10
R is 0.0625		R is 0.0625		R is 0.0625		R is 0.0625		R is 0.0625	
XmL = 1e7 cells/mL		XmL = 5e7 cells/mL		XmL = 1e8 cells/mL		XmL = 1.5e8 cells/mL		XmL = 5e8 cells/mL	
mmoles per day		mmoles per day		mmoles per day		mmoles per day		mmoles per day	
TCE in	1.11E-09	TCE in	1.11E-09	TCE in	1.0214E-08	TCE in	1.4488E-08	TCE in	3.4479E-08
DCE out	1.109E-09	DCE out	1.109E-09	DCE out	1.0129E-08	DCE out	1.4318E-08	DCE out	3.3511E-08
VC out	1.0126E-12	VC out	1.0126E-12	VC out	8.414E-11	VC out	1.6888E-10	VC out	9.4665E-10
TCE degraded	1.1194E-09	TCE degraded	1.1194E-09	TCE degraded	1.0311E-08	TCE degraded	1.4636E-08	TCE degraded	3.5014E-08
DCE degraded	1.0119E-12	DCE degraded	1.0119E-12	DCE degraded	8.468E-11	DCE degraded	1.7034E-10	DCE degraded	9.6604E-10
VC degraded	1.7534E-15	VC degraded	1.7534E-15	VC degraded	7.3862E-13	VC degraded	1.8399E-12	VC degraded	2.1014E-11

Table A1: *Degradation rates in biobeads with cell loadings from 1E7 to 5E8 cells/mL*

R is 1.5 cm		R is 1.5 cm		R is 1.5 cm		R is 1.5 cm		R is 1.5 cm		R is 1.5 cm	
XmL = 1E9 cells/mL		XmL = 5e9 cells/mL		XmL = 1e10 cells/mL		XmL = 1.5e10cells/mL		XmL = 5e10 cells/mL		XmL = 1e11 cells/mL	
mmoles per day		mmoles per day		mmoles per day		mmoles per day		mmoles per day		mmoles per day	
TCE in	2.854E-05	TCE in	5.2052E-05	TCE in	3.0449E-05	TCE in	3.0964E-05	TCE in	3.4698E-05	TCE in	3.9131E-05
DCE out	1.8308E-05	DCE out	1.269E-05	DCE out	4.2183E-05	DCE out	0	DCE out	0.00015917	DCE out	0.00028175
VC out	7.0913E-06	VC out	2.9586E-05	VC out	7.4215E-05	VC out	0.00012213	VC out	0.00046213	VC out	0.00092346
TCE degraded	4.4077E-05	TCE degraded	0.00014649	TCE degraded	0.00022621	TCE degraded	0.00036639	TCE degraded	0.00118114	TCE degraded	0.00225582
DCE degraded	1.0768E-05	DCE degraded	4.6818E-05	DCE degraded	0.00011389	DCE degraded	0.00018547	DCE degraded	0.00069898	DCE degraded	0.00140771
VC degraded	3.1574E-06	VC degraded	1.2168E-05	VC degraded	2.559E-05	VC degraded	3.9118E-05	VC degraded	0.00012847	VC degraded	0.00024849
R is 1.25 cm		R is 1.25 cm		R is 1.25 cm		R is 1.25 cm		R is 1.25 cm		R is 1.25 cm	
XmL = 1E9 cells/mL		XmL = 5e9 cells/mL		XmL = 1e10 cells/mL		XmL = 1.5e10cells/mL		XmL = 5e10 cells/mL		XmL = 1e11 cells/mL	
mmoles per day		mmoles per day		mmoles per day		mmoles per day		mmoles per day		mmoles per day	
TCE in	2.0583E-05	TCE in	3.6334E-05	TCE in	4.0709E-05	TCE in	2.5426E-05	TCE in	2.761E-05	TCE in	3.0455E-05
DCE out	1.4171E-05	DCE out	1.2861E-05	DCE out	3.7696E-06	DCE out	0.00012754	DCE out	0.00034403	DCE out	0.00061264
VC out	4.446E-06	VC out	1.6929E-05	VC out	3.6838E-05	VC out	6.4685E-05	VC out	0.00026152	VC out	0.00053869
TCE degraded	2.9574E-05	TCE degraded	8.426E-05	TCE degraded	0.00014365	TCE degraded	0.00018764	TCE degraded	0.00069353	TCE degraded	0.00134228
DCE degraded	6.6754E-06	DCE degraded	2.6706E-05	DCE degraded	5.7939E-05	DCE degraded	9.9372E-05	DCE degraded	0.0003952	DCE degraded	0.000817
VC degraded	1.9733E-06	VC degraded	7.2538E-06	VC degraded	1.4205E-05	VC degraded	2.2177E-05	VC degraded	7.5034E-05	VC degraded	0.00014679
R is 1.0 cm		R is 1.0 cm		R is 1.0 cm		R is 1.0 cm		R is 1.0 cm		R is 1.0 cm	
XmL = 1E9 cells/mL		XmL = 5e9 cells/mL		XmL = 1e10 cells/mL		XmL = 1.5e10cells/mL		XmL = 5e10 cells/mL		XmL = 1e11 cells/mL	
mmoles per day		mmoles per day		mmoles per day		mmoles per day		mmoles per day		mmoles per day	
TCE in	1.3664E-05	TCE in	2.5252E-05	TCE in	3.1478E-05	TCE in	3.8957E-05	TCE in	2.1186E-05	TCE in	2.276E-05
DCE out	1.0019E-05	DCE out	1.2258E-05	DCE out	8.5827E-06	DCE out	6.7997E-05	DCE out	0.00018977	DCE out	0.00033817
VC out	2.5389E-06	VC out	9.0491E-06	VC out	1.7344E-05	VC out	2.7754E-05	VC out	0.00012783	VC out	0.00027232
TCE degraded	1.8268E-05	TCE degraded	4.8272E-05	TCE degraded	8.232E-05	TCE degraded	0.00012775	TCE degraded	0.00035937	TCE degraded	0.00070364
DCE degraded	3.7551E-06	DCE degraded	1.4104E-05	DCE degraded	2.7442E-05	DCE degraded	4.3503E-05	DCE degraded	0.00019343	DCE degraded	0.00041168
VC degraded	1.109E-06	VC degraded	3.9766E-06	VC degraded	7.2556E-06	VC degraded	1.083E-05	VC degraded	3.8629E-05	VC degraded	7.6399E-05
R is 0.75cm		R is 0.75cm		R is 0.75cm		R is 0.75cm		R is 0.75cm		R is 0.75cm	
XmL = 1E9 cells/mL		XmL = 5e9 cells/mL		XmL = 1e10 cells/mL		XmL = 1.5e10cells/mL		XmL = 5e10 cells/mL		XmL = 1e11 cells/mL	
mmoles per day		mmoles per day		mmoles per day		mmoles per day		mmoles per day		mmoles per day	
TCE in	7.9574E-06	TCE in	1.5524E-05	TCE in	1.9639E-05	TCE in	2.1473E-05	TCE in	1.5339E-05	TCE in	1.6042E-05
DCE out	6.1791E-06	DCE out	9.4158E-06	DCE out	8.9078E-06	DCE out	7.1327E-06	DCE out	0.00013081	DCE out	0.00013081
VC out	1.2566E-06	VC out	4.236E-06	VC out	7.4968E-06	VC out	1.0954E-05	VC out	4.9261E-05	VC out	0.0001094
TCE degraded	9.8993E-06	TCE degraded	2.5235E-05	TCE degraded	3.9016E-05	TCE degraded	4.9363E-05	TCE degraded	0.00015303	TCE degraded	0.00030242
DCE degraded	1.814E-06	DCE degraded	6.4772E-06	DCE degraded	1.1733E-05	DCE degraded	1.731E-05	DCE degraded	7.5004E-05	DCE degraded	0.00016544
VC degraded	5.2275E-07	VC degraded	1.8836E-06	VC degraded	3.2821E-06	VC degraded	4.6613E-06	VC degraded	1.6276E-05	VC degraded	3.2566E-05

R is 0.5cm		R is 0.5cm		R is 0.5cm		R is 0.5cm		R is 0.5cm		R is 0.5cm	
XmL = 1E9 cells/mL		XmL = 5e9 cells/mL		XmL = 1e10 cells/mL		XmL = 1.5e10cells/mL		XmL = 5e10 cells/mL		XmL = 1e11 cells/mL	
mmoles per day		mmoles per day		mmoles per day		mmoles per day		mmoles per day		mmoles per day	
TCE in	3.6478E-06	TCE in	7.5085E-06	TCE in	9.9031E-06	TCE in	1.1473E-05	TCE in	1.465E-05	TCE in	1.0197E-05
DCE out	2.9913E-06	DCE out	5.3489E-06	DCE out	6.1959E-06	DCE out	6.3384E-06	DCE out	2.6086E-06	DCE out	2.9809E-05
VC out	4.8574E-07	VC out	1.5001E-06	VC out	2.5699E-06	VC out	3.5664E-06	VC out	1.1065E-05	VC out	2.7811E-05
TCE degraded	4.2231E-06	TCE degraded	1.0386E-05	TCE degraded	1.5658E-05	TCE degraded	2.0104E-05	TCE degraded	4.5689E-05	TCE degraded	7.6232E-05
DCE degraded	6.6359E-07	DCE degraded	2.2361E-06	DCE degraded	3.9151E-06	DCE degraded	5.5039E-06	DCE degraded	1.7514E-05	DCE degraded	4.2786E-05
VC degraded	1.7087E-07	VC degraded	6.6178E-07	VC degraded	1.1438E-06	VC degraded	1.5786E-06	VC degraded	4.4867E-06	VC degraded	9.4464E-06
R is 0.25cm		R is 0.25cm		R is 0.25cm		R is 0.25cm		R is 0.25cm		R is 0.25cm	
XmL = 1E9 cells/mL		XmL = 5e9 cells/mL		XmL = 1e10 cells/mL		XmL = 1.5e10cells/mL		XmL = 5e10 cells/mL		XmL = 1e11 cells/mL	
mmoles per day		mmoles per day		mmoles per day		mmoles per day		mmoles per day		mmoles per day	
TCE in	9.2814E-07	TCE in	2.0243E-06	TCE in	2.7809E-06	TCE in	3.3226E-06	TCE in	5.3779E-06	TCE in	6.7809E-06
DCE out	8.0921E-07	DCE out	1.641E-06	DCE out	2.1399E-06	DCE out	2.4547E-06	DCE out	3.1623E-06	DCE out	2.8651E-06
VC out	1.0045E-07	VC out	2.8071E-07	VC out	4.5123E-07	VC out	6.0514E-07	VC out	1.5372E-06	VC out	2.7409E-06
TCE degraded	9.9998E-07	TCE degraded	2.386E-06	TCE degraded	3.4999E-06	TCE degraded	4.4014E-06	TCE degraded	8.9747E-06	TCE degraded	1.4137E-05
DCE degraded	1.1929E-07	DCE degraded	3.9137E-07	DCE degraded	6.5472E-07	DCE degraded	8.9291E-07	DCE degraded	2.3584E-06	DCE degraded	4.3037E-06
VC degraded	1.8392E-08	VC degraded	1.0526E-07	VC degraded	1.8998E-07	VC degraded	2.6337E-07	VC degraded	6.8265E-07	VC degraded	1.1943E-06
R is 0.125cm		R is 0.125cm		R is 0.125cm		R is 0.125cm		R is 0.125cm		R is 0.125cm	
XmL = 1E9 cells/mL		XmL = 5e9 cells/mL		XmL = 1e10 cells/mL		XmL = 1.5e10cells/mL		XmL = 5e10 cells/mL		XmL = 1e11 cells/mL	
mmoles per day		mmoles per day		mmoles per day		mmoles per day		mmoles per day		mmoles per day	
TCE in	2.2707E-07	TCE in	5.1872E-07	TCE in	7.2854E-07	TCE in	8.8456E-07	TCE in	1.5346E-06	TCE in	2.0583E-06
DCE out	2.0843E-07	DCE out	4.4837E-07	DCE out	6.1164E-07	DCE out	7.2788E-07	DCE out	1.1563E-06	DCE out	1.4171E-06
VC out	1.7163E-08	VC out	5.8304E-08	VC out	9.0544E-08	VC out	1.1657E-07	VC out	2.6481E-07	VC out	4.446E-07
TCE degraded	2.3601E-07	TCE degraded	5.6363E-07	TCE degraded	8.184E-07	TCE degraded	1.0194E-06	TCE degraded	1.9841E-06	TCE degraded	2.9574E-06
DCE degraded	1.8637E-08	DCE degraded	7.0619E-08	DCE degraded	1.1774E-07	DCE degraded	1.5826E-07	DCE degraded	3.8796E-07	DCE degraded	6.6754E-07
VC degraded	1.442E-09	VC degraded	1.2008E-08	VC degraded	2.6335E-08	VC degraded	4.0116E-08	VC degraded	1.138E-07	VC degraded	1.9733E-07
R is 0.0625		R is 0.0625		R is 0.0625		R is 0.0625		R is 0.0625		R is 0.0625	
XmL = 1E9 cells/mL		XmL = 5e9 cells/mL		XmL = 1e10 cells/mL		XmL = 1.5e10cells/mL		XmL = 5e10 cells/mL		XmL = 1e11 cells/mL	
mmoles per day		mmoles per day		mmoles per day		mmoles per day		mmoles per day		mmoles per day	
TCE in	5.2588E-08	TCE in	1.2776E-07	TCE in	1.8295E-07	TCE in	2.2465E-07	TCE in	4.0552E-07	TCE in	5.6164E-07
DCE out	5.0368E-08	DCE out	1.1633E-07	DCE out	1.6235E-07	DCE out	1.9634E-07	DCE out	3.3685E-07	DCE out	4.4819E-07
VC out	2.146E-09	VC out	1.0428E-08	VC out	1.8032E-08	VC out	2.4049E-08	VC out	5.1996E-08	VC out	8.1437E-08
TCE degraded	5.3685E-08	TCE degraded	1.3335E-07	TCE degraded	1.9416E-07	TCE degraded	2.4148E-07	TCE degraded	4.6171E-07	TCE degraded	6.7401E-07
DCE degraded	2.2184E-09	DCE degraded	1.1431E-08	DCE degraded	2.0625E-08	DCE degraded	2.8382E-08	DCE degraded	6.9275E-08	DCE degraded	1.1517E-07
VC degraded	7.5045E-11	VC degraded	9.9886E-10	VC degraded	2.5577E-09	VC degraded	4.2526E-09	VC degraded	1.6683E-08	VC degraded	3.2039E-08

Table A2: *Degradation rates in biobeads with cell loadings from 1E9 to 1E11 cells/mL*

Appendix B: Diffusion Data

Diffusion data includes the final thickness (cm) of the membrane averaged over five measurements with calipers. Also included are the sink compartment volume (mL), concentration of solute in the source compartment (ppm), membrane cross sectional area (cm^2), and change in sink concentration with time ($\frac{d(ppm)}{d(t)}$). These values are used with Equation 1 to determine effective diffusivity, D_e ($\frac{cm^2}{sec}$).

Caffeine Diffusion

Calibration: Caffeine was diluted from 775ppm in DI water down to 155ppm. The ThermoFisher Evolution UV-Vis Spectrophotometer was blanked with deionized water, providing the zero point.

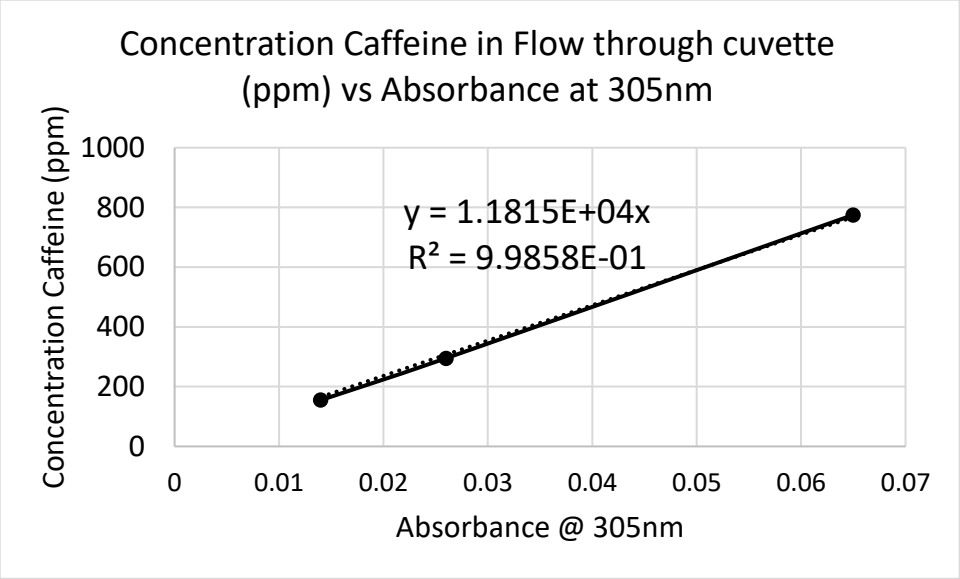

Figure B1: *Calibration curve for Caffeine*

Conc (ppm)	Abs @ 305nm
775	0.065
295.238095	0.026
155	0.014
0	0

Table B.1: *Caffeine Dilution/calibration data*

Caffeine diffusion in 10% PVA 2% SA membranes (chemically crosslinked in saturated boric acid, 2% (w/v) $CaCl_2$ for 4.5 hours). Diffusion carried out in deionized water.

Caffeine Diffusion A													
4/11/19													
Jonathan 'Jonny' Counts - 10% PVA 2%SA Crosslinked in Sat. boric acid 2% (w/v) CaCl2 for 4.5 hours. Equilibrated in water for 1 hour													
Run was conducted in DI water													
Post Experiment Membrane thickness													
	Initial	0.805	Real (in)		Vsink	z (cm)	d(ppm)/dt	Area (cm^2)	Csource (ppm)				
	1	1.293	1.293		19	1.2156	37.566	7.0709	3100				
	2	1.266	1.266										
	3	1.32	1.32		De								
	4	1.245	1.245		1.0995E-05								
	5	1.294	1.294										
		Ave (in)	1.2836										
		Ave (cm)	3.260344										
Caffeine Diffusion C													
4/15/19													
Jonathan 'Jonny' Counts - 10% PVA 2%SA Crosslinked in Sat. boric acid 2% (w/v) CaCl2 for 4.5 hours. Equilibrated in water for 1 hour													
Run was conducted in DI water													
Post Expt Membrane thick													
	Initial	0.802	Real (in)		Vsink	z (cm)	d(ppm)/dt	Area (cm^2)	Csource (ppm)				
	1	1.226	0.424		36	1.083564	20.397	7.0709	3100				
	2	1.236	0.434										
	3	1.224	0.422		De								
	4	1.24	0.438		1.0083E-05								
	5	1.217	0.415										
		Ave (in)	0.4266										
		Ave (cm)	1.083564										
Caffeine Diffusion D													
4/24/19 Jonathan 'Jonny' Counts - 10% PVA 2%SA Crosslinked in Sat. boric acid 2% (w/v) CaCl2 for 4.5 hours. Equilibrated in water for 1 hour													
Run was conducted in DI water													
Pre Expt Membrane thick					Post Expt Membrane thick								
Initial	0.804	Real (in)		Initial	0.805	Real (in)		Vsink	z (cm)	d(ppm)/dt	Area (cm^2)	Csource (ppm)	
1	1.191	1.191		1	1.29	1.29		38.2	1.095	19.758	7.0709	3100	
2	1.178	1.178		2	1.288	1.288							
3	1.168	1.168		3	1.296	1.296		De					
4	1.17	1.17		4	1.305	1.305		1.047E-05					
5	1.183	1.183		5	1.287	1.287							
	Ave (in)	1.178			Ave (in)	1.2932							
	Ave (cm)	2.99212			Ave (cm)	3.284728							
	% Swell	9.77928693											
	Ave z (cm)	3.138424											
Caffeine Diffusion E													
4/27/19 Jonathan 'Jonny' Counts - 10% PVA 2%SA Crosslinked in Sat. boric acid 2% (w/v) CaCl2 for 4.5 hours. Equilibrated in water for 1 hour													
Run was conducted in DI water													
Pre Expt Membrane thick					Post Expt Membrane thick								
Initial	0.805	Real (in)		Initial	0.8	Real (in)		Vsink	z (cm)	d(ppm)/dt	Area (cm^2)	Csource (ppm)	
1	1.165	0.36		1	1.214	0.414		38.1	0.971042	22.502	7.0709	3100	
2	1.168	0.363		2	1.186	0.386							
3	1.161	0.356		3	1.209	0.409		De					
4	1.161	0.356		4	1.211	0.411		1.055E-05					
5	1.165	0.36		5	1.208	0.408							
	Ave (in)	0.359			Ave (in)	0.4056							
	Ave (cm)	0.91186			Ave (cm)	1.030224							
	% Swell	12.9805014											
	Ave z (cm)	0.971042											

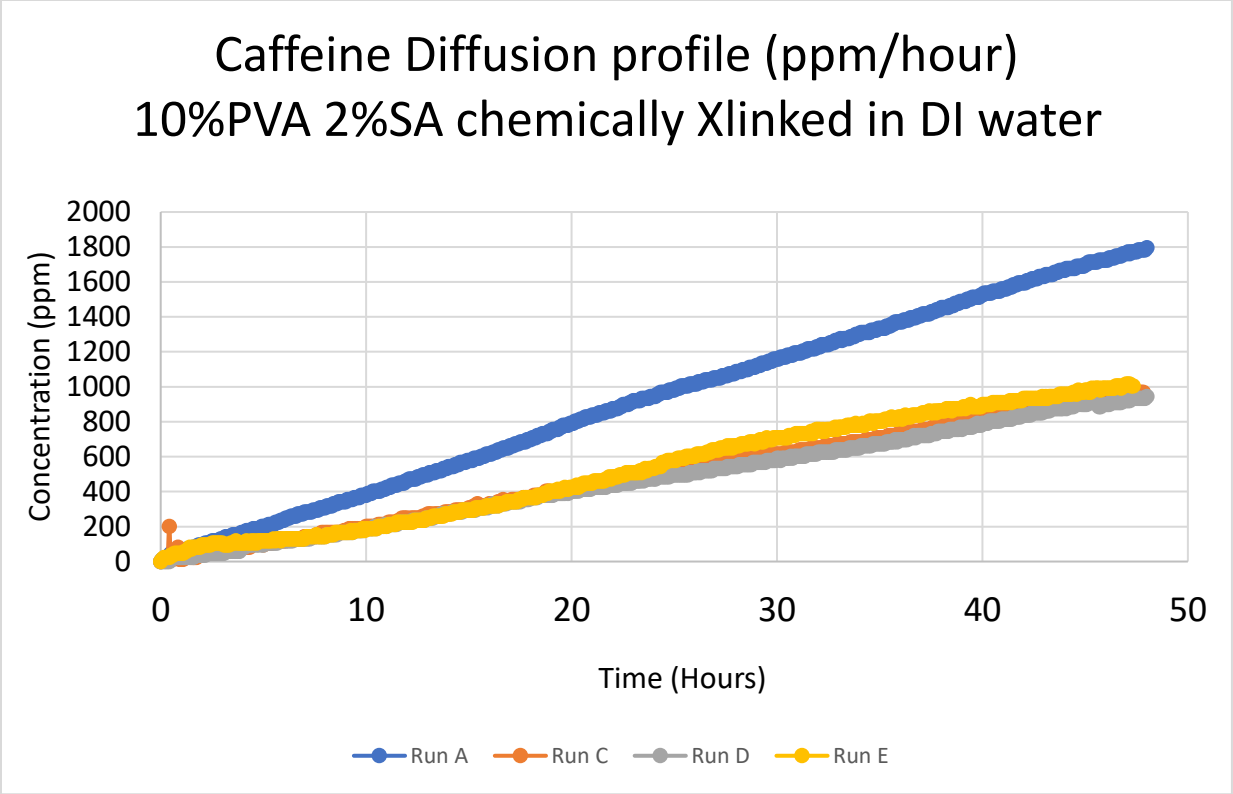

Figure B.2: *Concentration profile for caffeine diffusion*

Caffeine diffusion in 10% PVA 2% SA membranes (physically crosslinked by 5 freeze/thaw cycles of 1 hour each). Diffusion carried out in deionized water.

Run A													
9/24/19													
Caffeine Diffusion through 10% PVA 2% SA Membrane (F/T 5x in -20C freezer)													
Pre Expt Membrane thick				Post Expt Membrane thick									
	Initial	0.839	Real (in)		Initial	0.844	Real (in)		Vsink	z (cm)	d(M)/dt	Area (cm^2)	Csource (ppm)
	1	1.175	0.336		1	1.197	0.353		39.8	0.919988	9.9194	7.0709	3100
	2	1.217	0.378		2	1.231	0.387						
	3	1.175	0.336		3	1.238	0.394		De				
	4	1.195	0.356		4	1.183	0.339		4.6027E-06				
	5	1.177	0.338		5	1.249	0.405						
		Ave (in)	0.3488			Ave (in)	0.3756						
		Ave (cm)	0.885952			Ave (cm)	0.954024						
		% Swell	7.68348624										
Run B													
43734													
Caffeine Diffusion through 10% PVA 2% SA Membrane (F/T 5x in -20C freezer)													
Pre Expt Membrane thick				Post Expt Membrane thick									
	Initial	0.851	Real (in)		Initial	0.84	Real (in)		Vsink	z (cm)	d(ppm)/dt	Area (cm^2)	Csource (ppm)
	1	1.184	0.333		1	1.258	0.418		38.3	0.97282	14.019	7.0709	3100
	2	1.199	0.348		2	1.262	0.422						
	3	1.209	0.358		3	1.258	0.418		De				
	4	1.205	0.354		4	1.277	0.437		6.6193E-06				
	5	1.198	0.347		5	1.235	0.395						
		Ave (in)	0.348			Ave (in)	0.418						
		Ave (cm)	0.88392			Ave (cm)	1.06172						
		% Swell	20.1149425										
Run C													
9/27/19													
Caffeine Diffusion through 10% PVA 2% SA membrane (Freeze/Thawed 5x in -20C freezer)													
Pre Expt Membrane thick				Post Expt Membrane thick									
	Initial	0.839	Real (in)		Initial	0.842	Real (in)		Vsink	z (cm)	d(ppm)/dt	Area (cm^2)	Csource (ppm)
	1	1.182	0.343		1	1.217	0.375		45	0.922528	1.31E+01	7.0709	3100
	2	1.167	0.328		2	1.245	0.403						
	3	1.17	0.331		3	1.235	0.393		De				
	4	1.184	0.345		4	1.238	0.396		6.89E-06				
	5	1.187	0.348		5	1.212	0.37						
		Ave (in)	0.339			Ave (in)	0.3874						
		Ave (cm)	0.86106			Ave (cm)	0.983996						
		% Swell	14.2772861										
Run D													
10/1/19													
Caffeine Diffusion through 10% PVA 2% SA membrane (Freeze/Thawed 5x in -20C freezer)													
Pre Expt Membrane thick				Post Expt Membrane thick									
	Initial	0.839	Real (in)		Initial	0.838	Real (in)		Vsink	z (cm)	d(ppm)/dt	Area (cm^2)	Csource (ppm)
	1	1.145	0.306		1	1.207	0.369		39.3	0.851916	11.877	7.0709	3100
	2	1.13	0.291		2	1.217	0.379						
	3	1.148	0.309		3	1.187	0.349		De				
	4	1.151	0.312		4	1.202	0.364		5.0391E-06				
	5	1.148	0.309		5	1.204	0.366						
		Ave (in)	0.3054			Ave (in)	0.3654						
		Ave (cm)	0.775716			Ave (cm)	0.928116						
		% Swell	19.6463654										

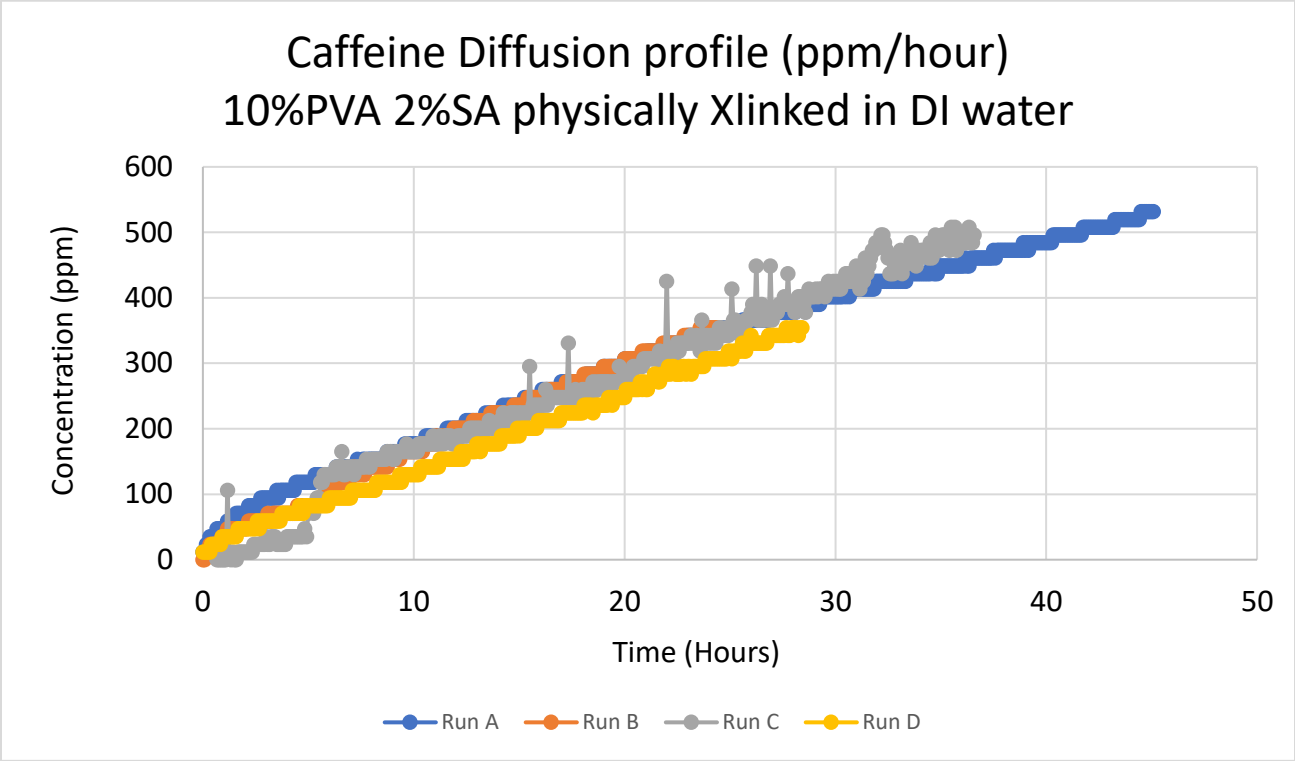

Figure B.3: *Caffeine concentration profile Freeze/Thawed*

Caffeine diffusion in 10% PVA 2% SA membranes (chemically crosslinked in saturated boric acid, 2% (w/v) $CaCl_2$ for 4.5 hours). Diffusion carried out in 0.5M KCl water.

Run A									
Run conducted in 0.5M KCl									
1/9/19 Jonathan 'Jonny' Counts Caffeine run through 10% PVA 2%SA Membrane Xlinked for 4.5 hours in Saturated boric acid 2% (w/v) CaCl2									
dC/dt	Membrane (cm)	V. sink	Membrane (cm^2)	C.source		De (cm^2/sec)			
7.98E+00	1.0678	30	7.079	3100		3.236E-06			
Membrane Pre Experiment					Membrane Post Experiment				
Initial	0.839				Initial	0.838			
1	1.248	Real in	0.409		1	1.273	Real in	0.435	
2	1.238		0.399		2	1.269		0.431	
3	1.246		0.407		3	1.266		0.428	
4	1.246		0.407		4	1.279		0.441	
5	1.245		0.406		5	1.279		0.441	
		Ave (in)	0.4056				Ave (in)	0.4352	
		Ave (cm)	1.030224				Ave (cm)	1.105408	
		Pre/Post Ave	1.067816						
Run B									
Run conducted in 0.5 M KCl water									
1/9/19 Jonathan 'Jonny' Counts Caffeine run through 10% PVA 2%SA Membrane Xlinked for 4.5 hours in Saturated boric acid 2% (w/v) CaCl2									
dC/dt	Membrane (cm)	V. sink	Membrane (cm^2)	C.source		De (cm^2/sec)			
11.824	0.993648	25.8	7.079	3100		3.8369E-06			
Membrane Pre Experiment					Membrane Post Experiment				
Initial	0.836				Initial	0.841			
1	1.186	Real in	0.35		1	1.237	Real in	0.396	
2	1.201		0.365		2	1.281		0.44	
3	1.2		0.364		3	1.323		0.482	
4	1.183		0.347		4	1.24		0.399	
5	1.18		0.344		5	1.266		0.425	
		Ave (in)	0.354		Ave (in)	0.4284			
		Ave (cm)	0.89916		Ave (cm)	1.088136			
		Pre/Post Ave	0.993648						
Run C									
Run conducted in 0.5M KCl									
1/11/19 Jonathan 'Jonny' Counts Caffeine run through 10% PVA 2%SA Membrane Xlinked for 4.5 hours in Saturated boric acid 2% (w/v) CaCl2									
dC/dt	Membrane (cm)	V. sink	Membrane (cm^2)	C.source		De (cm^2/sec)			
10.328	1.237	23	7.079	3100		3.71944E-06			
Membrane Post Experiment									
Initial	0.837								
1	1.304	Real in	0.467						
2	1.309		0.472						
3	1.345		0.508						
4	1.336		0.499						
5	1.327		0.49						
Ave (in)	0.4872								
Ave (cm)	1.237488								
Run D									
Run conducted in 0.5M KCl									
1/13/19 Jonathan 'Jonny' Counts Caffeine run through 10% PVA 2%SA Membrane Xlinked for 4.5 hours in Saturated boric acid 2% (w/v) CaCl2									
dC/dt	Membrane (cm)	V. sink	Membrane (cm^2)	C.source		De			
1.75E+01	0.5682	26.4	7.079	3100		3.331E-06	cm^2/s		
Membrane Pre Experiment					Membrane Post Experiment				
Initial	0.838				Initial	0.838			
1	1.032	Real in	0.194		1	1.086	Real in	0.248	
2	1.037		0.199		2	1.077		0.239	
3	1.033		0.195		3	1.094		0.256	
4	1.05		0.212		4	1.077		0.239	
5	1.04		0.202		5	1.091		0.253	
		Ave (in)	0.2004				Ave (in)	0.247	
		Ave (cm)	0.509016				Ave (cm)	0.62738	
		Pre/Post Ave	0.568198						

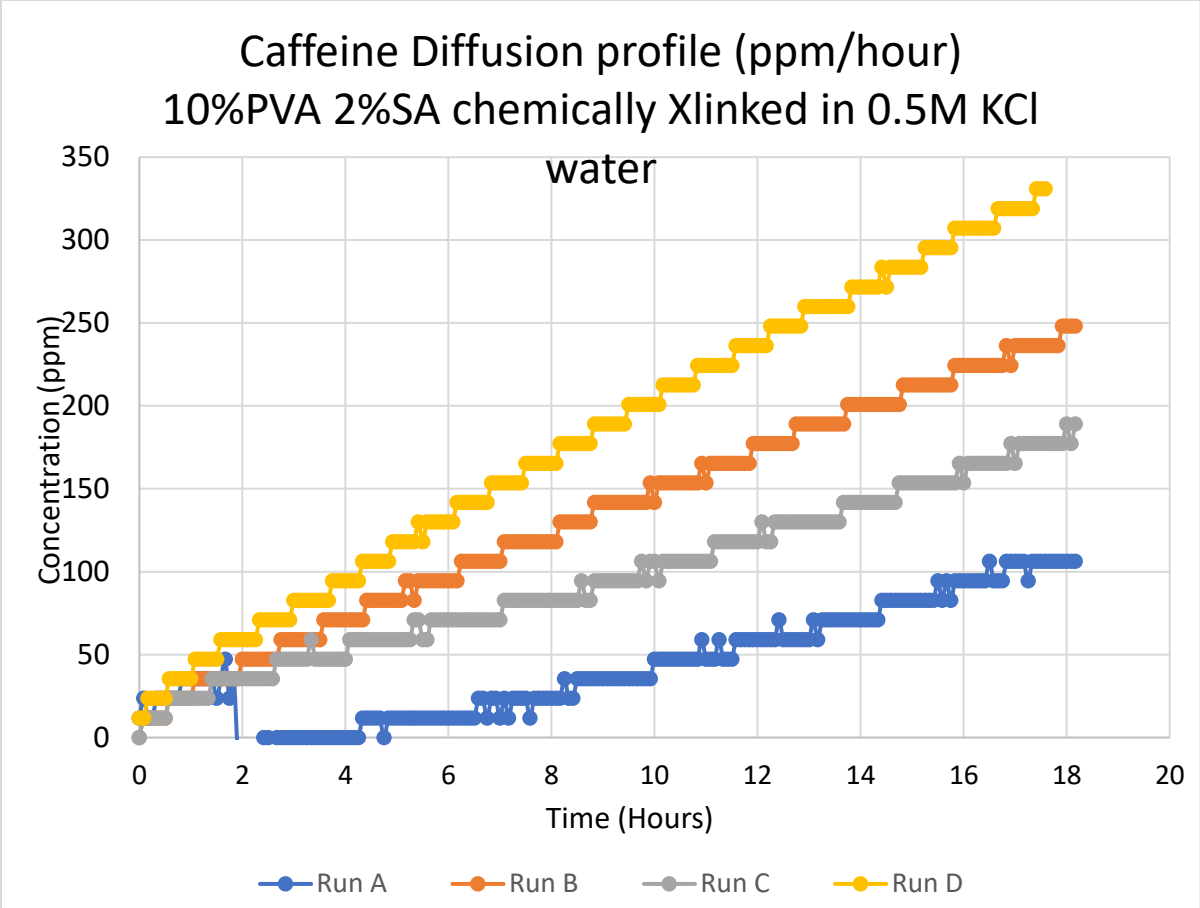

Figure B.4: *Concentration profile for caffeine (ionic)*

Caffeine diffusion in 10% PVA 2% SA membranes (physically crosslinked by 5 freeze/thaw cycles of 1 hour each). Diffusion carried out in 0.5M KCl water.

Run A													
3/18/20													
Jonathan 'Jonny' Counts - 10% PVA 2% SA Freeze/Thawed 5x in -20C. Equilibrated in 0.5M KCl for 4 hours													
Run was conducted in 0.5M KCl water													
Pre Expt Membrane thick				Post Expt Membrane thick									
	Initial	0.834	Real (in)		Initial	0.833	Real (in)		Vsink	z (cm)	d(ppm)/dt	Area (cm^2)	Csource (ppm)
	1	1.287	0.453		1	1.287	0.454		30.6	1.161288	10.931	7.0709	3100
	2	1.279	0.445		2	1.3	0.467						
	3	1.298	0.464		3	1.3	0.467		De				
	4	1.274	0.44		4	1.314	0.481		2.59E-06				
	5	1.26	0.426		5	1.308	0.475						
		Ave (in)	0.4456			Ave (in)	0.4688						
		Ave (cm)	1.131824			Ave (cm)	1.190752						
		% Swell	5.2064632										
		Ave z (cm)	1.161288										
Run B													
3/19/20													
Jonathan 'Jonny' Counts - 10% PVA 2% SA Freeze/Thawed 5x in -20C. Equilibrated in 0.5M KCl for 4 hours													
Run was conducted in 0.5M KCl water													
Pre Expt Membrane thick				Post Expt Membrane thick									
	Initial	0.834	Real (in)		Initial	0.834	Real (in)		Vsink	z (cm)	d(ppm)/dt	Area (cm^2)	Csource (ppm)
	1	1.255	0.453		1	1.276	0.454		26.3	1.161288	11.589	7.0709	3100
	2	1.272	0.445		2	1.266	0.467						
	3	1.263	0.464		3	1.278	0.467		De				
	4	1.261	0.44		4	1.285	0.481		4.4854E-06				
	5	1.275	0.426		5	1.249	0.475						
		Ave (in)	0.4456			Ave (in)	0.4688						
		Ave (cm)	1.131824			Ave (cm)	1.190752						
		% Swell	5.2064632										
		Ave z (cm)	1.161288										
Run C													
3/21/20													
3/21/20 Jonathan 'Jonny' Counts - 10% PVA 2%SA Freeze/Thawed 5x in -20C													
Run was conducted in 0.5M KCl			Membrane equilibrated in 0.5M KCl for 2 days				Cuvette was cleaed before run						
Source is considered 1full (unit of concentration since we don't know exactly what the molarity is) Cinnamon derivative is very hard to measure/dissolve/it's really sticky													
Pre Expt Membrane thick				Post Expt Membrane thick									
	Initial	0.833	Real (in)		Initial	0.833	Real (in)		Vsink	z (cm)	d(ppm)/dt	Area (cm^2)	Csource (ppm)
	1	1.309	0.476		1	1.257	0.424		25	1.143	10.068	7.0709	3100
	2	1.303	0.47		2	1.254	0.421						
	3	1.316	0.483		3	1.259	0.426		De				
	4	1.312	0.479		4	1.261	0.428		3.6458E-06				
	5	1.308	0.475		5	1.251	0.418						
		Ave (in)	0.4766			Ave (in)	0.4234						
		Ave (cm)	1.210564			Ave (cm)	1.075436						
		% Swell	-11.1624										
		Ave z (cm)	1.143										

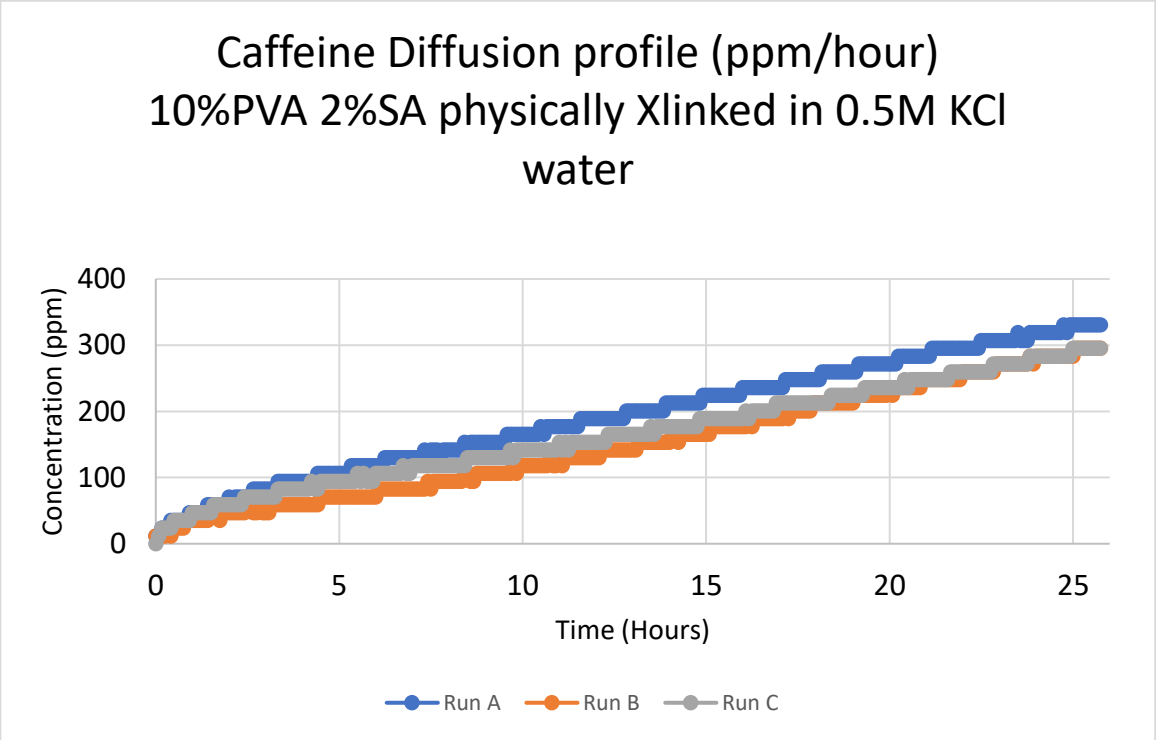

Figure B.5: *Concentration profile for caffeine (F/T, ionic)*

Caffeine diffusion in 10% PVA membranes (physically crosslinked by 5 freeze/thaw cycles of 1 hour each). Diffusion carried out in deionized water.

Run A													
1/27/20													
Membrane Pre Expt:		Initial in	0.838			Jonathan 'Jonny' Counts Caffeine Diff through 10% PVA (F/T 5x in -20C) Equilibrated in water for 4 days							
		1	1.316	Real inches	0.478		PVA was 146 kDa						
		2	1.299		0.461		Area cm^2	Sink V (mL)	z (cm)	d(M)/dt	Csource (M)		
		3	1.288		0.45		7.0709	22.3	1.195832	11.618	3100		
		4	1.329		0.491								
		5	1.293		0.455		De (cm^2/sec)						
				Average in	0.467		3.92616E-06						
				Average cm	1.18618								
Membrane Post Expt:		Initial in	0.836										
		1	1.336	Real inches	0.5								
		2	1.298		0.462								
		3	1.303		0.467								
		4	1.314		0.478								
		5	1.302		0.466								
				Average in	0.4746								
				Average cm	1.205484								
Run B													
1/28/20													
Jonathan 'Jonny' Counts - 10% PVA Freeze/Thawed 5x in -20C. Equilibrated in water for 5 days.													
Run was conducted in DI water													
Pre Expt Membrane thick				Post Expt Membrane thick									
	Initial	0.837	Real (in)		Initial	0.839	Real (in)		Vsink	z (cm)	d(ppm)/dt	Area (cm^2)	Csource (ppm)
	1	1.301	0.464		1	1.322	0.483		21.2	1.217041	15.21	7.0709	3100
	2	1.298	0.461		2	1.36	0.521						
	3	1.298	0.461		3	1.299	0.46		De				
	4	1.322	0.485		4	1.322	0.483		4.9731E-06				
	5	1.34	0.503		5	1.332	0.493						
						1.3	0.461						
		Ave (in)	0.4748			Ave (in)	0.4835						
		Ave (cm)	1.205992			Ave (cm)	1.22809						
		% Swell	1.83235046										
		Ave z (cm)	1.217041										
Run C													
1/30/20													
Jonathan 'Jonny' Counts - 10% PVA Freeze/Thawed 5x in -20C. Equilibrated in water for 3 days													
Run was conducted in DI water													
Pre Expt Membrane thick				Post Expt Membrane thick									
	Initial	0.84	Real (in)		Initial	0.838	Real (in)		Vsink	z (cm)	d(ppm)/dt	Area (cm^2)	Csource (ppm)
	1	1.314	0.474		1	1.33	0.492		21.2	1.226566	17.812	7.0709	3100
	2	1.32	0.48		2	1.33	0.492						
	3	1.319	0.479		3	1.343	0.505		De				
	4	1.298	0.458		4	1.332	0.494		5.8695E-06				
	5	1.306	0.466		5	1.327	0.489						
		Ave (in)	0.4714			Ave (in)	0.4944						
		Ave (cm)	1.197356			Ave (cm)	1.255776						
		% Swell	4.87908358										
		Ave z (cm)	1.226566										

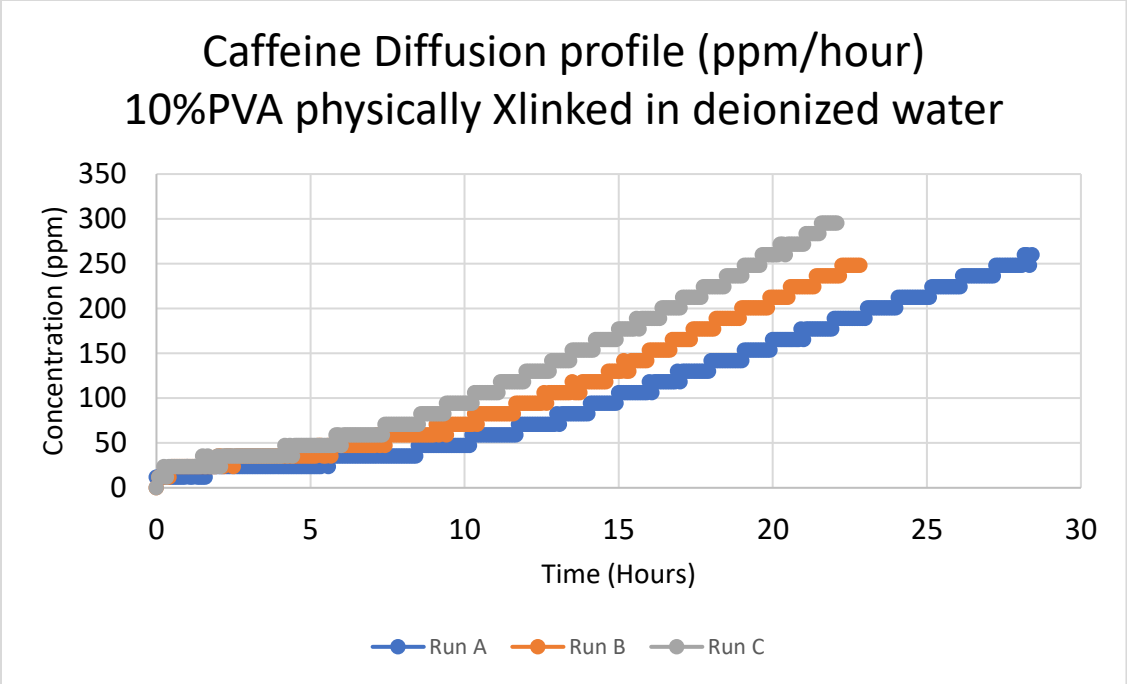

Figure B.6: *Concentration profile for caffeine F/T (10%PVA)*

Saccharin Diffusion

Calibration: Sodium saccharin was diluted from 1570.5ppm in DI water down to 157ppm. The ThermoFisher Evolution UV-Vis Spectrophotometer was blanked with deionized water, providing the zero point.

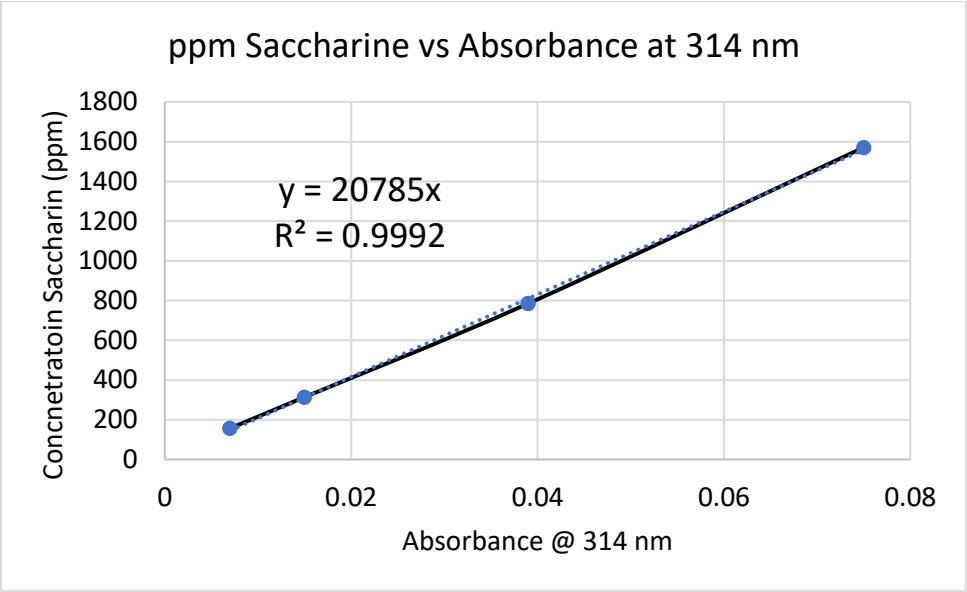

Figure B.7: *Calibration curve for saccharin*

Conc (ppm)	Abs @ 314 nm
3141	0.121
1570.5	0.075
785.25	0.039
314.1	0.015
157.05	0.007

Table B.2: *Saccharin Dilution/calibration data*

Saccharin diffusion in 10% PVA 2% SA membranes (chemically crosslinked in saturated boric acid, 2% (w/v) $CaCl_2$ for 4.5 hours). Diffusion carried out in deionized water.

Run A		Saccharine diffusion through 10% PVA 2% SA chemically Xlinked in Sat boric acid 2% (w/v) CaCl2 for 4.5 hours											
2/14/20		Equilibrated in water for 2 days prior and run starting 2/14/2020.											
Pre Expt Membrane thick				Post Expt Membrane thick									
	Initial	0.837	Real (in)		Initial	0.836	Real (in)		Vsink	z (cm)	d(ppm)/dt	Area (cm^2)	Csource (ppm)
	1	1.275	0.438		1	1.282	0.446		23.1	1.139952	29.533	7.0709	3100
	2	1.277	0.44		2	1.314	0.478						
	3	1.26	0.423		3	1.317	0.481		De				
	4	1.26	0.423		4	1.294	0.458		9.8552E-06				
	5	1.259	0.422		5	1.315	0.479						
		Ave (in)	0.4292			Ave (in)	0.4684						
		Ave (cm)	1.090168			Ave (cm)	1.189736						
		% Swell	9.1332712										
		Ave z (cm)	1.139952										
Run B		Saccharine diffusion through 10% PVA 2% SA chemically Xlinked in Sat boric acid 2% (w/v) CaCl2 for 4.5 hours											
2/17/20		Equilibrated in water for 2 days prior and run starting 2/17/2020.											
Pre Expt Membrane thick				Post Expt Membrane thick									
	Initial	0.838	Real (in)		Initial	0.839	Real (in)		Vsink	z (cm)	d(ppm)/dt	Area (cm^2)	Csource (ppm)
	1	1.277	0.439		1	1.311	0.472		23	1.161288	40.334	7.0709	3100
	2	1.288	0.45		2	1.329	0.49						
	3	1.287	0.449		3	1.3	0.461		De				
	4	1.261	0.423		4	1.319	0.48		1.3652E-05				
	5	1.263	0.425		5	1.322	0.483						
		Ave (in)	0.4372			Ave (in)	0.4772						
		Ave (cm)	1.110488			Ave (cm)	1.212088						
		% Swell	9.14913083										
		Ave z (cm)	1.161288										
Run C		Saccharine diffusion through 10% PVA 2% SA chemically Xlinked in Sat boric acid 2% (w/v) CaCl2 for 4.5 hours											
2/18/20		Equilibrated in water for 2 days prior and run starting 2/18/2020.											
Pre Expt Membrane thick				Post Expt Membrane thick									
	Initial	0.838	Real (in)		Initial	0.841	Real (in)		Vsink	z (cm)	d(ppm)/dt	Area (cm^2)	Csource (ppm)
	1	1.217	0.379		1	1.255	0.414		23.9	0.976122	23.754	7.0709	3100
	2	1.215	0.377		2	1.22	0.379						
	3	1.212	0.374		3	1.226	0.385		De				
	4	1.201	0.363		4	1.241	0.4		7.0226E-06				
	5	1.225	0.387		5	1.226	0.385						
		Ave (in)	0.376			Ave (in)	0.3926						
		Ave (cm)	0.95504			Ave (cm)	0.997204						
		% Swell	4.41489362										
		Ave z (cm)	0.976122										

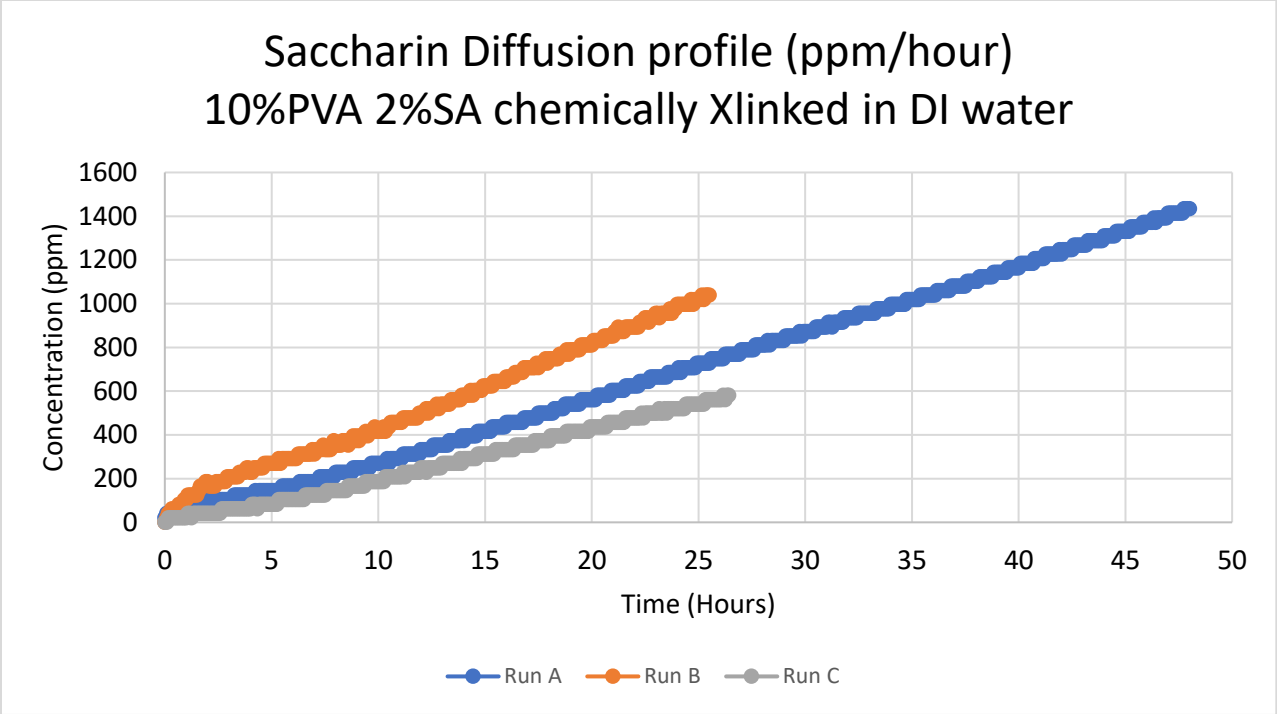

Figure B.8: *Concentration profile for saccharin (chemical crosslink)*

Saccharin diffusion in 10% PVA 2% SA membranes (chemically crosslinked in saturated boric acid, 2% (w/v) $CaCl_2$ for 4.5 hours). Diffusion carried out in 0.5M KCl water.

Run A		Saccharine diffusion through 10% PVA 2% SA chemically Xlinked in Sat boric acid 2% (w/v) CaCl2 for 4.5 hours										
2/20/20		Equilibrated in 0.5M KCl water for 2 days prior and run starting 2/20/20.					Run conducted in 0.5M KCl					
Pre Expt Membrane thick				Post Expt Membrane thick								
	Initial	0.84	Real (in)		Initial	0.839	Real (in)		Vsink	z (cm)	d(ppm)/dt	Area (cm^2)	Csource (ppm)
	1	1.169	0.329		1	1.21	0.371		25.1	0.913892	22.237	7.0709	3100
	2	1.173	0.333		2	1.239	0.4						
	3	1.171	0.331		3	1.234	0.395		De				
	4	1.175	0.335		4	1.215	0.376		6.4641E-06				
	5	1.18	0.34		5	1.227	0.388						
		Ave (in)	0.3336			Ave (in)	0.386						
		Ave (cm)	0.847344			Ave (cm)	0.98044						
		% Swell	15.7074341										
		Ave z (cm)	0.913892										
Run B		Saccharine diffusion through 10% PVA 2% SA chemically Xlinked in Sat boric acid 2% (w/v) CaCl2 for 4.5 hours										
2/21/20		Equilibrated in 0.5M KCl water for 2 days prior and run starting 2/21/20.					Run conducted in 0.5M KCl					
Pre Expt Membrane thick				Post Expt Membrane thick								
	Initial	0.839	Real (in)		Initial	0.839	Real (in)		Vsink	z (cm)	d(ppm)/dt	Area (cm^2)	Csource (ppm)
	1	1.283	0.444		1	1.299	0.46		28.4	1.142238	17.092	7.0709	3100
	2	1.268	0.429		2	1.306	0.467						
	3	1.258	0.419		3	1.33	0.491		De				
	4	1.247	0.408		4	1.317	0.478		7.0263E-06				
	5	1.275	0.436		5	1.304	0.465						
		Ave (in)	0.4272			Ave (in)	0.4722						
		Ave (cm)	1.085088			Ave (cm)	1.199388						
		% Swell	10.5337079										
		Ave z (cm)	1.142238										
Run C		Saccharine diffusion through 10% PVA 2% SA chemically Xlinked in Sat boric acid 2% (w/v) CaCl2 for 4.5 hours										
2/24/20		Equilibrated in 0.5M KCl water for 5 days prior and run starting 2/24/20.					Run conducted in 0.5M KCl					
Pre Expt Membrane thick				Post Expt Membrane thick								
	Initial	0.834	Real (in)		Initial	0.829	Real (in)		Vsink	z (cm)	d(ppm)/dt	Area (cm^2)	Csource (ppm)
	1	1.29	0.456		1	1.28	0.451		19	1.152144	23.54	7.0709	3100
	2	1.271	0.437		2	1.29	0.461						
	3	1.282	0.448		3	1.285	0.456		De				
	4	1.287	0.453		4	1.302	0.473		6.5302E-06				
	5	1.273	0.439		5	1.291	0.462						
		Ave (in)	0.4466			Ave (in)	0.4606						
		Ave (cm)	1.134364			Ave (cm)	1.169924						
		% Swell	3.13479624										
		Ave z (cm)	1.152144										
Run D		Saccharine diffusion through 10% PVA 2% SA chemically Xlinked in Sat boric acid 2% (w/v) CaCl2 for 4.5 hours										
2/25/20		Equilibrated in 0.5M KCl water for 6 days prior and run starting 2/25/20.					Run conducted in 0.5M KCl					
Pre Expt Membrane thick				Post Expt Membrane thick								
	Initial	0.829	Real (in)		Initial	0.83	Real (in)		Vsink	z (cm)	d(ppm)/dt	Area (cm^2)	Csource (ppm)
	1	1.303	0.474		1	1.301	0.471		23.8	1.1938	17.771	7.0709	3100
	2	1.303	0.474		2	1.305	0.475						
	3	1.298	0.469		3	1.285	0.455		De				
	4	1.302	0.473		4	1.317	0.487		6.3985E-06				
	5	1.276	0.447		5	1.305	0.475						
		Ave (in)	0.4674			Ave (in)	0.4726						
		Ave (cm)	1.187196			Ave (cm)	1.200404						
		% Swell	1.11253744										
		Ave z (cm)	1.1938										

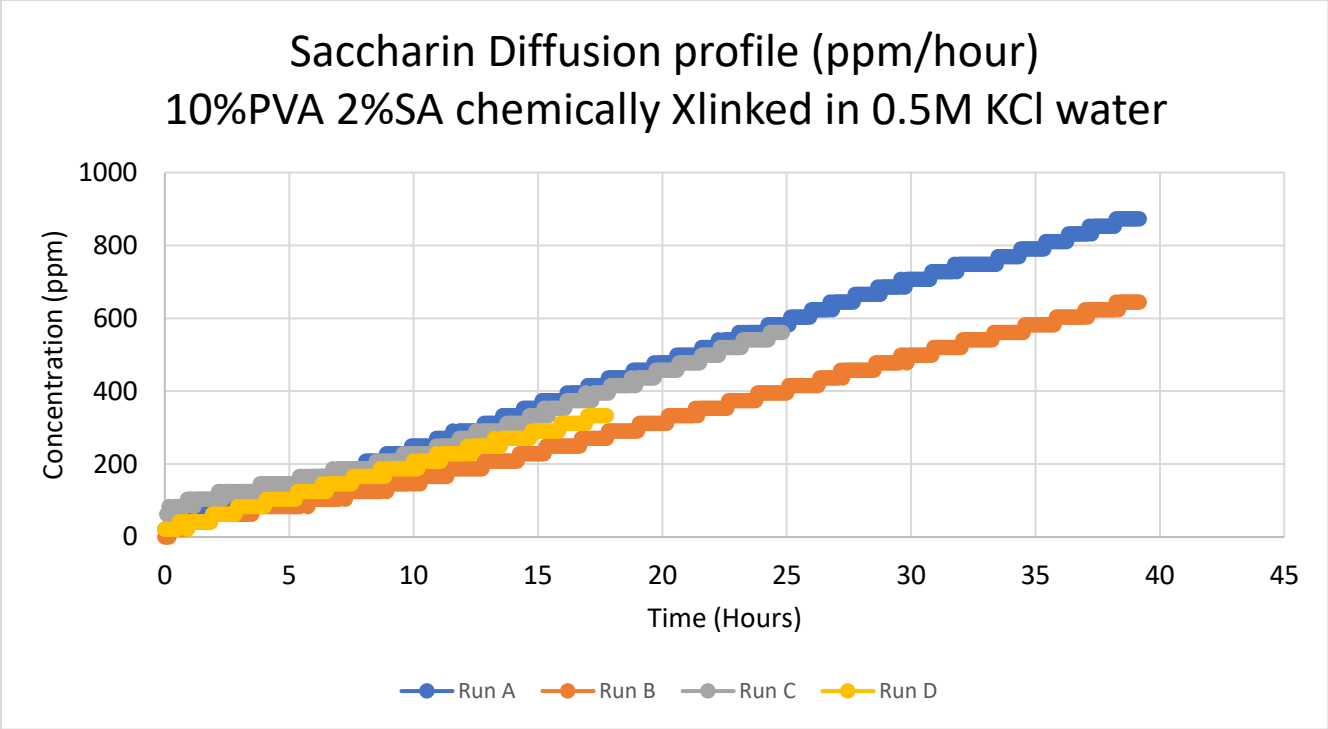

Figure B.9: *Concentration profile for saccharin chemical crosslink (ionic)*

Metanil Yellow Diffusion

Calibration: Metanil yellow was diluted from 65.8ppm in DI water down to 4.11ppm. The ThermoFisher Evolution UV-Vis Spectrophotometer was blanked with deionized water, providing the zero point.

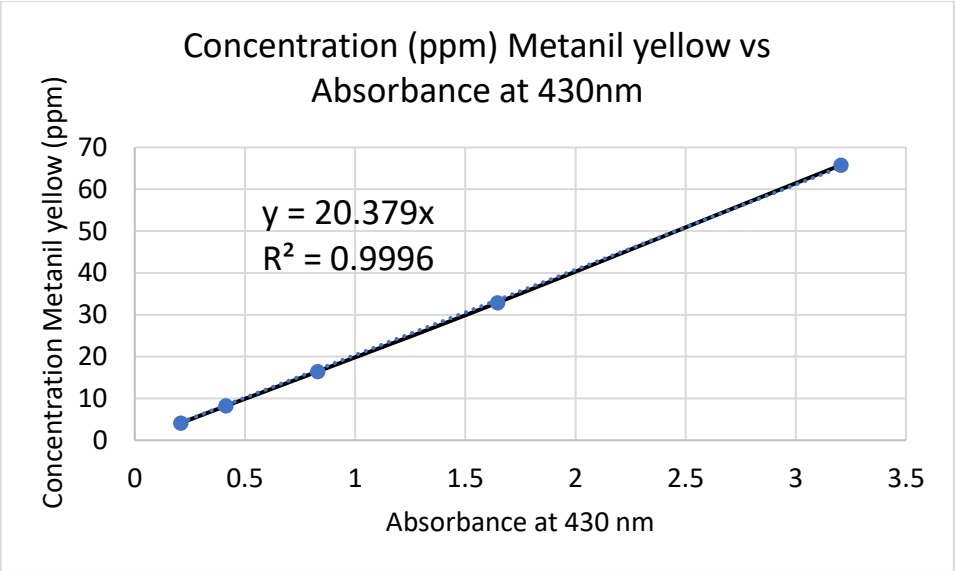

Figure B10: *Calibration curve for metanil yellow*

Conc (ppm)	Abs @ 430 nm
65.8	3.205
32.9	1.646
16.45	0.83
8.225	0.414
4.1125	0.208

Table B.3: *Metanil yellow dilution/calibration data*

Metanil yellow diffusion in 10% PVA 2% SA membranes (chemically crosslinked in saturated boric acid, 2% (w/v) $CaCl_2$ for 4.5 hours). Diffusion carried out in deionized water.

Run A													
6/23/19		10% PVA 2% SA membrane Xlinked Chemically for 4.5 hours. Equilibrated in DI water one hour. Run conducted in DI water.											
Pre Expt Membrane thick				Post Expt Membrane thick									
	Initial	0.84	Real (in)		Initial	0.842	Real (in)		Vsink	z (cm)	d(ppm)/dt	Area (cm^2)	Csource (ppm)
	1	1.167	0.327		1	1.24	0.398		unrecorded	0.897885	0.0752	7.0709	164.8
	2	1.166	0.326		2	1.21	0.368						
	3	1.156	0.316		3	1.218	0.376		De				
	4	1.168	0.328		4	1.214	0.372		6.9519E-07				
	5	1.166	0.326		5	1.24	0.398						
		Ave (in)	0.3246			Ave (in)	0.3824						
		Ave (cm)	0.824484			Ave (cm)	0.971296						
		% Swell	17.8065311										
Run B													
6/27/19		10% PVA 2% SA membrane Xlinked Chemically for 4.5 hours. Equilibrated in DI water one hour. Run conducted in DI water.											
Pre Expt Membrane thick				Post Expt Membrane thick									
	Initial	0.848	Real (in)		Initial	0.816	Real (in)		Vsink	z (cm)	d(ppm)/dt	Area (cm^2)	Csource (ppm)
	1	1.208	0.36		1	1.32	0.504		38	1.07315	0.03805	7.0709	131.6
	2	1.207	0.359		2	1.298	0.482						
	3	1.222	0.374		3	1.3	0.484		De				
	4	1.19	0.342		4	1.27	0.454		4.632E-07				
	5	1.217	0.369		5	1.313	0.497						
		Ave (in)	0.3608			Ave (in)	0.4842						
		Ave (cm)	0.916432			Ave (cm)	1.229868						
		% Swell	34.2017738										
Run C		Metanil Yellow diffusion run with Spectrophotometer (SN: ends in 2203)											
7/3/19		10% PVA 2% SA membrane Xlinked in Saturated boric acid solution (2% w/v CaCl2)							Equiil in DI water for one hour				
Pre Expt Membrane thick				Post Expt Membrane thick									
	Initial	0.818	Real (in)		Initial	0.82	Real (in)		Vsink	z (cm)	d(ppm)/dt	Area (cm^2)	Csource (ppm)
	1	1.093	0.275		1	1.228	0.408		31.5	0.880618	0.064787	7.0709	131.6
	2	1.086	0.268		2	1.258	0.438						
	3	1.098	0.28		3	1.233	0.413		De				
	4	1.112	0.294		4	1.215	0.395		5.3648E-07				
	5	1.104	0.286		5	1.23	0.41						
		Ave (in)	0.2806			Ave (in)	0.4128						
		Ave (cm)	0.712724			Ave (cm)	1.048512						
		% Swell	47.1133286										
Run D													
7/11/19													
Jonathan 'Jonny' Counts Metanil Yellow diffusion in a 10% PVA 2% SA Membrane													
Xlinked 4 1/2 hours in Sat. Boric acid and 2% (w/v) CaCl2					Equilibrated in DI water for one hour.								
The first 18 hours showed spotty data and were not saved. (cuvette problems- most data points were ****) After 18 hours, the sink was rinsed out and reloaded, then blanked and run for 46													
Pre Expt Membrane thick				Post Expt Membrane thick									
	Initial	0.819	Real (in)		Initial	0.82	Real (in)		Vsink	z (cm)	d(ppm)/dt	Area (cm^2)	Csource (ppm)
	1	1.101	0.282		1	1.238	0.418		25	0.876554	0.08644	7.0709	131.2
	2	1.103	0.284		2	1.209	0.389						
	3	1.114	0.295		3	1.208	0.388		De				
	4	1.104	0.285		4	1.239	0.419		5.6718E-07				
	5	1.098	0.279		5	1.232	0.412						
		Ave (in)	0.285			Ave (in)	0.4052						
		Ave (cm)	0.7239			Ave (cm)	1.029208						
		% Swell	42.1754386										

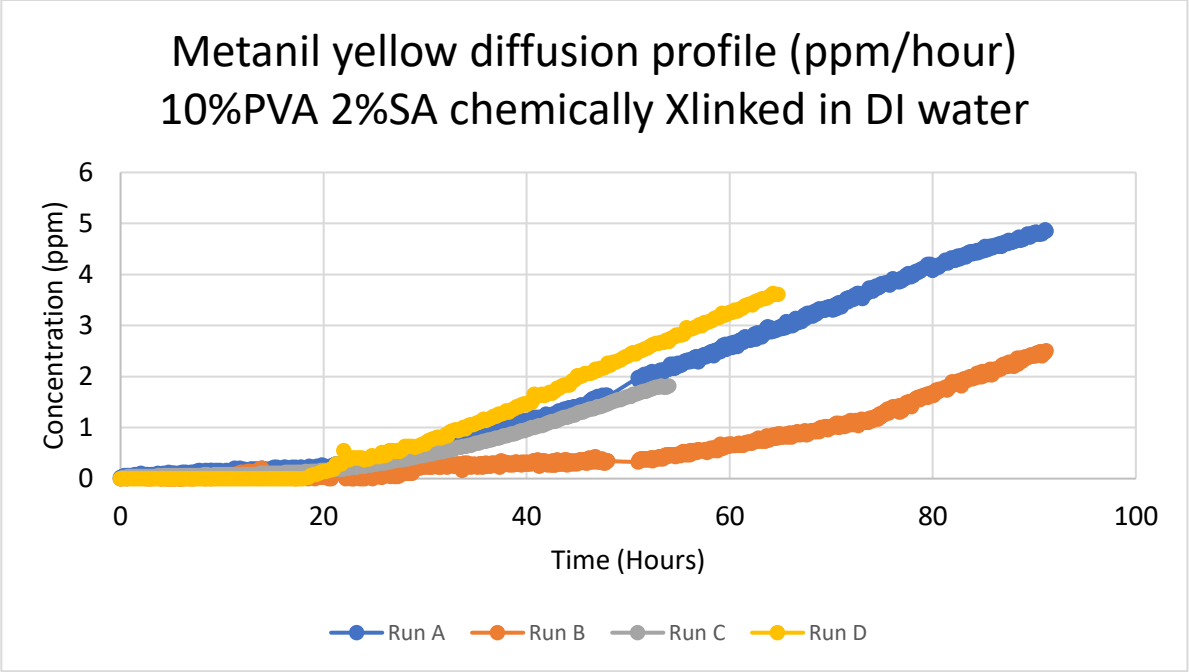

Figure B.11: *Concentration profile for metanil yellow chemical crosslink*

Metanil yellow diffusion in 10% PVA 2% SA membranes (chemically crosslinked in saturated boric acid, 2% (w/v) $CaCl_2$ for 4.5 hours). Diffusion carried out in 0.5M or 1.0M KCl.

Run A													
3/14/19													
10% PVA 2% SA Membrane Xlinked 4 1/2 hours in Sat. Boric acid 2% (w/v) CaCl2													
Jonathan 'Jonny' Counts													
Metanil yellow diffusion for 72 hours followed by more diffusion without blanking													
Run conducted in 0.5M KCl													
Pre Expt Membrane thick				Post Expt Membrane thick									
	Initial	N/A	Real (in)		Initial	0.833	Real (in)		Vsink	z (cm)	d(ppm)/dt	Area (cm^2)	Csource (ppm)
	1	N/A	N/A		1	1.258	0.425		31.4	1.104392	0.073024	7.0709	128.0487805
	2	N/A	N/A		2	1.262	0.429						
	3	N/A	N/A		3	1.25	0.417		De				
	4	N/A	N/A		4	1.278	0.445		7.769E-07				
	5	N/A	N/A		5	1.291	0.458						
		Ave (in)	N/A			Ave (in)	0.4348						
		Ave (cm)	N/A			Ave (cm)	1.104392						
Run B													
3/5/20													
Jonathan 'Jonny' Counts - 10% PVA 2%SA Chem Xlinked 4.5 hours in sat boric acid (2% w/v CaCl2)													
Run was conducted in 0.5M KCl			Membrane equilibrated in 0.5M KCl for 2 days										
Metanil yellow diffusion in 0.5M KCl													
Pre Expt Membrane thick				Post Expt Membrane thick									
	Initial	0.829	Real (in)		Initial	0.832	Real (in)		Vsink	z (cm)	d(ppm)/dt	Area (cm^2)	Csource (ppm)
	1	1.193	0.364		1	1.285	0.453		20	1.156208	0.0938	7.0709	187.5
	2	1.204	0.375		2	1.278	0.446						
	3	1.21	0.381		3	1.301	0.469		De				
	4	1.183	0.354		4	1.291	0.459		4.5445E-07				
	5	1.23	0.401		5	1.281	0.449						
		Ave (in)	0.375			Ave (in)	0.4552						
		Ave (cm)	0.9525			Ave (cm)	1.156208						
		% Swell	21.3866667										
		Ave z (cm)	1.054354										
Run C													
7/16/19													
Jonathan 'Jonny' Counts setup for Metanil Yellow diffusion in 1M KCl						10% PVA 2% SA Membrane Xlinked 4 1/2 hours in Sat. Boric acid 2% (w/v) CaCl2								
						Equilibrated in 0.5M KCl for one day							
Pre Expt Membrane thick				Post Expt Membrane thick									
	Initial	0.82	Real (in)		Initial	0.842	Real (in)		Vsink	z (cm)	d(ppm)/dt	Area (cm^2)	Csource (ppm)
	1	1.194	0.374		1	1.215	0.373		32.4	0.954532	0.03937	7.0709	92.67
	2	1.201	0.381		2	1.215	0.373						
	3	1.19	0.37		3	1.225	0.383		De				
	4	1.198	0.378		4	1.214	0.372		5.1616E-07				
	5	1.201	0.381		5	1.215	0.373						
		Ave (in)	0.3768			Ave (in)	0.3748						
		Ave (cm)	0.957072			Ave (cm)	0.951992						
		% Swell	-0.5307856										

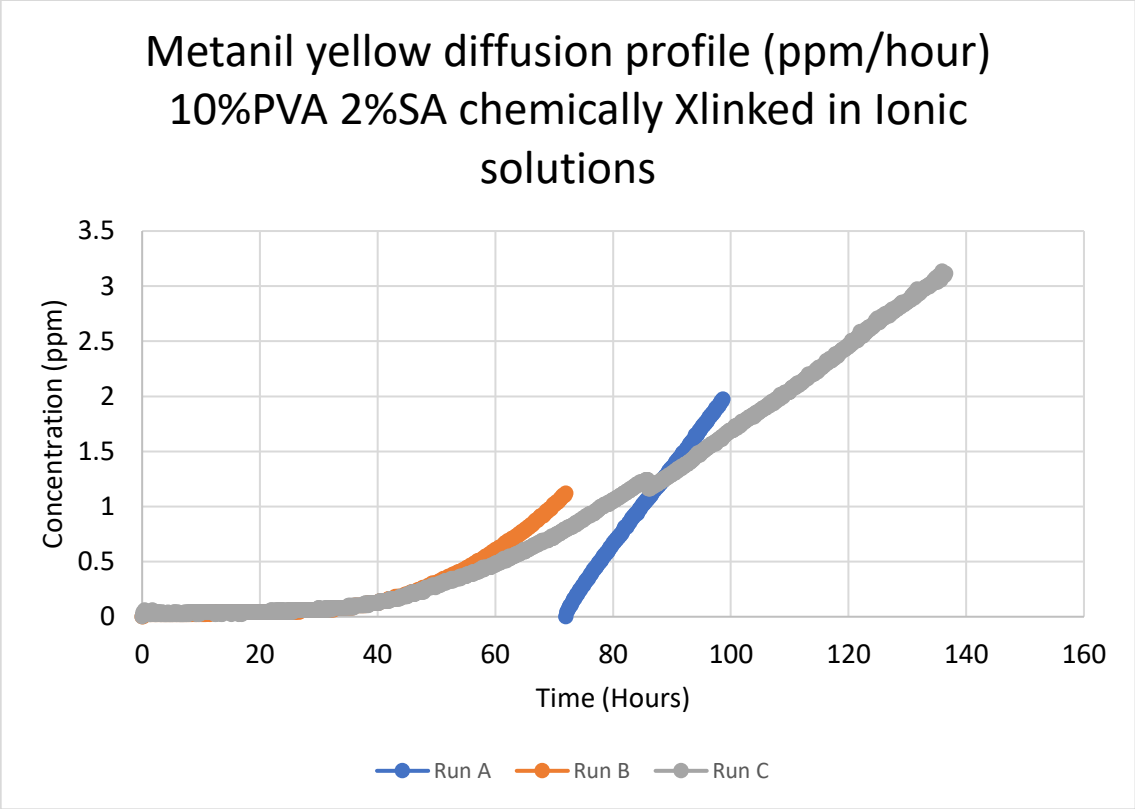

Figure B.12: *Concentration profile for metanil yellow chemical crosslink (ionic)*

Methylene blue Diffusion

Calibration: Methylene blue was diluted from 5.15ppm in DI water down to 0.322ppm. The ThermoFisher Evolution UV-Vis Spectrophotometer was blanked with deionized water, providing the zero point.

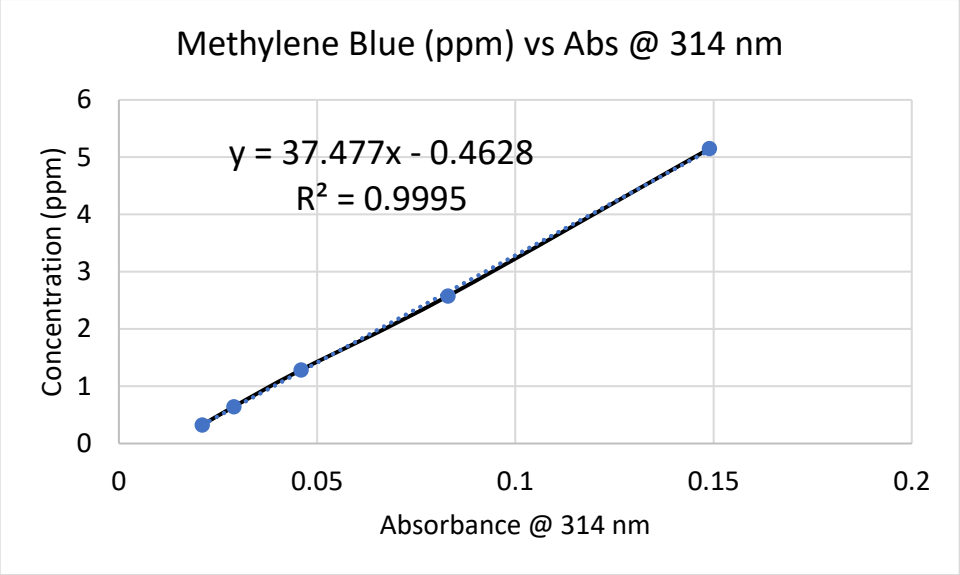

Figure B.13: *Calibration curve for methylene blue*

Conc (ppm)	Absorbance at 314 nm
5.15	0.149
2.575	0.083
1.2875	0.046
0.64375	0.029
0.321875	0.021

Table B.4: *Methylene blue dilution/calibration data*

Methylene blue diffusion in 10% PVA 2% SA membranes (chemically crosslinked in saturated boric acid, 2% (w/v) $CaCl_2$ for 4.5 hours). Diffusion carried out in deionized water.

Run A 5/25/2019

10% PVA 2%SA Chemically Crosslinked for 4.5 hours in sat. boric acid 2% (w/v) CaCl2. Equilibrated in DI water for one hour. Run conducted in DI water.

Membrane Pre Expt				Membrane Post Expt								
	(in)				(in)							
Initial	0.831	Real (in)		Initial	0.829	Real (in)		Vsink (mL)	z (cm)	Area (cm^2)	Csource (ppm	d(ppm)/dt
1	1.145	0.314		1	1.212	0.383		37.6	0.884174	7.0709	164.8	0.0548
2	1.141	0.31		2	1.215	0.384						
3	1.142	0.311		3	1.214	0.383		De				
4	1.141	0.31		4	1.219	0.388		4.3428E-07				
5	1.141	0.31		5	1.219	0.388						
	Ave (in)	0.311										
	Ave (cm)	0.78994			Ave (in)	0.3852						
					Ave (cm)	0.978408						
	% Swell											
	23.8585209											

Run B

6/3/19 10% PVA 2%SA Chemically Crosslinked for 4.5 hours in sat. boric acid 2% (w/v) CaCl2. Equilibrated in DI water for one hour. Run conducted in DI water.

Pre Expt Membrane thick				Post Expt Membrane thick								
Initial	0.837	Real (in)		Initial	0.834	Real (in)		Vsink	z (cm)	d(ppm)/dt	Area (cm^2)	Csource (ppm)
1	1.265	0.428		1	1.319	0.485		33.3	1.163594	0.059177	7.0709	164.8
2	1.265	0.428		2	1.341	0.507						
3	1.267	0.43		3	1.339	0.505		De				
4	1.245	0.408		4	1.317	0.483		5.4659E-07				
5	1.25	0.413		5	1.315	0.481						
	Ave (in)	0.4214			Ave (in)	0.4922						
	Ave (cm)	1.070356			Ave (cm)	1.250188						
	% Swell	16.8011391										

Run C

6/10/19 10% PVA 2%SA Chemically Crosslinked for 4.5 hours in sat. boric acid 2% (w/v) CaCl2. Equilibrated in DI water for one hour. Run conducted in DI water.

Membrane Pre Expt				Membrane Post Expt				d(ppm)/dt	Vsink	z (cm)	Area	Csource ppm
Initial	0.837	Real		Initial	0.841	Real		0.028837	40	1.097	7.0709	164.8
1	1.197	0.36		1	1.34	0.499						
2	1.197	0.36		2	1.342	0.501						
3	1.195	0.358		3	1.343	0.502		De				
4	1.194	0.357		4	1.365	0.524		3.0164E-07				
5	1.192	0.355		5	1.345	0.504						
	Ave(in)	0.358										
	Ave(cm)	0.90932			Ave(in)	0.506						
					Ave(cm)	1.28524						
	%Swell	41.3407821										
	Ave z (cm)	1.09728										

Run D

6/14/19 10% PVA 2%SA Chemically Crosslinked for 4.5 hours in sat. boric acid 2% (w/v) CaCl2. Equilibrated in DI water for one hour. Run conducted in DI water.

Membrane Pre Expt				Membrane Post Expt:				d(ppm)/dt	z (cm)	Area (cm^2)	Vsink (mL)	Csource (ppm)
Initial	0.836	Real (in)		Initial	0.839	Real (in)		0.0429	0.843026	7.0709	34	164.8
1	1.117	0.281		1	1.217	0.378						
2	1.115	0.279		2	1.24	0.401		De				
3	1.109	0.273		3	1.222	0.383		2.9312E-07				
4	1.113	0.277		4	1.218	0.379						
5	1.11	0.274		5	1.233	0.394						
	Ave (in)	0.2768										
	Ave (cm)	0.703072			Ave (in)	0.387						
	% Swell	39.8121387			Ave (cm)	0.98298						

Run E

7/12/19

10% PVA 2%SA Chemically Crosslinked for 4.5 hours in sat. boric acid 2% (w/v) CaCl2. Equilibrated in DI water for one hour. Run conducted in DI water.

Jonathan 'Jonny' Counts 7_12_19

Pre Expt Membrane thick				Post Expt Membrane thick				Vsink	z (cm)	d(ppm)/dt	Area (cm^2)	Csource (ppm)
Initial	0.817	Real (in)		Initial	0.824	Real (in)		33.9	0.739648	0.11638	7.0709	164.2
1	1.064	0.247		1	1.145	0.321						
2	1.064	0.247		2	1.154	0.33		De				
3	1.077	0.26		3	1.164	0.34		6.9816E-07				
4	1.068	0.251		4	1.19	0.366						
5	1.07	0.253		5	1.121	0.297						
	Ave (in)	0.2516			Ave (in)	0.3308						
	Ave (cm)	0.639064			Ave (cm)	0.840232						
	% Swell	31.4785374										

Run F

7/15/19

This was a weekend run of methylene blue through 10% PVA 2% SA membrane Xlinked 4 1/2 hours in Sat. Boric acid (2% w/v CaCl2)

Jonathan 'Jonny' Counts Flow through cuvette was just washed with pirahna solution.

	Pre Expt Membrane thick				Post Expt Membrane thick			Vsink	z (cm)	d(ppm)/dt	Area (cm^2)	Csource (ppm)
Initial	0.818	Real (in)		Initial	0.828	Real (in)		39	0.809752	0.078838	7.0709	164.2
1	1.101	0.283		1	1.168	0.34						
2	1.11	0.292		2	1.17	0.342		De				
3	1.134	0.316		3	1.159	0.331		5.9566E-07				
4	1.122	0.304		4	1.17	0.342						
5	1.107	0.289		5	1.177	0.349						
	Ave (in)	0.2968			Ave (in)	0.3408						
	Ave (cm)	0.753872			Ave (cm)	0.865632						
	% Swell	14.8247978										

Run G

1/17/19

Methylene Blue diffusion in 10% PVA 2% SA membrane Xlinked in Sat Boric acid (2% w/v CaCl2) for 4 1/2 hours

Equilibrated in DI water for one hour. Run conducted in DI water.

Pre Expt Membrane thick				Post Expt Membrane thick				Vsink	z (cm)	d(ppm)/dt	Area (cm^2)	Csource (ppm)
Initial	0.818	Real (in)		Initial	0.835	Real (in)		34.3	0.87757	0.091988	7.0709	164.2
1	1.102	0.284		1	1.225	0.39						
2	1.108	0.29		2	1.246	0.411						
3	1.103	0.285		3	1.221	0.386		De				
4	1.108	0.29		4	1.225	0.39		6.6246E-07				
5	1.118	0.3		5	1.264	0.429						
	Ave (in)	0.2898			Ave (in)	0.4012						
	Ave (cm)	0.736092			Ave (cm)	1.019048						
	% Swell	38.4403037										

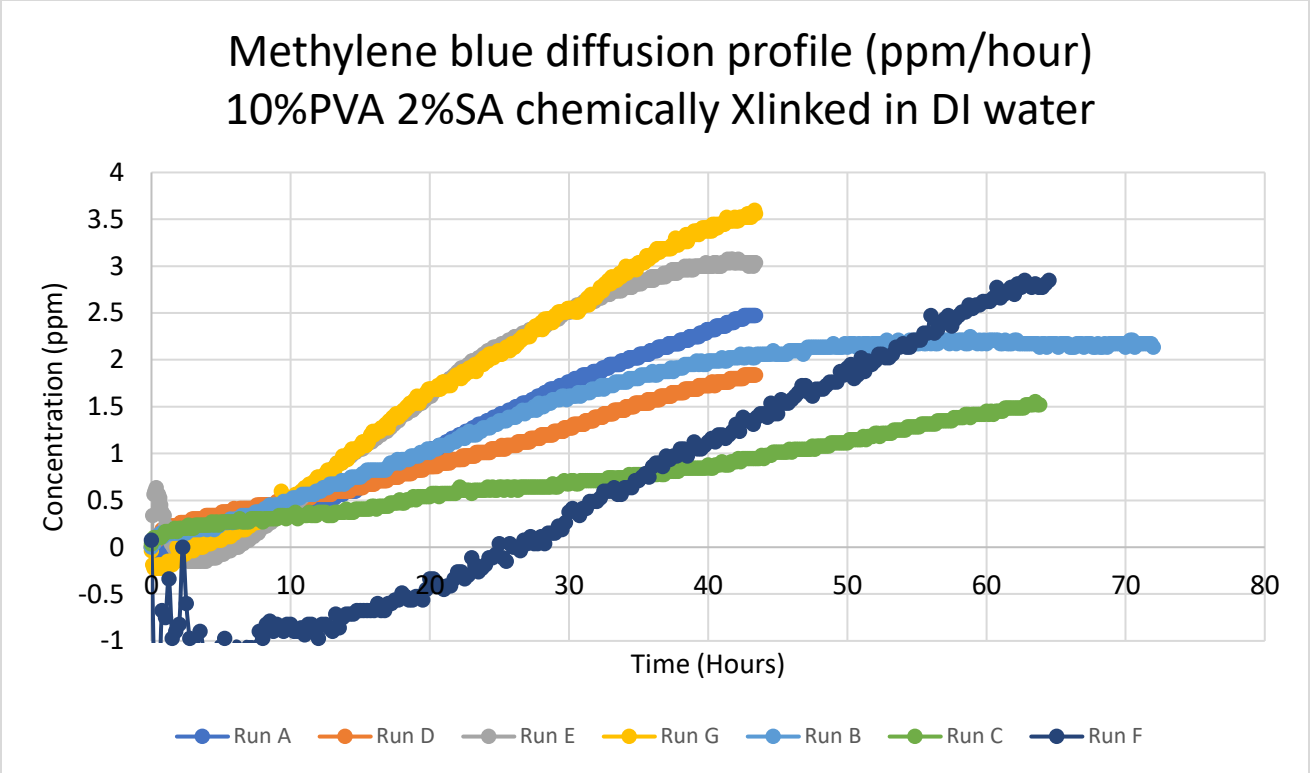

Figure B.14: *Concentration profile for methylene blue chemically crosslinked*

Methylene blue diffusion in 10% PVA 2% SA membranes (chemically crosslinked in saturated boric acid, 2% (w/v) $CaCl_2$ for 4.5 hours). Diffusion carried out in 0.5M KCl.

Run A												
8/1/19												
Methylene blue diffusion in 10% PVA 2% SA membrane Xlinked in Sat. Boric Acid 4 1/2 hours							Diffusion took place in 0.5M KCl solution in water					
Membrane was equilbrated in salt solution 2 hours				Spec SN: 2203								
Membrane Pre Expt				Membrane Post Expt.				Vsink	z (cm)	d(ppm)/dt	Area (cm^2)	Csource (ppm)
Initial	0.846			Initial	0.845			36	1.154938	0.0722	7.0709	164.5
1	1.285	0.439		1	1.343	0.498						
2	1.291	0.445		2	1.339	0.494		De				
3	1.267	0.421		3	1.325	0.48		7.1689E-07				
4	1.259	0.413		4	1.315	0.47						
5	1.264	0.418		5	1.314	0.469						
	Ave (in)	0.4272		Ave (in)		0.4822						
	Ave (cm)	1.085088		Ave (cm)		1.224788						
	% Swell	12.8745318										
Run B			Methylene blue diffusion in 10% PVA 2% SA membrane Xlinked in Sat. Boric Acid 4 1/2 hours									
8/5/19			Membrane was equilbrated in 0.5M KCl salt solution 2 hours									
Pre Expt Membrane thick				Post Expt Membrane thick								
Initial	0.853	Real (in)		Initial	0.843	Real (in)		Vsink	z (cm)	d(ppm)/dt	Area (cm^2)	Csource (ppm)
1	1.204	0.351		1	1.277	0.434		31.2	1.013968	0.08893	7.0709	164.5
2	1.209	0.356		2	1.283	0.44						
3	1.217	0.364		3	1.284	0.441		De				
4	1.222	0.369		4	1.288	0.445		6.7187E-07				
5	1.2	0.347		5	1.288	0.445						
	Ave (in)	0.3574			Ave (in)	0.441						
	Ave (cm)	0.907796			Ave (cm)	1.12014						
	% Swell	23.3911584										
Run C			Methylene blue diffusion in 10% PVA 2% SA membrane Xlinked in Sat. Boric Acid 4 1/2 hours									
8/7/19			Membrane was equilbrated in 0.5M KCl salt solution 2 hours									
Pre Expt Membrane thick				Post Expt Membrane thick								
Initial	0.846	Real (in)		Initial	0.845	Real (in)		Vsink	z (cm)	d(ppm)/dt	Area (cm^2)	Csource (ppm)
1	1.128	0.282		1	1.229	0.384		33	0.86233	0.087671	7.0709	164.5
2	1.135	0.289		2	1.234	0.389						
3	1.137	0.291		3	1.226	0.381		De				
4	1.149	0.303		4	1.258	0.413		5.958E-07				
5	1.12	0.274		5	1.234	0.389						
	Ave (in)	0.2878			Ave (in)	0.3912						
	Ave (cm)	0.731012			Ave (cm)	0.993648						
	% Swell	0.35927728										

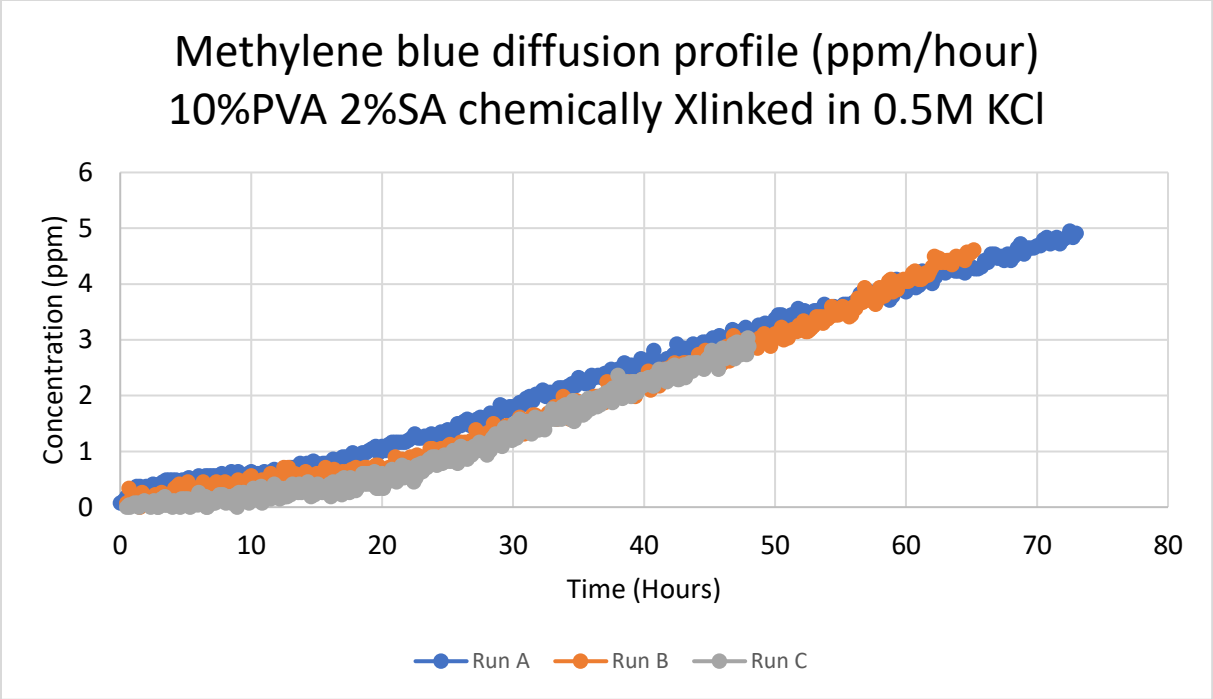

Figure B.15: *Concentration profile for methylene blue chemically crosslinked (ionic)*

Cinnamon Diffusion

Calibration: Positively charged cinnamaldehyde derivative, (E)-*N*,*N*,*N*-trimethyl-3-prop-2-en-1-aminium iodide, was diluted from 5.15ppm in DI water down to 0.322ppm. The ThermoFisher Evolution UV-Vis Spectrophotometer was blanked with deionized water, providing the zero point.

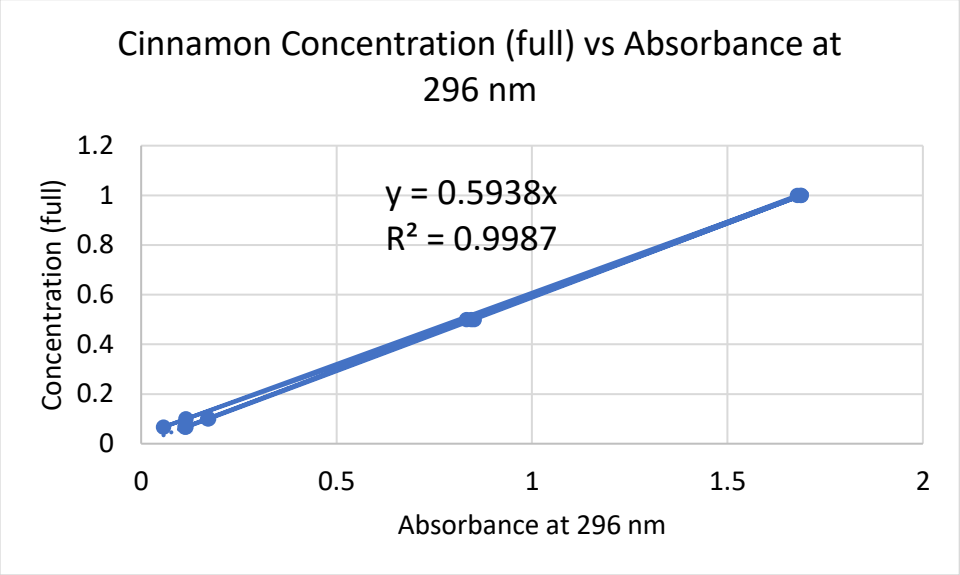

Figure B.16: *Calibration curve for cinnamon*

3/11/2020 Cinnamon (MW: 176 g/mol) obtained from Dr. Waynant. It did not easily dissolve in water and was impossible to measure accurately (very viscous), so roughly 1 gram was placed in 1 liter of deionized water. This is regarded as the "full" concentration and was used as the stock solution and the source solution for all diffusion runs. A new calibration will have to be made for any new stock solution.

Conc (full)	Abs 296nm
1	1.679
0.5	0.833
0.1	0.115
0.06666667	0.057
1	1.687
0.5	0.845
0.1	0.17
0.06666667	0.112
1	1.689
0.5	0.852
0.1	0.173
0.06666667	0.115

Table B.5: *Cinnamon dilution/calibration data*

Cinnamon diffusion in 10% PVA 2% SA membranes (chemically crosslinked in saturated boric acid, 2% (w/v) $CaCl_2$ for 4.5 hours). Diffusion carried out in deionized water.

Run A												
3/12/20												
Jonathan 'Jonny' Counts - 10% PVA 2%SA Chem Xlinked 4.5 hours in sat boric acid (2% w/v CaCl2)												
Run was conducted in DI water			Membrane equilibrated in DI for 2 days									
Source is considered 1full (unit of concentration since we don't know exactly what the molarity is) Cinnamon derivative is very hard to measure/dissolve/it's really sticky												
Pre Expt Membrane thick				Post Expt Membrane thick								
Initial	0.83	Real (in)		Initial	0.837	Real (in)		Vsink	z (cm)	d(full)/dt	Area (cm^2)	Csource (full)
1	1.178	0.348		1	1.224	0.387		28.1	0.985012	0.007483	7.0709	1
2	1.181	0.351		2	1.221	0.384						
3	1.187	0.357		3	1.223	0.386		De				
4	1.184	0.354		4	1.224	0.387		8.1367E-06				
5	1.183	0.353		5	1.232	0.395						
	Ave (in)	0.3526			Ave (in)	0.3878						
	Ave (cm)	0.895604			Ave (cm)	0.985012						
	% Swell	9.98298355										
	Ave z (cm)	0.940308										
Run B												
3/14/20												
Jonathan 'Jonny' Counts - 10% PVA 2%SA Chem Xlinked 4.5 hours in sat boric acid (2% w/v CaCl2)												
Run was conducted in DI water			Membrane equilibrated in DI for 2 days									
Source is considered 1full (unit of concentration since we don't know exactly what the molarity is) Cinnamon derivative is very hard to measure/dissolve/it's really sticky												
Pre Expt Membrane thick				Post Expt Membrane thick								
Initial	N/A	Real (in)		Initial	0.836	Real (in)		Vsink	z (cm)	d(full)/dt	Area (cm^2)	Csource (full)
1	N/A	N/A		1	1.22	0.384		26.7	0.993648	0.0051628	7.0709	1
2	N/A	N/A		2	1.232	0.396						
3	N/A	N/A		3	1.225	0.389		De				
4	N/A	N/A		4	1.227	0.391		5.3809E-06				
5	N/A	N/A		5	1.232	0.396						
	Ave (in)	N/A			Ave (in)	0.3912						
	Ave (cm)	N/A			Ave (cm)	0.993648						
Run C												
3/16/20												
Jonathan 'Jonny' Counts - 10% PVA 2%SA Chem Xlinked 4.5 hours in sat boric acid (2% w/v CaCl2)												
Run was conducted in DI water			Membrane equilibrated in DI for 2 days									
Source is considered 1full (unit of concentration since we don't know exactly what the molarity is) Cinnamon derivative is very hard to measure/dissolve/it's really sticky												
Pre Expt Membrane thick				Post Expt Membrane thick								
Initial	0.837	Real (in)		Initial	0.832	Real (in)		Vsink	z (cm)	d(full)/dt	Area (cm^2)	Csource (full)
1	1.133	0.296		1	1.124	0.292		28.9	0.75946	0.0060811	7.0709	1
2	1.1	0.263		2	1.131	0.299						
3	1.128	0.291		3	1.133	0.301		De				
4	1.113	0.276		4	1.127	0.295		5.2433E-06				
5	1.117	0.28		5	1.14	0.308						
	Ave (in)	0.2812			Ave (in)	0.299						
	Ave (cm)	0.714248			Ave (cm)	0.75946						
	% Swell	6.33001422										
	Ave z (cm)	0.736854										

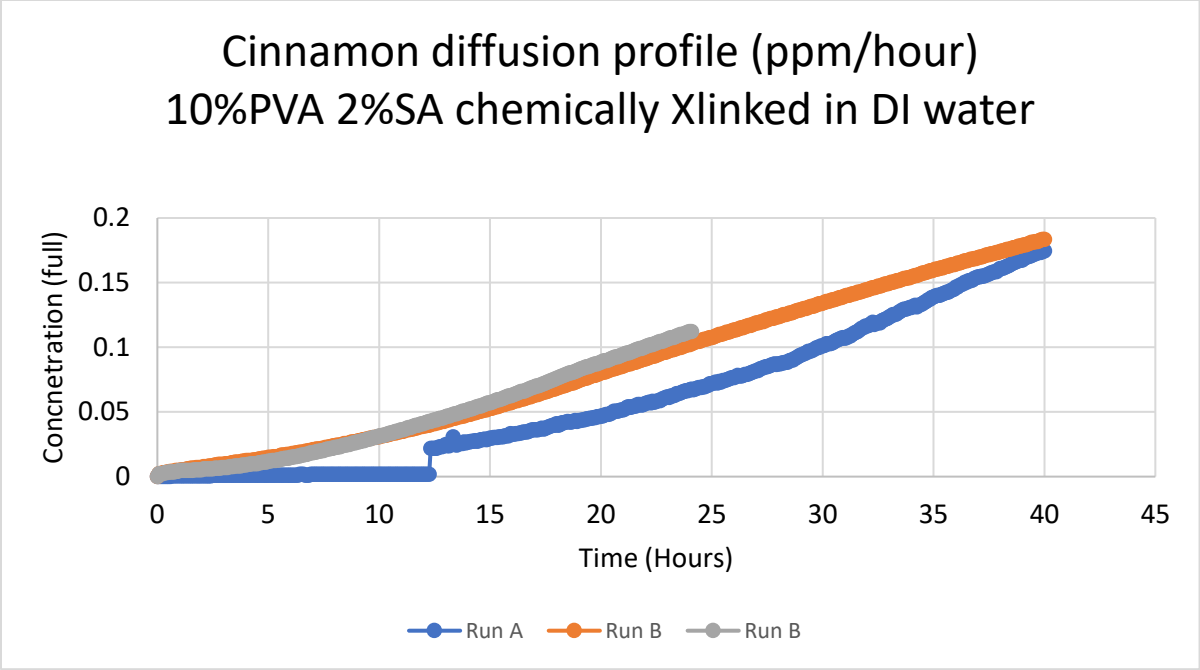

Figure B.17: *Concentration profile for cinnamon chemical crosslink*

Cinnamon diffusion in 10% PVA 2% SA membranes (chemically crosslinked in saturated boric acid, 2% (w/v) $CaCl_2$ for 4.5 hours). Diffusion carried out in 0.5M KCl.

Run A												
3/17/20												
Jonathan 'Jonny' Counts - 10% PVA 2%SA Chem Xlinked 4.5 hours in sat boric acid (2% w/v CaCl2)												
Run was conducted in 0.5M KCl			Membrane equilibrated in 0.5M KCl for 1 day									
Source is considered 1full (unit of concentration since we don't know exactly what the molarity is) Cinnamon derivative is very hard to measure/dissolve/it's really sticky												
Pre Expt Membrane thick				Post Expt Membrane thick								
Initial	0.835	Real (in)		Initial	0.831	Real (in)		Vsink	z (cm)	d(full)/dt	Area (cm^2)	Csource (full)
1	1.275	0.44		1	1.293	0.462		24	1.151128	0.002147	7.0709	1
2	1.28	0.445		2	1.293	0.462						
3	1.253	0.418		3	1.303	0.472		De				
4	1.274	0.439		4	1.26	0.429		2.3302E-06				
5	1.28	0.445		5	1.272	0.441						
	Ave (in)	0.4374			Ave (in)	0.4532						
	Ave (cm)	1.110996			Ave (cm)	1.151128						
	% Swell	6.33001423										
	Ave z (cm)	0.736854										
Run B												
3/19/20												
Jonathan 'Jonny' Counts - 10% PVA 2%SA Chem Xlinked 4.5 hours in sat boric acid (2% w/v CaCl2)												
Run was conducted in 0.5M KCl			Membrane equilibrated in 0.5M KCl for 2 days				Cuvette was cleane after this run (dirty)					
Source is considered 1full (unit of concentration since we don't know exactly what the molarity is) Cinnamon derivative is very hard to measure/dissolve/it's really sticky												
Pre Expt Membrane thick				Post Expt Membrane thick								
Initial	0.834	Real (in)		Initial	0.834	Real (in)		Vsink	z (cm)	d(full)/dt	Area (cm^2)	Csource (full)
1	1.343	0.509		1	1.365	0.531		23	1.360424	0.002786	7.0709	1
2	1.32	0.486		2	1.354	0.52						
3	1.352	0.518		3	1.372	0.538		De				
4	1.332	0.498		4	1.377	0.543		3.4246E-06				
5	1.33	0.496		5	1.38	0.546						
	Ave (in)	0.5014			Ave (in)	0.5356						
	Ave (cm)	1.273556			Ave (cm)	1.360424						
	% Swell	6.82090148										
	Ave z (cm)	1.31699										
Run C												
3/20/20												
Jonathan 'Jonny' Counts - 10% PVA 2%SA Chem Xlinked 4.5 hours in sat boric acid (2% w/v CaCl2)												
Run was conducted in 0.5M KCl			Membrane equilibrated in 0.5M KCl for 2 days				Cuvette was cleaed before run					
Source is considered 1full (unit of concentration since we don't know exactly what the molarity is) Cinnamon derivative is very hard to measure/dissolve/it's really sticky												
Pre Expt Membrane thick				Post Expt Membrane thick								
Initial	0.838	Real (in)		Initial	0.832	Real (in)		Vsink	z (cm)	d(full)/dt	Area (cm^2)	Csource (full)
1	1.252	0.414		1	1.298	0.466		24.3	1.1938	0.002322	7.0709	1
2	1.271	0.433		2	1.295	0.463						
3	1.261	0.423		3	1.3	0.468		De				
4	1.252	0.414		4	1.316	0.484		2.6462E-06				
5	1.258	0.42		5	1.301	0.469						
	Ave (in)	0.4208			Ave (in)	0.47						
	Ave (cm)	1.068832			Ave (cm)	1.1938						
	% Swell	11.6920152										
	Ave z (cm)	1.131316										

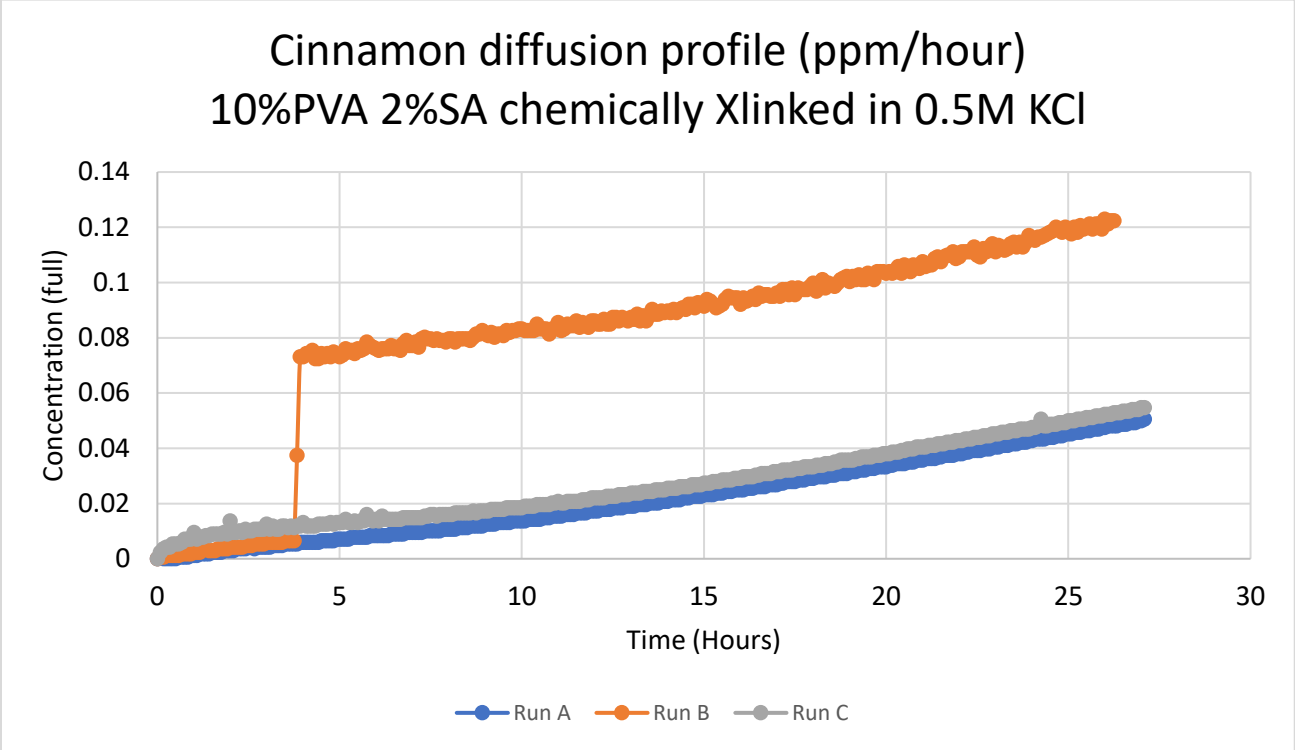

Figure B.18: *Concentration profile for cinnamon chemical crosslink (ionic)*

TCE diffusion:

TCE diffusion in 10% PVA 2% SA membranes (chemically crosslinked in saturated boric acid, 2% (w/v) $CaCl_2$). Diffusion carried out in MilliQ water.

Run conducted by Sam Wolfe in 2018			
TCE difusion in 10% PVA 2% SA membranes crosslinked chemically			
in saturated boric acid and 2% (w/v) CaCl2			
z1 (cm)	z2 (cm)	z3 (cm)	Area (cm^2)
0.97282	0.97282	0.6985	7.0709
Vol (mL) 1	Vol (mL) 2	Vol (mL) 3	
65	70	70	
[TCE] source (ppm)	[TCE] source (ppm)	[TCE] source (ppm)	
150	150	150	
De (cm^2/sec) 1	De (cm^2/sec) 2	De (cm^2/sec) 3	
1.25E-05	1.24E-05	8.08E-06	

Conc (ppm)	Abs @ 200nm
25	0.171
50	0.489
75	0.871
100	1.323

Table B.6: *TCE dilution/calibration data*

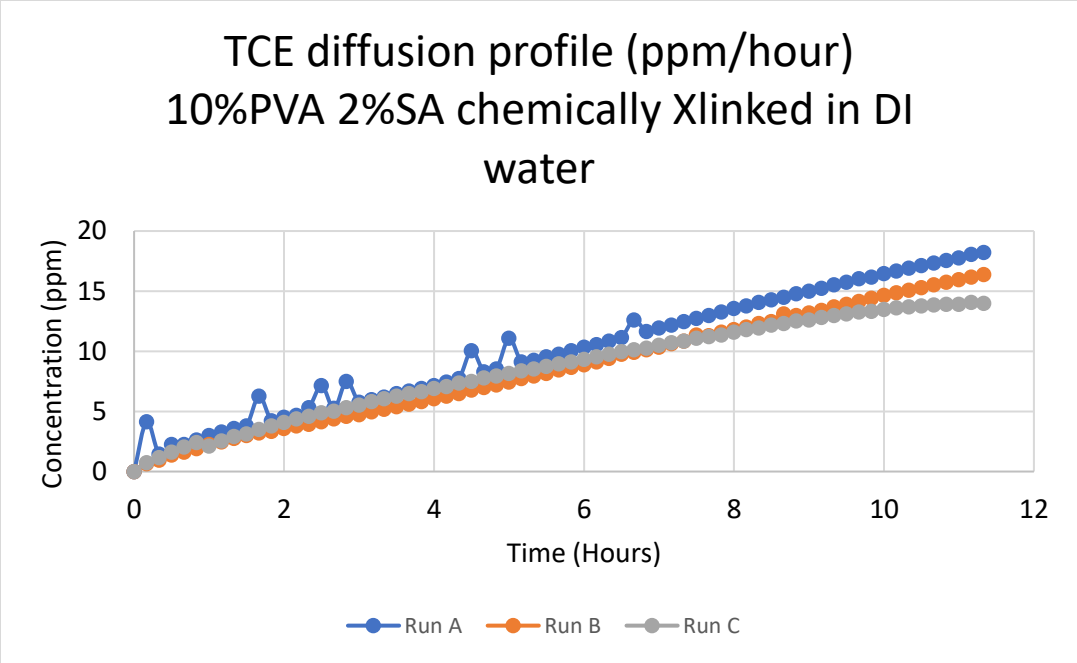

Figure B:19: *Concentration profile for TCE diffusion*

DCE Diffusion:

DCE diffusion in 10% PVA 2% SA membranes (chemically crosslinked in saturated boric acid, 2% (w/v) $CaCl_2$). Diffusion carried out in MilliQ water.

Run conducted by Sam Wolfe in 2018			
DCE difusion in 10% PVA 2% SA membranes crosslinked chemically			
in saturated boric acid and 2% (w/v) CaCl2			
z1 (cm)	z2 (cm)	z3 (cm)	Area (cm^2)
0.84328	1.1303	0.7874	7.0709
Vol (mL) 1	Vol (mL) 2	Vol (mL) 3	
65	65	65	
[TCE] source (ppm)	[TCE] source (ppm	[TCE] source (ppm)	
150	150	150	
De (cm^2/sec) 1	De (cm^2/sec) 2	De (cm^2/sec) 3	
6.49E-06	8.23E-06	5.99E-06	

Conc (ppm)	Abs @ 200nm
0	0
0.03556	0.049
25	0.644
50	1.252
75	1.833
100	2.258

Table B.7: *cDCE dilution/calibration data*

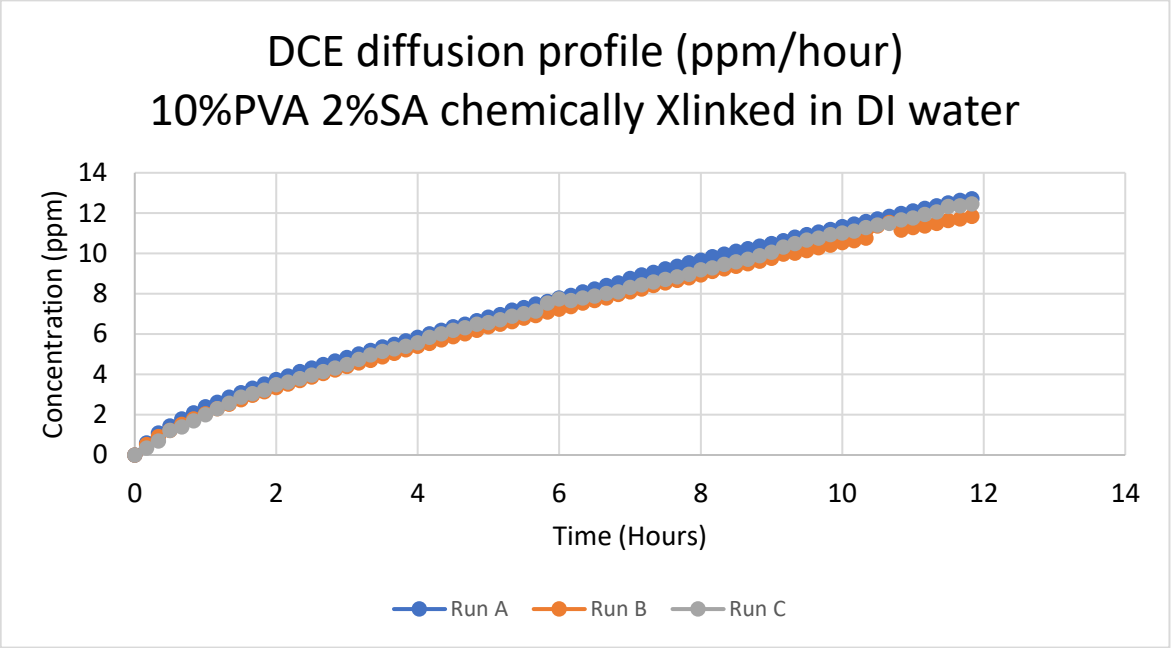

Figure B20: *Concentration Gradient for DCE Diffusion*

VC Diffusion:

VC diffusion in 10% PVA 2% SA membranes (chemically crosslinked in saturated boric acid, 2% (w/v) $CaCl_2$). Diffusion carried out in MilliQ water.

Run conducted by Sam Wolfe in 2018			
DCE difusion in 10% PVA 2% SA membranes crosslinked chemically			
in saturated boric acid and 2% (w/v) CaCl2			
z1 (cm)	z2 (cm)	z3 (cm)	Area (cm^2)
0.63652	0.6228	0.71679	7.0709
Vol (mL) 1	Vol (mL) 2	Vol (mL) 3	
14.5	14.5	16.7	
[TCE] source (ppm	[TCE] source (ppm)	[TCE] source (ppm)	
98.765	154.9	152.01	
De (cm^2/sec) 1	De (cm^2/sec) 2	De (cm^2/sec) 3	
6.55E-06	2.45E-06	3.11E-06	

Conc (ppm)	Abs @ 202nm
0	0
6.51	0.0306
13.02	0.0656
26.04	0.1488
52.08	0.3629

Table B.8: *VC dilution/calibration data*

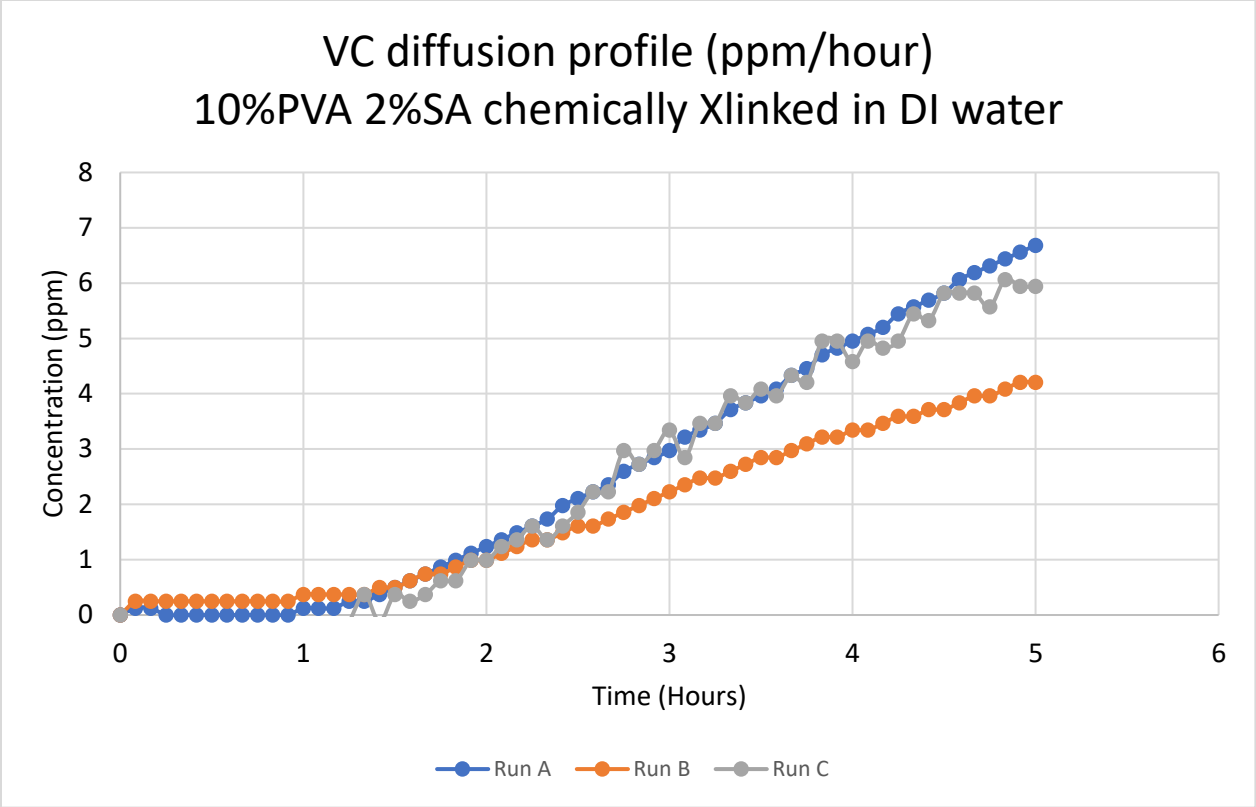

Figure B21: *Concentration gradient for VC diffusion*

Proton Diffusion:

Proton diffusion in 10% PVA 2% SA membranes (chemically crosslinked in saturated boric acid, 2% (w/v) $CaCl_2$). Diffusion carried out in MilliQ water.

10% PVA 2% SA membranes Xlinked in sat. boric acid 2% (w/v) CaCl2 for 4.5 hours												
Equilibrated in DI water for one hour												
Run A and B only show diffusion after the lag period (proton adsorption)												
	Run A	Run B	Run C	Run D	Run E							
d(M)/d(Hrs)	Slope 1	Slope 2	Slope 3	Slope 4	Slope 5			Run A	Run B	Run C	Run D	Run E
	1.3677E-05	2.3749E-05	1.3469E-05	1.2916E-05	2.6983E-05			Pre M1	Pre M2	Final M3	Final M4	Final M5
							:	0.84	0.84	0.838	0.838	0.83
	Vol 1	Vol 2	Vol 3	Vol 4	Vol		1	1.252	1.165	1.224	1.209	1.3
	35.2	29.5	32	37	34.3		2	1.249	1.182	1.224	1.227	1.305
							3	1.252	1.195	1.22	1.253	1.309
	Area	Area	Area	Area	Area		4	1.258	1.192	1.215	1.277	1.304
	7.0709	7.0709	7.0709	7.0709	7.816		5	1.249	1.186	1.219	1.211	1.301
	Csource (M)	Csource (M)	Csource (M)	Csource (M)	Csource			0.412	0.325	0.386	0.371	0.47
	0.00338844	0.00338844	0.00151356	0.00151356	0.00331131			0.409	0.342	0.386	0.389	0.475
								0.412	0.355	0.382	0.415	0.479
	z1	z2	z3	z4	z5			0.418	0.352	0.377	0.439	0.474
	1.04648	0.87376	0.971296	1.009396	1.203452			0.409	0.346	0.381	0.373	0.471
							Ave (in)	0.412	0.344	0.3824	0.3974	0.4738
	De 1	De 2	De 3	De 4	De 5		Ave (cm)	1.04648	0.87376	0.971296	1.009396	1.203452
	5.841E-06	7.0971E-06	1.0866E-05	1.252E-05	1.1954E-05							
					m is the slope of pH vs mV							
	Calibration Data				b is the intercept							
		Run A	Run B			Run C	Run D					
	pH	Probe 1 (mV	Probe 2 (mV)		pH	Probe 1 (mV	Probe 2 (mV)					
	4	3.67724167	54278.5079		4	58417.9375	51636.5					
	7	1.34710833	53770.7451		7	51762.6875	44934.1875					
	10	0.40655972	52932.6964									
					m	-0.0004508	-0.0004476					
	m	-4.49E-04	-4.51E-04		b	30.333	27.113					
	b	27.159	30.499									

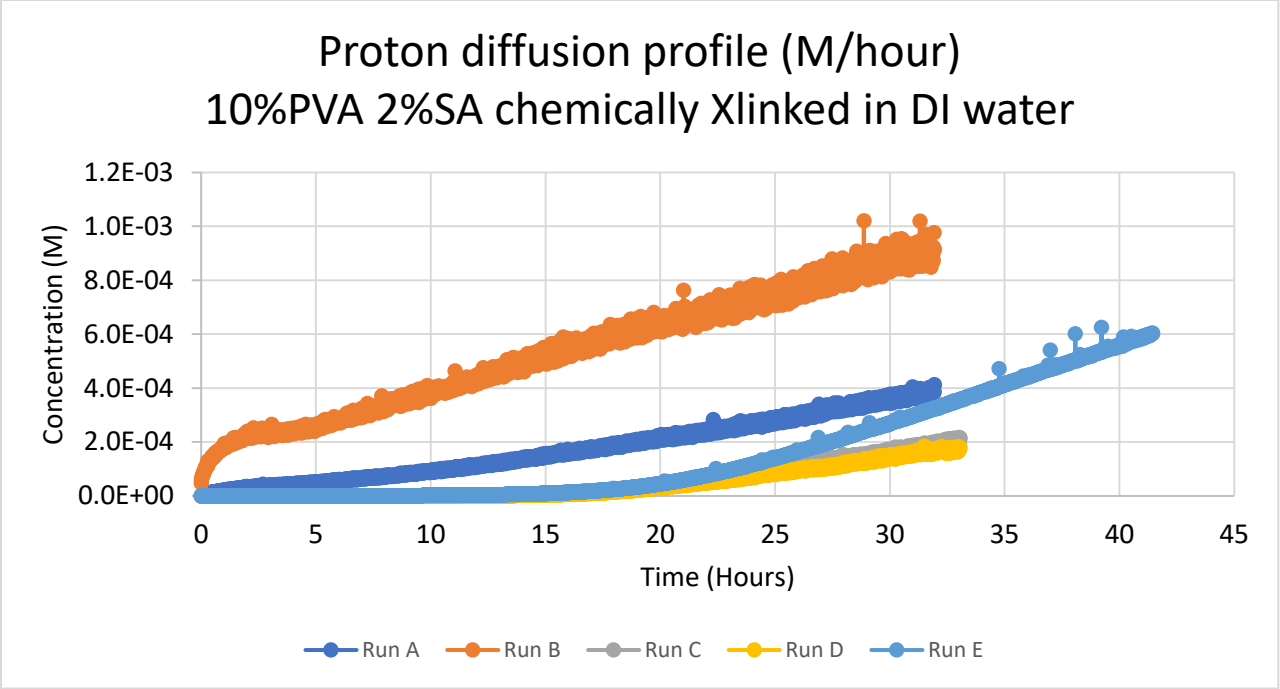

Figure B22: *Concentration gradient for proton diffusion (chemically crosslinked) – 10% PVA 2% SA*

Proton diffusion in 10% PVA 2%SA membranes (frozen/thawed 5x in -20ºC). Diffusion carried out in MilliQ water.

10% PVA 2%SA Membranes (Freeze/Thawed 5x in -20C)									
Equilibrated in DI water for one hour									
						Run A	Run B	Run C	Run D
	Run A	Run B	Run C	Run D	thickness (in)	M1	M2	M3	M4
	d[H]/dt 1	d[H]/dt 2	d[H]/dt 3	d[H]/dt 4	Initial:	0.839	0.837	0.838	0.84
	0.0000558	2.4085E-05	2.06338E-05	2.3255E-05	1	1.145	1.298	1.383	1.359
					2	1.13	1.31	1.39	1.36
	Vol 1	Vol 2	Vol 3	Vol 4	3	1.148	1.333	1.322	1.382
	28.5	92	92	92	4	1.151	1.298	1.368	1.342
					5	1.148	1.292	1.379	1.349
	Area (cm^2)	Area (cm^2)	Area (cm^2)	Area (cm^2)					
	7.816	7.816	7.816	7.816					
					Real 1	0.306	0.461	0.545	0.519
	Csource (M)	Csource (M)	Csource (M)	Csource (M)	Real 2	0.291	0.473	0.552	0.52
	0.003890451	0.004786301	0.004786301	0.004786301	Real 3	0.309	0.496	0.484	0.542
					Real 4	0.312	0.461	0.53	0.502
	z1 (cm)	z2 (cm)	z3 (cm)	z4 (cm)	Real 5	0.309	0.455	0.541	0.509
	0.77572	1.191768	1.347216	1.316736					
					Ave (in)	0.3054	0.4692	0.5304	0.5184
	De (cm^2/s) 1	De (cm^2/s) 2	De (cm^2/s) 3	De (cm^2/s) 4	Ave (cm)	0.775716	1.191768	1.347216	1.316736
	1.12692E-05	1.96083E-05	1.89896E-05	2.09178E-05					

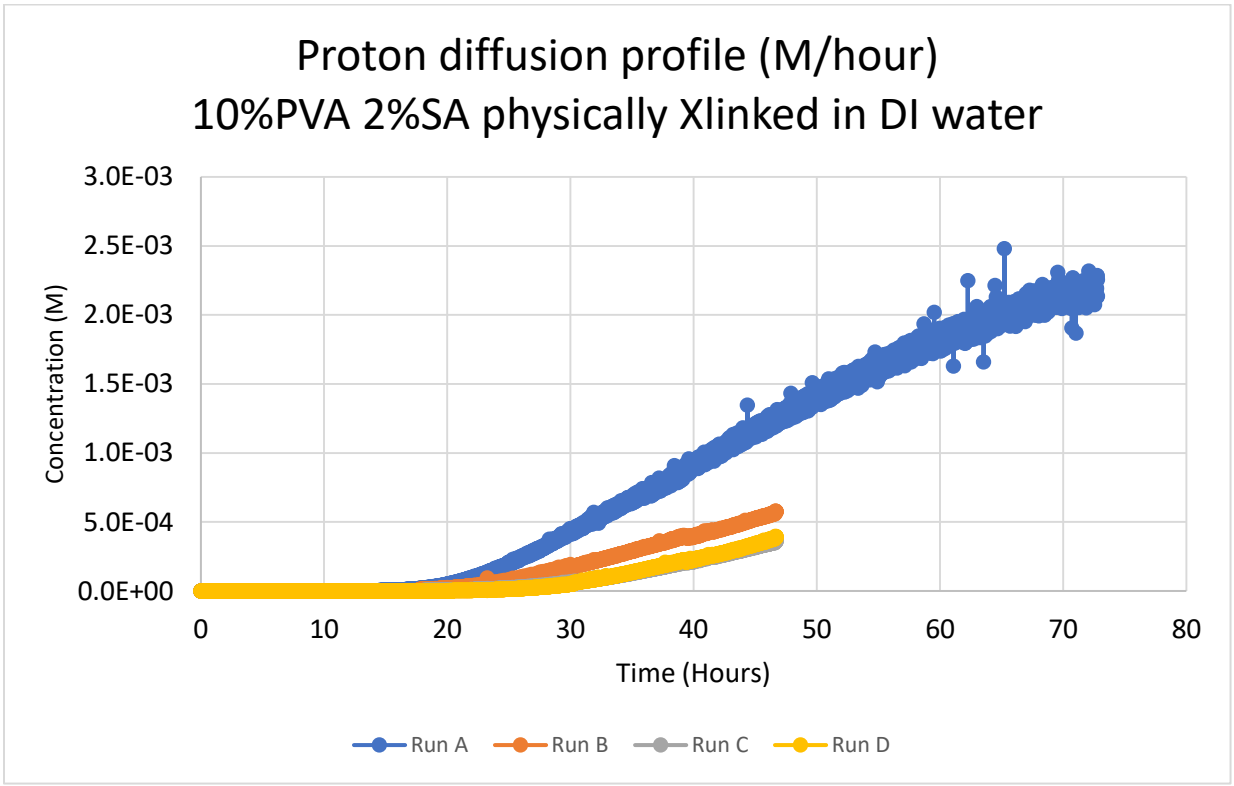

Figure B23: *Concentration gradient for proton diffusion (physically crosslinked) – 10% PVA 2% SA*

Proton diffusion in 10% PVA (frozen/thawed 5x in -20°C). Diffusion carried out in MilliQ water.

10% PVA (MW: 184kDa)Membranes (Freeze/Thawed 5x in -20C)										
Equilibrated in DI water for one hour										
						Run A	Run B	Run C	Run D	
	Run A	Run B	Run C	Run D	thickness (in)	Puck 1	Puck 2	M1 Pre	M3 Pre	
	d[H]/dt 1	d[H]/dt 2	d[H]/dt 3	d[H]/dt 4	Initial:	0.839	0.837	0.837	0.838	
	8.64314E-06	8.61452E-06	2.13869E-05	2.42615E-05	1	1.265	1.265	1.26	1.242	
					2	1.283	1.306	1.232	1.225	
	Vol 1	Vol 2	Vol 3	Vol 4	3	1.275	1.307	1.232	1.266	
	95	95	92	92	4	1.288	1.25	1.239	1.208	
					5	1.277	1.281	1.233	1.229	
	Area (cm^2)	Area (cm^2)	Area (cm^2)	Area (cm^2)						
	7.81606	7.81606	7.81	7.81						
					Real 1	0.426	0.428	0.423	0.404	
	Csource (M)	Csource (M)	Csource (M)	Csource (M)	Real 2	0.444	0.469	0.395	0.387	
	0.001995262	0.001995262	0.00402717	0.00402717	Real 3	0.436	0.47	0.395	0.428	
					Real 4	0.449	0.413	0.402	0.37	
	z1 (cm)	z2 (cm)	z3 (cm)	z4 (cm)	Real 5	0.438	0.444	0.396	0.391	
	1.114	1.129	1.021588	1.00584						
					Ave (in)	0.4386	0.4448	0.4022	0.396	
	De (cm^2/s) 1	De (cm^2/s) 2	De (cm^2/s) 3	De (cm^2/s) 4	Ave (cm)	1.114044	1.129792	1.021588	1.00584	
	1.62926E-05	1.64573E-05	1.77525E-05	1.98281E-05						

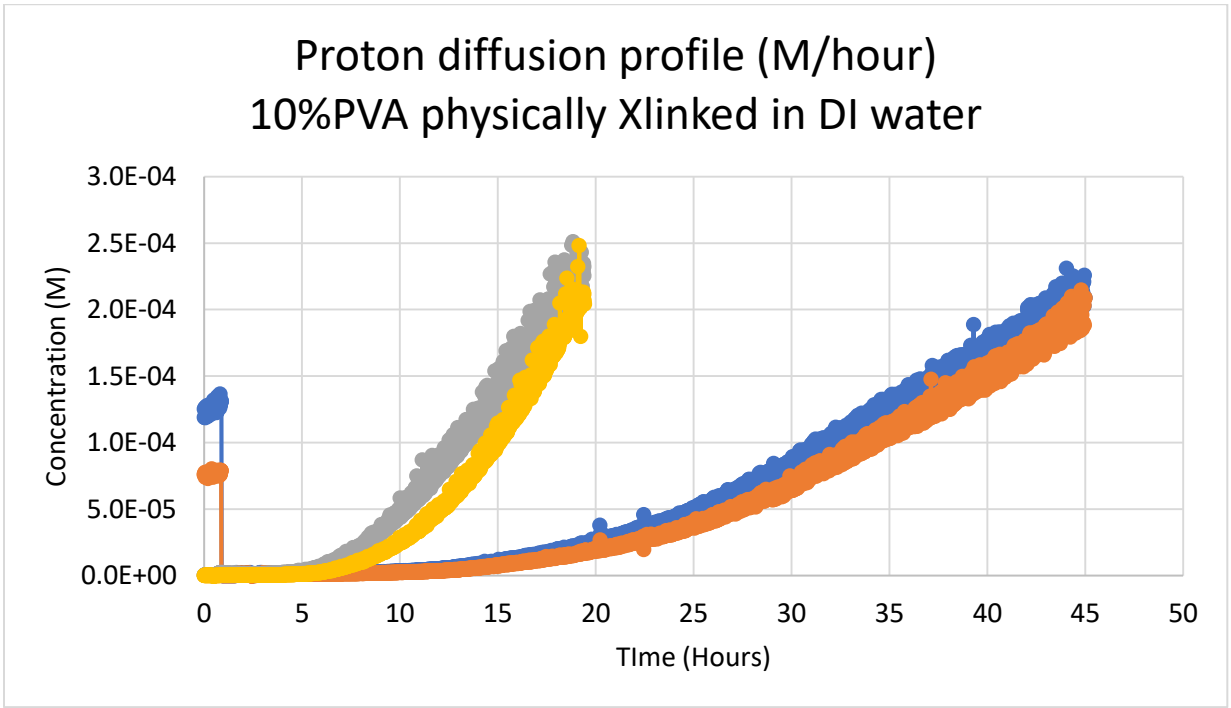

Figure B24: *Concentration gradient for proton diffusion (physically crosslinked) – 10% PVA*

Proton diffusion in 15% PVA membranes (frozen/thawed 5x in -20C). Diffusion carried out in MilliQ water.

15% PVA (MW: 184kDa)Membranes (Freeze/Thawed 5x in -20C)								
Equilibrated in DI water for one hour								
						Run A	Run B	Run C
	Run A	Run B	Run C		thickness (in	Puck 1	Puck 2	M1 Pre
	d[H]/dt 1	d[H]/dt 2	d[H]/dt 3		Initial:	0.83	0.828	0.828
	1.34165E-05	1.01125E-05	2.05432E-05		1	1.334	1.335	1.318
					2	1.31	1.347	1.299
	Vol 1	Vol 2	Vol 3		3	1.346	1.347	1.32
	92	92	92		4	1.296	1.333	1.31
					5	1.33	1.356	1.314
	Area (cm^2)	Area (cm^2)	Area (cm^2)					
	7.81606	7.81606	7.81			0.504	0.507	0.49
					Real 1	0.48	0.519	0.471
	Csource (M)	Csource (M)	Csource (M)		Real 2	0.516	0.519	0.492
	0.003890451	0.003890451	0.003981072		Real 3	0.466	0.505	0.482
					Real 4	0.5	0.528	0.486
	z1 (cm)	z2 (cm)	z3 (cm)		Real 5			
	1.250188	1.19126	1.09677			0.4932	0.5156	0.4842
					Ave (in)	1.252728	1.309624	1.229868
	De (cm^2/s) 1	De (cm^2/s) 2	De (cm^2/s) 3		Ave (cm)	1.250188	1.19126	1.096772
	1.41075E-05	1.01321E-05	1.85191E-05					

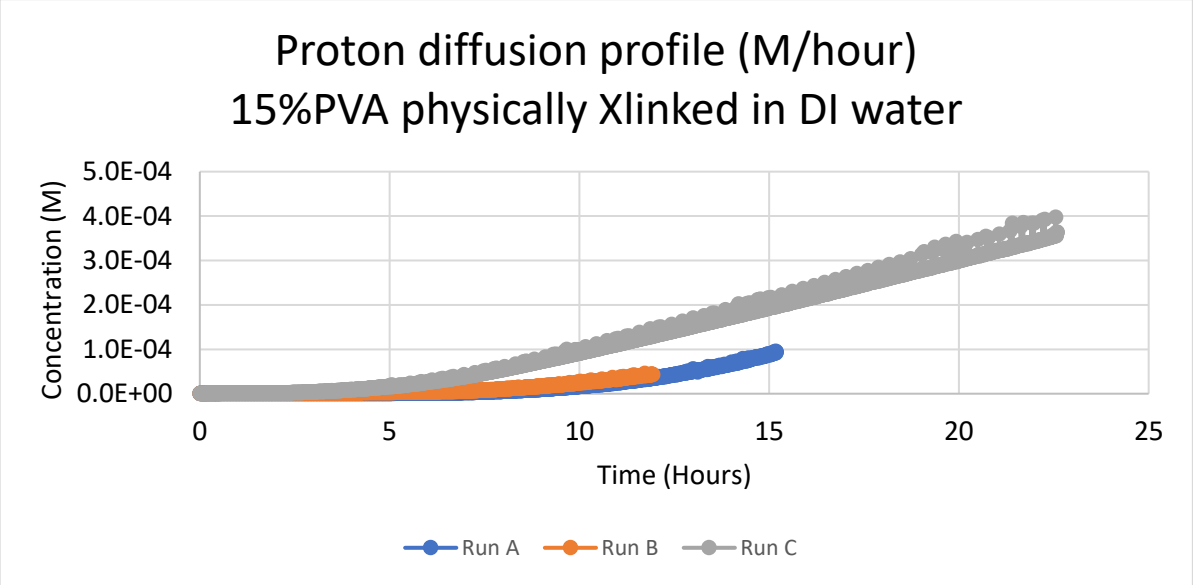

Figure B25: *Concentration gradient for proton diffusion (physically crosslinked) – 15% PVA*

Proton diffusion in 30% PVA membranes (frozen/thawed 5x in -20°C). Diffusion carried out in DI Water.

30% PVA (MW: 31kDa)Membranes (Freeze/Thawed 5x in -20C)							
Equilibrated in DI water for 2 days							
					Run A	Run B	Run C
	Run A	Run B	Run C	thickness (in)	Puck 1	Puck 2	M1 Pre
	d[H]/dt 1	d[H]/dt 2	d[H]/dt 3	Initial:	0.838	0.839	0.839
	1.44887E-05	1.67841E-05	1.56787E-05	1	1.404	1.417	1.385
				2	1.415	1.418	1.367
	Vol 1	Vol 2	Vol 3	3	1.393	1.427	1.362
	92	92	92	4	1.408	1.412	1.361
				5	1.386	1.41	1.361
	Area (cm^2)	Area (cm^2)	Area (cm^2)				
	7.816	7.816	7.816				
				Real 1	0.566	0.578	0.546
	Csource (M)	Csource (M)	Csource (M)	Real 2	0.577	0.579	0.528
	0.004265795	0.004265795	0.004265795	Real 3	0.555	0.588	0.523
				Real 4	0.57	0.573	0.522
	z1 (cm)	z2 (cm)	z3 (cm)	Real 5	0.548	0.571	0.522
	1.430528	1.467612	1.341628				
				Ave (in)	0.5632	0.5778	0.5282
	De (cm^2/s) 1	De (cm^2/s) 2	De (cm^2/s) 3	Ave (cm)	1.430528	1.467612	1.341628
	1.58865E-05	1.88803E-05	1.61229E-05				

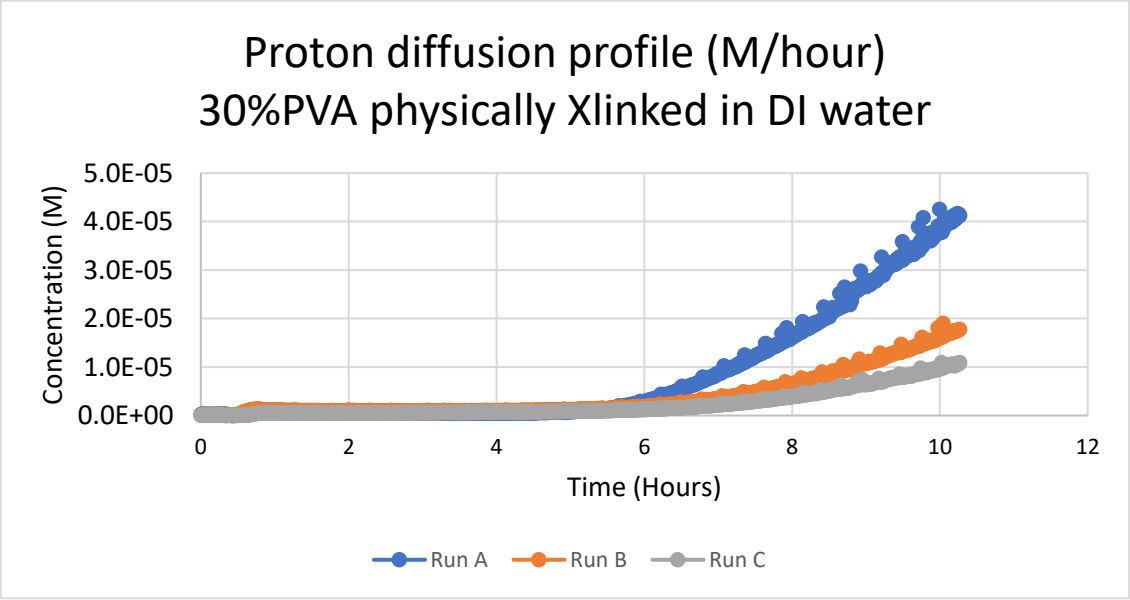

Figure B26: *Concentration gradient for DI proton diffusion (physically crosslinked) – 30% PVA*

Proton diffusion in 10% PVA 50% glycerol membranes (covered and set at room temperature for 4 days). Diffusion carried out in MilliQ water.

10g PVA (MW: 148kDa) and 50mL glycerol and 50mL DI water, dissolved and left coverered to set 4 days							
Equilibrated in DI water for 2 days.							
					Run A	Run B	Run C
Slope 1	Slope 2	Slope 3		thickness (in)	Puck 1	Puck 2	M1 Pre
1.84E-05	1.5641E-05	2.0617E-05		Initial:	0.83	0.828	0.828
				1	1.334	1.335	1.318
Vol (mL)	Vol (mL)	Vol (mL)		2	1.31	1.347	1.299
92	92	92		3	1.346	1.347	1.32
				4	1.296	1.333	1.31
Area (cm^2)	Area (cm^2)	Area (cm^2)		5	1.33	1.356	1.314
7.816	7.816	7.816					
				Real 1	0.504	0.507	0.49
Csource (M)	Csource (M)	Csource (M)		Real 2	0.48	0.519	0.471
0.00371535	0.00371535	0.00371535		Real 3	0.516	0.519	0.492
				Real 4	0.466	0.505	0.482
z1 (cm)	z2 (cm)	z3 (cm)		Real 5	0.5	0.528	0.486
1.252728	1.309624	1.229868					
				Ave (in)	0.4932	0.5156	0.4842
De 1	De 2	De 3		Ave (cm)	1.252728	1.309624	1.229868
2.03E-05	1.80E-05	2.23E-05					
Calibration data							
	mV	mV	mV				
pH	Probe 1	Probe 2	probe3				
4	52880.7561	54196.0244	52119.6585				
7	46436	47825.1026	45867.6923				
m	-0.0004655	-0.0004709	-0.0004798		m is the slope of pH (y) vs mV (x)		
b	28.6157133	29.5203372	29.0095682		b is the intercept of a linear eqn.		
	-0.1555725	0.58794759	-0.1428731				

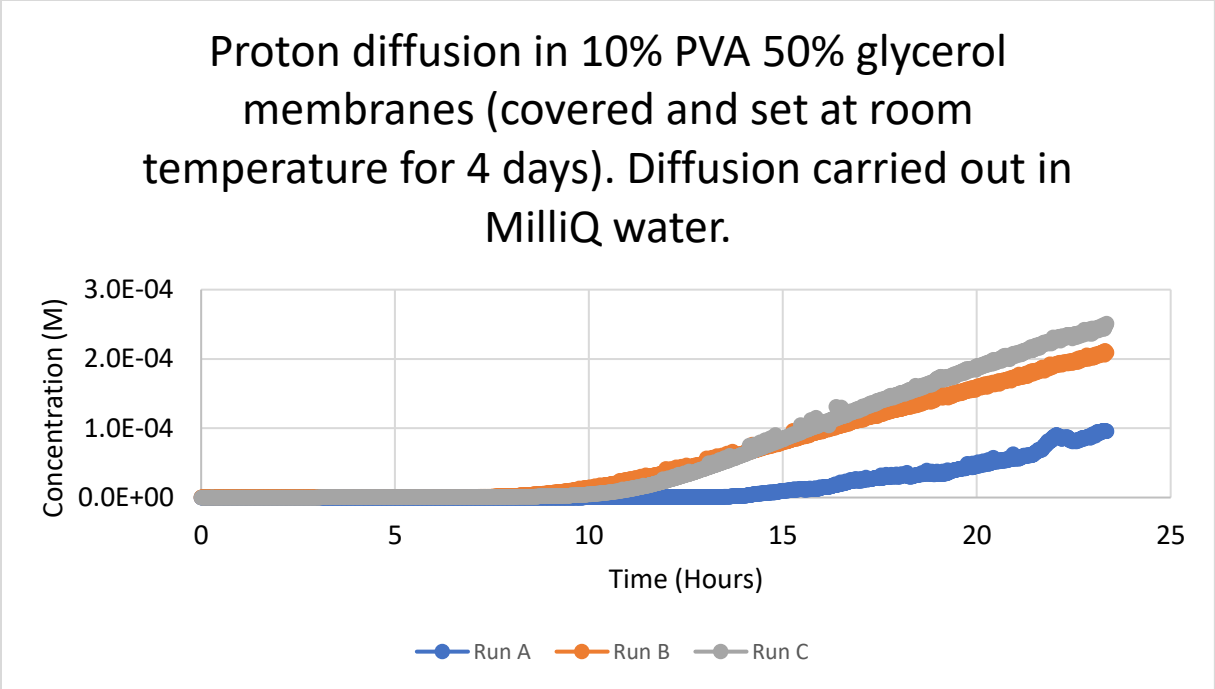

Figure B27: *Concentration gradient for proton diffusion (physically crosslinked) – 10% PVA 50% Glycerol*

Proton diffusion in 10% PVA 2% SA membranes (frozen/thawed 5x at -20ºC). Diffusion carried out in 0.1M KCl.

10% PVA 2%SA Membranes (Freeze/Thawed 5x in -20C)								
Equilibrated in 0.1M KCl water for 5 days					Membrane thickness determination (5 measurements)			
	Run A	Run B	Run C			Run A	Run B	Run C
	d[H]/dt 1	d[H]/dt 2	d[H]/dt 3		thickness (in)	M1	M2	M3
	3.38716E-05	3.68106E-05	4.18618E-05		Initial:	0.839	0.842	0.84
					1	1.281	1.253	1.297
	Vol 1	Vol 2	Vol 3		2	1.291	1.265	1.321
	92	92	92		3	1.296	1.246	1.267
					4	1.292	1.258	1.299
	Area (cm^2)	Area (cm^2)	Area (cm^2)		5	1.295	1.267	1.295
	7.816	7.816	7.816					
	Csource (M)	Csource (M)	Csource (M)		Real 1	0.442	0.411	0.457
	0.004265795	0.003801894	0.004265795		Real 2	0.452	0.423	0.481
					Real 3	0.457	0.404	0.427
	z1 (cm)	z2 (cm)	z3 (cm)		Real 4	0.453	0.416	0.459
	1.14808	1.056132	1.157732		Real 5	0.456	0.425	0.455
	De (cm^2/s) 1	De (cm^2/s) 2	De (cm^2/s) 3		Ave (in)	0.452	0.4158	0.4558
	2.98064E-05	3.34343E-05	3.71473E-05		Ave (cm)	1.14808	1.056132	1.157732

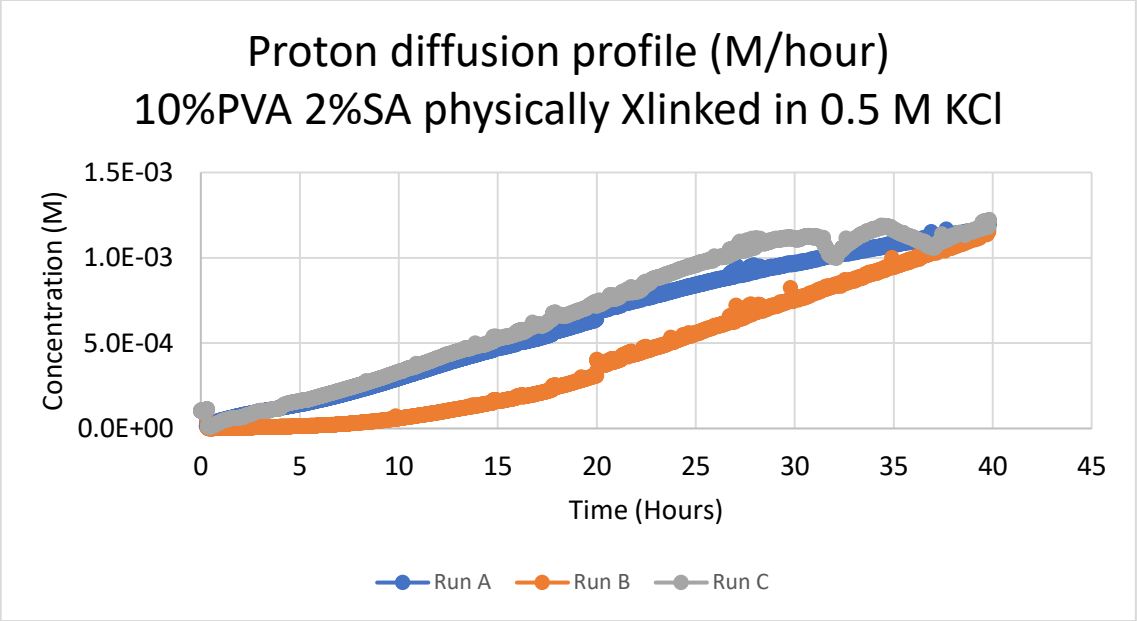

Figure B28: *Concentration gradient for ionic proton diffusion (physically crosslinked) – 10% PVA 2% SA*

Proton diffusion in 30% PVA membranes (31kDa, frozen/thawed 5x at -20ºC). Diffusion carried out in 0.1M KCl.

30% PVA (MW: 51kDa)Membranes (Freeze/Thawed 5x in -20C)						Run A	Run B	Run C
Equilibrated in DI water for one hour					thickness (in)	Post M1	Post M2	Post M3
					Initial:	0.832	0.832	0.832
	Run A	Run B	Run C		1	1.303	1.258	1.354
	d[H]/dt 1	d[H]/dt 2	d[H]/dt 3		2	1.305	1.26	1.36
	0.000029969	0.000031589	0.000027095		3	1.307	1.264	1.36
					4	1.309	1.257	1.355
	Vol 1	Vol 2	Vol 3		5	1.308	1.268	1.36
	92	92	92					
	Area (cm^2)	Area (cm^2)	Area (cm^2)		Real 1	0.471	0.426	0.522
	7.816	7.816	7.816		Real 2	0.473	0.428	0.528
					Real 3	0.475	0.432	0.528
	Csource (M)	Csource (M)	Csource (M)		Real 4	0.477	0.425	0.523
	0.004073803	0.004073803	0.004073803		Real 5	0.476	0.436	0.528
	z1 (cm)	z2 (cm)	z3 (cm)		Ave (in)	0.4744	0.4294	0.5258
	1.204976	1.090676	1.335532		Ave (cm)	1.204976	1.090676	1.335532
	De (cm^2/s) 1	De (cm^2/s) 2	De (cm^2/s) 3					
	2.89835E-05	2.76524E-05	2.90432E-05		Calibration Data			
					pH	Probe 1 (mV)	probe 2 (mV)	probe 3 (mV)
					4	53516.89286	54847.51786	53101.83929
					7	47018.38776	48371.36735	46569.85714
					m	-0.000461645	-0.000463238	-0.000459279
					b	28.70578634	29.40746286	28.38854154
						-0.160908828	0.564553749	-0.252446725

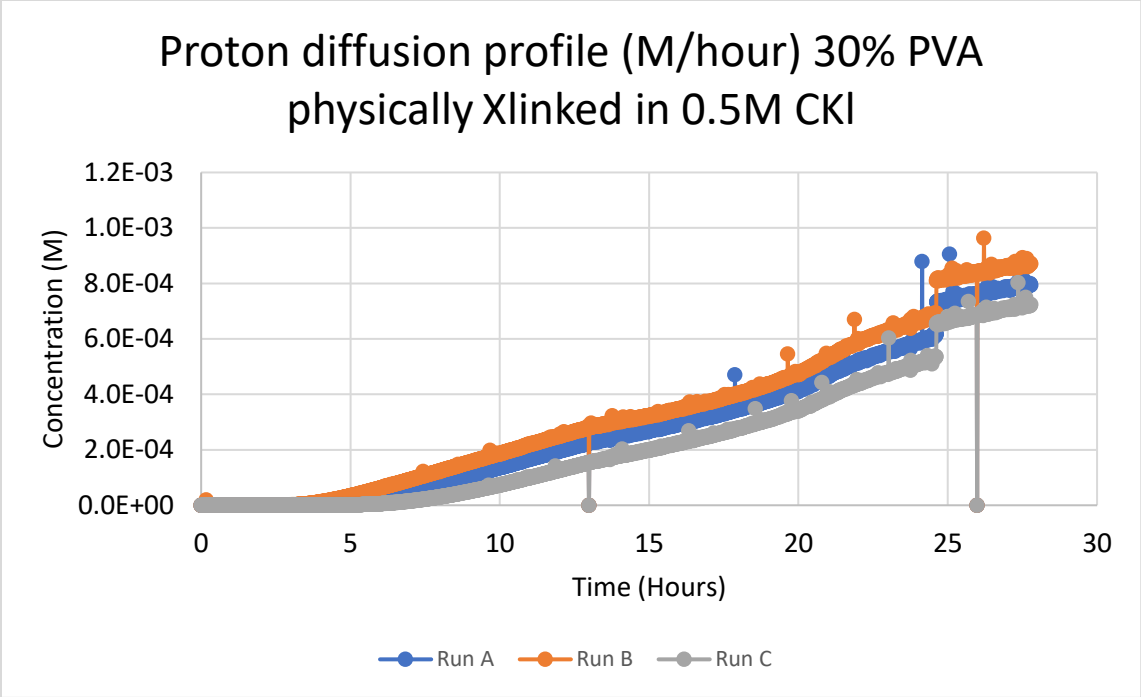

Figure B29: *Concentration gradient for ionic proton diffusion (physically crosslinked) – 30% PVA*

Proton diffusion in 10% PVA membranes (frozen/thawed 5x at -20°C). Diffusion carried out in 0.5M KCl.

10% PVA 2% SA (MW: 184kDa)Membranes (Freeze/Thawed 5x in -20C)														
Equilibrated in 0.5M KCl water for six days														
	Run A	Run B	Run C	Run D	Run E	Run F			Run A	Run B	Run C	Run D	Run E	Run F
	d[H]/dt 1	d[H]/dt 2	d[H]/dt 3	d[H]/dt 4	d[H]/dt 5	d[H]/dt 6		thickness (in	Puck 1	Puck 2	Puck 3	Puck 4	Puck 5	Puck 6
	5.50487E-05	5.35066E-05	5.81716E-05	4.81334E-05	4.65725E-05	5.12154E-05		Initial:	0.838	0.838	0.838	0.836	0.838	0.839
								1	1.299	1.341	1.281	1.27	1.24	1.256
	Vol 1	Vol 2	Vol 3	Vol 4	Vol 5	Vol 6		2	1.296	1.356	1.292	1.277	1.24	1.226
	92	92	92	92	92	92		3	1.291	1.359	1.301	1.288	1.272	1.237
								4	1.286	1.331	1.28	1.261	1.257	1.243
	Area (cm^2)	Area (cm^2)	Area (cm^2)	Area (cm^2)	Area (cm^2)	Area (cm^2)		5	1.285	1.332	1.298	1.277	1.254	1.233
	7.816	7.816	7.816	7.816	7.816	7.816								
	Csource (M)	Csource (M)	Csource (M)	Csource (M)	Csource (M)	Csource (M)		Real 1	0.461	0.503	0.443	0.434	0.402	0.417
	0.005623413	0.005623413	0.005623413	0.004073803	0.004073803	0.004073803		Real 2	0.458	0.518	0.454	0.441	0.402	0.387
								Real 3	0.453	0.521	0.463	0.452	0.434	0.398
	z1 (cm)	z2 (cm)	z3 (cm)	z4 (cm)	z5 (cm)	z6 (cm)		Real 4	0.448	0.493	0.442	0.425	0.419	0.404
	1.151636	1.284732	1.149096	1.114044	1.053084	1.016		Real 5	0.447	0.494	0.46	0.441	0.416	0.394
	De (cm^2/s) 1	De (cm^2/s) 2	De (cm^2/s) 3	De (cm^2/s) 4	De (cm^2/s) 5	De (cm^2/s) 6		Ave (in)	0.4534	0.5058	0.4524	0.4386	0.4146	0.4
	3.68607E-05	3.99688E-05	3.88658E-05	4.30377E-05	3.93635E-05	4.17633E-05		Ave (cm)	1.151636	1.284732	1.149096	1.114044	1.053084	1.016
m	-0.000450709	-0.000448043	-0.000452923	-0.0004517	-0.0004489	-0.0004528								
b	29.62334829	28.1560421	27.98631041	29	29	29								
b correction	1.055342918	-0.386299428	-0.802915625	0.4572463	0.4871784	0.3136992								
y = m*x + b		Where y is the pH and x is mV reading for each pH probe												

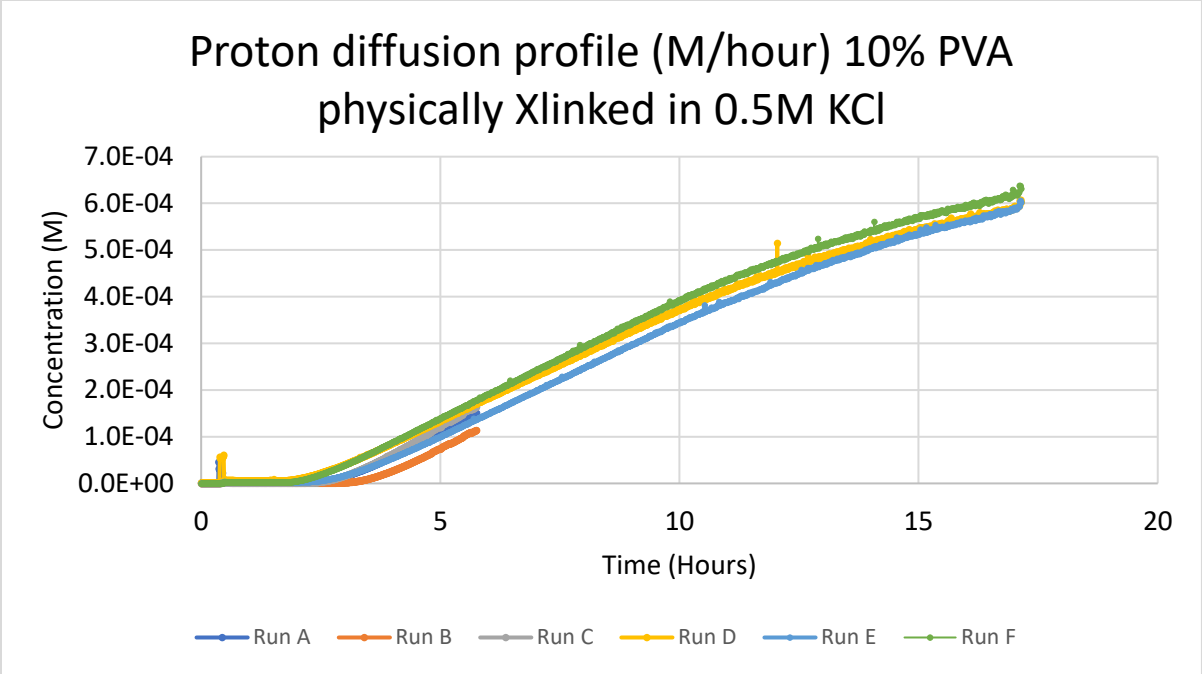

Figure B30: *Concentration gradient for ionic proton diffusion (physically crosslinked) – 10% PVA*

Polymer volume (physically crosslinked 10% PVA membranes) in deionized water vs time. (Swelling data)

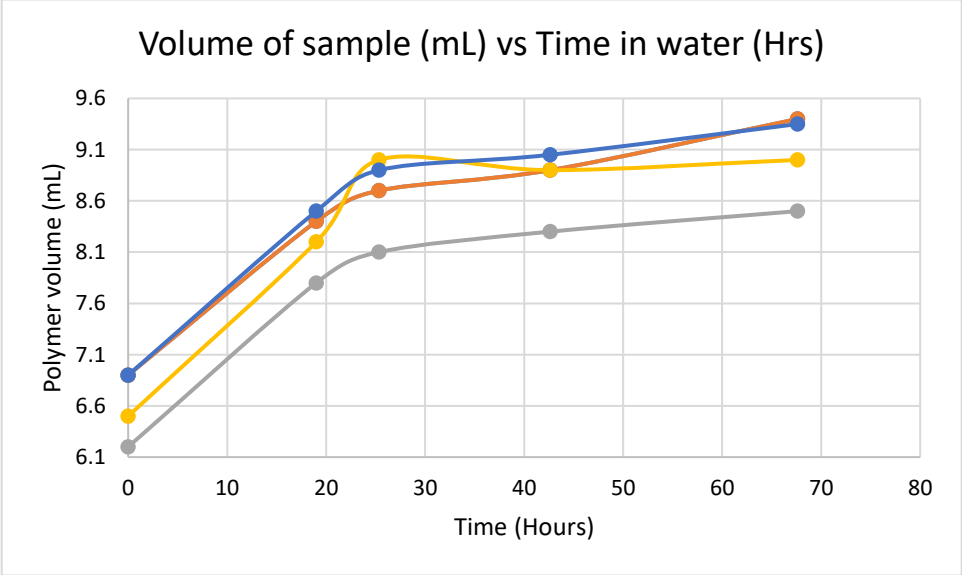

Figure B31: *Volume increase in polymers with time*

Appendix C: GellipHish Standard Operating Procedure

GellipHish Diffusion Procedure:

1. Prepare Membranes

   Polymer is poured into molds and sequential freezing and thawing conducted to form solid membranes in the mold. Upon finishing the last freeze cycle, pucks should be placed in water to equilibrate for at least 1 hour. Pucks equilibrated for over one week show negligible swelling throughout the run. Alternatively, a sheet of membrane can be frozen, dunked in chemical crosslinker for 4 ½ hours and cut with a cookie-cutter. The cut pieces can then be inserted into molds, then placed in water to swell for 1 hour.

2. Calibration

   GellipHish is turned on and a python script selected which employs 4, 8, 12, or 16 pH probes. Clicking "Open File" will set up a csv file to record values. This file must be named in the box below the button prior to running (name the program with the date, followed by 'GelliRun'). Probes are rinsed with DI water and each probe is place in 10+mL of 4.01 pH buffer. Clicking the "pH" button starts measurements and collects mV readings for each probe over time. Once the probe readings stabilize (30-45 minutes) the probes can be rinsed and placed in pH 7.0 buffer. The probes are then allowed to equilibrate again, then are removed and the program results saved. A new instance of the script is run for the actual diffusion experiment. A three point calibration may also be conducted with pH 5.0 or 10.0 buffer, though the slope between mV and pH does not significantly change.

3. Puck Preparation

   Puck thicknesses are measured before the experiment is conducted. Five measurements are taken with calipers and recorded for each puck, allowing determination of average thickness and standard deviation of measurement. Pucks are then placed in the sink

arms, and arms are securely inserted into the PVC cross adapter (check that arms are pushed in as far as possible).

4. Diffusion Sink Setup

Sink arms are turned upside-down, so puck is at the bottom. A stir bar is inserted through the pH probe adapter and 92.0 mL of DI water is added (record volume of water). The pH probe is then inserted through the adapter slowly, and the probe is slowly moved up and down to prevent compression of air in the sink. Forcing the probe may have a piston effect which breaks the seal of the membrane and causes leakage. The probe adapter is then turned clockwise to tighten the seal around the probe. Any leakage of sink arm should be noted in lab notebook.

5. Final Setup

Three sink arms are now ready within the PVC Cross adapter. A long source tube with elbow end is inserted. A magnetic stir bar is added at the elbow and guided to the PVC cross with an exterior magnet. Acidic solution (pH ~ 2.3, record this value!) is poured into the source at the elbow. Volume of source solution is recorded.

The GellipHish should be mounted above a secondary spill container with a custom stir motor plate below it. Alternatively, a regular stir plate may be used to stir sinks and sources, provided the PVC cross is centered on the plate. A magnet should be used to move stir bars to the center of the sinks, where the motors can stir them.

6. Running the code

A GellipHish python script is run to monitor pH with time. Clicking “Open File” will set up a csv file to record values. This file must be named in the box below the button prior to running (name the program with the date, followed by ‘GelliRun’). Then click the pH button to start measurements. Record the time interval between successive probe measurements (this number is not recorded by the program). A 5-25 hour lag period is common before sink pH begins to drop. If a probe reading indicates a large, rapid drop in pH, a membrane leak is likely. Unfortunately, there is no way to remove a leaking sink without compromising the entire run. Source pH should be monitored manually

using a calibrated pH probe and values recorded every few hours. The source pH will rise until pseudo-steady state diffusion begins and will then remain nearly constant.

7. End of Run

Run the program for at least 12 hours to achieve pseudo steady state flux. Membranes incorporating SA or other adsorbing polymers such as chitosan may require more time. Upon shutting down the program, pour the source solution out, and measure and record final pH with a Hach probe or other high quality probe. Remove each sink and measure final pH. Measure membrane thicknesses once again as swelling has been known to occur. Neutralize acidic solutions and pour down the drain.